# DELIVERY OF ZINC TO RED BLOOD CELLS AND THE DOWNSTREAM EFFECTS IN MULTIPLE SCLEROSIS

Ву

Suzanne Letourneau

# A DISSERTATION

Submitted to
Michigan State University
in partial fulfillment of the requirements
for the degree of

Chemistry – Doctor of Philosophy

2013

#### **ABSTRACT**

# DELIVERY OF ZINC TO RED BLOOD CELLS AND THE DOWNSTREAM EFFECTS IN MULTIPLE SCLEROSIS

Ву

#### Suzanne Letourneau

The research presented here shows that zinc is delivered to the red blood cell (RBC) and

investigates the effects of this in multiple sclerosis. A review of MS, as well as prior research investigating RBC-derived adenosine triphosphate (ATP) and the stimulation of nitric oxide (NO) are presented here. This dissertation hypothesizes that the increase in RBC-derived ATP seen in MS patients may be the result of increased zinc levels and leads to increased levels of NO, a molecule known to increase the permeability of the blood brain barrier (BBB), which is a precursor to lesion formation. C-peptide, a biologically active byproduct in the formation of insulin, also increases the release of ATP from RBCs, but only when bound to Zn<sup>2+</sup>. Evidence is presented here showing that C-peptide can deliver  $Zn^{2+}$  to RBCs. When bound to C-peptide, 2.54  $\pm$  0.23 pmol of  $Zn^{2+}$  were delivered to RBCs, compared to 0.09  $\pm$  0.21 pmol when  $Zn^{2+}$  alone was introduced RBCs. The significance of this in diabetes mellitus will be discussed. Because of these findings, C-peptide was used to deliver  $\mathrm{Zn}^{2+}$  to the RBCs of MS patients. Significantly more Zn<sup>2+</sup> is delivered to the RBCs of MS patients, at a value of 3.61  $\pm$  0.22 pmol, than to those of healthy controls, at a value of 2.26  $\pm$  0.24 pmol. Additionally, the basal level of Zn<sup>2+</sup> in the RBCs of MS patients and those of healthy

controls was measured. The RBCs of MS patients were found to have 41.8  $\pm$  1.7  $\mu$ g of Zn<sup>2+</sup>/g Hb where the RBCs of healthy controls only had 32.9  $\pm$  2.2  $\mu$ g Zn<sup>2+</sup>/g Hb.

To further the research into the increase ATP release from the RBCs of MS patients, this was measured in a flow system that mimics the shear stress experienced by the RBCs in vivo. It was found that the RBCs of MS patients release significantly more ATP, at a value of  $344.7 \pm 46.8$  nM, than those of healthy controls, at a value of  $132.1 \pm 14.1$  nM. Glybenclamide, an inhibitor of ATP release from the RBC, decreased this value to  $65.3 \pm 11.6$  nM in the RBCs of MS patients, showing that this is indeed the result of increase release of ATP, as opposed to cell lysis. The glucose uptake into these cells that may be leading to the increased ATP release is also discussed.

Finally, reports have shown that estrogens have a protective effect in MS. Here, the effect of estradiol and estriol on the RBC-derived ATP was measured. Estradiol and estriol reduced the ATP release from healthy RBCs to  $74 \pm 4\%$  and  $70 \pm 11\%$  that of healthy controls, respectively. Through the use of a microfluidic device, the effects of estradiol on RBC-derived ATP and the subsequent endothelial cell NO production were investigated. When these RBCs were incubated estradiol, the NO production from the endothelial cells was attenuated to a value that was only  $59 \pm 7\%$  of RBCs in the absence of estradiol. The ability of estrogens to decrease the ATP release from RBCs and subsequently the NO production of endothelial cells has major implications in the treatment of MS.

#### **ACKNOWLEDGMENTS**

First I would like to thank Michigan State University for the funding that made this work possible. The chemistry department here at Michigan State has provided an environment that fosters cooperation and resource sharing that creates a vast knowledge base and allows for increase productivity. In this area, I would especially like to thank Kathy Severin for all of her assistance in the training on and maintenance of the instruments in the teaching laboratories. She is always willing to spend her time helping others. During my time at Michigan State, I was also privileged to be part of a collaboration with Michigan State University's Neurology and Ophthalmology Clinic. I would like to thank Dr. Eric Eggenberger, Dr. Jayne Ward, and Doozie Russell for their help in obtaining blood samples from MS patients, to who I am also grateful.

I'd also like to thank my advisor, Dana Spence, for his role in helping me to get where I am today. His unique leadership style fosters productive and publishable results while leaving time for students to have a life outside of the laboratory. The research environment he has created promotes critical thinking and independent investigation, which are invaluable skills, no matter what field his students end up in.

A lot of this work would not have been possible without the teamwork of the Spence group members, past and present. I'd especially like to thank Wathsala Medawala, who collected the C-peptide data presented in this thesis. In addition to working together, I enjoyed sitting next to her for my first three years in the laboratory. I would also like to

thank the current Spence group members: Kari Anderson, Yimeng Wang, Yueli Liu, Jayda Erkal, Sarah Lockwood, Bethany Gross, Chengpeng Chen, Kristen Entwistle, and Ruipeng Mu. Yueli and Jayda were extremely instrumental in the research on the RBCs of MS patients, taking time away from their own research to help with mine, and for that I am truly indebted to them. Kari and I entered the program here in the same year, and she was not only an excellent labmate, but also became one of my closest friends.

I would like to than my parents, AnneMarie and Peter, and my sister, Lisa, for their support all of these years. They have been by biggest cheerleaders throughout this process, and I am lucky to have grown up in such a wonderful environment. My parents, Lisa, and Jackie and Bella Robbins have all helped to keep me smiling.

Finally, I would like to thank my soon-to-be husband, Jonathan, for all the love and support he has shown me since the day we first met. His patience and encouragement throughout the dissertation and defense process kept me going. He is my sunshine.

# TABLE OF CONTENTS

LIST OF TABLES				
LIST OF FIGURES	ix			
Chapter 1 – Introduction	1			
1.1 Multiple Sclerosis	1			
1.2 Classification, Diagnosis, and Treatment of MS	3			
1.3 Animal Model of MS	11			
1.4 Adenosine Triphosphate and Nitric Oxide	12			
1.5 Pregnancy and Estrogens in MS	15			
1.6 Zinc and MS	20			
REFERENCES	22			
Chapter 2 – The Effect on Estrogen on Endothelial Nitric Oxide Stimulation via Red				
Blood Cell Derived Adenosine Triphosphate	30			
2.1 Red Blood Cell Derived ATP and NO Stimulation	30			
2.1.1 Red Blood Cell Glycolysis	30			
2.1.2 ATP Release and NO Stimulation	33			
2.1.3 Estrogens and MS	37			
2.2 Microfluidic Devices	38			
2.3 Experimental	41			
2.3.1 Collection and Purification of Rabbit RBCs	41			
2.3.2 Preparation of Reagents	42			
2.3.3 Preparation of Microfluidic Device	43			
<ul><li>2.3.4 Chemiluminescence Detection of ATP Release from RBCs</li><li>2.3.5 Adhering Cells to a Microfluidic Device and Fluorescence</li></ul>	44			
Determination of NO	48			
2.4 Results	52			
2.5 Discussion	63			
REFERENCES	66			
Chapter 3 – Delivery of Zn <sup>2+</sup> to the Red Blood Cell by C-Peptide	72			
3.1 Diabetes Mellitus	72			
3.1.1 Classifications	72			
3.1.2 Complications	75			
3.2 Insulin and C-Peptide	77			
3.2.1 Discovery of Insulin	77			
3.2.2 Insulin and C-Peptide Production and Release	78			
3.2.3 Structure of C-Peptide	81			

3.2.4 Biological Effects of C-Peptide	83			
3.3 Experimental	86			
3.3.1 Preparation of Reagents	86			
3.3.2 Collection and Preparation of Human RBCs	87			
3.3.3 Radiolabeled Zn <sup>2+</sup> Assays for Determination of the Amount				
of Zn <sup>2+</sup> Interacting with the RBC	87			
3.4 Results	88			
3.5 Discussion	97			
REFERENCES	105			
Chapter 4 – Potential Multiple Sclerosis Biomarkers	113			
4.1 MS Diagnosis and the Need for Biomarkers	113			
4.2 Experimental	117			
4.2.1 Preparation of Reagents	117			
4.2.2 Collection and Preparation of Patient and Control Samples	118			
4.2.3 Determination of Radiolabelled Zn <sup>2+</sup> Interaction with				
MS Patient RBCs	119			
4.2.4 Determination of Radiolabelled Glucose Uptake of MS				
Patient RBCs	119			
4.2.5 Determination of ATP Release from MS Patient RBCs in	424			
Response to Flow	121			
4.2.6 Determination of C-peptide Interaction with MS Patient RBCs and the Plasma Concentration of C-Peptide by				
Enzyme Linked Immunosorbent Assay	123			
4.2.7 Determination of Basal Zn <sup>2+</sup> Levels in MS Patient RBCs	123			
	422			
by Atomic Absorption Spectroscopy 4.3 Results	123 126			
4.4 Discussion	131			
REFERENCES	139			
NEI ENERGES	133			
Chapter 5 – Overall Conclusions and Future Directions	143			
5.1 Overall Conclusions				
5.2 Future Directions	153			
5.2.1 Zn <sup>2+</sup> and C-Peptide Binding	153			
5.2.2 Future MS Studies	155			
5.2.3 Microfluidics and MS Studies	156			
REFERENCES	158			

# LIST OF TABLES

Table 1.1 – Medications used in MS. \*IFNs inhibit the proliferation of T cells, decreases the production of proinflammatory cytokines 8

#### LIST OF FIGURES

- Figure 1.1 Common Lesions in MS The diagnosis of MS requires lesions to be found in two of the four following areas of the CNS: juxtacortical, periventricular, infratentorial, and the spinal cord. Above are MRI images of lesions in these regions of the brain, as well as in the spinal cord. For interpretation of the references to color in this and all other figures, the reader is referred to the electronic version of this dissertation.
- Figure 1.2 Proposed mechanism of ATP release from RBCs and subsequent NO production It has been proposed that G-protein coupled receptor (GPCR), cyclic adenosine monophosphate (cAMP), and the cystic fibrosis transmembrane conductance regulation (CFTR) protein are all required for the release of ATP by mechanical deformation, though how the ATP leaves the cell remains in question. In this proposed mechanism, the binding of ATP to the P2Y receptor on the endothelial cell results in the activation NOS and the production of NO.
- Figure 1.3 Steroid structures Dehydroxyepiandosterone (DHEA) is a precursor of both estradiol and estriol, and all three steroids have similar structures leading to the hypothesis that the estrogens will have a similar effect on the ATP release from the RBC as that of DHEA.
- Figure 2.1 Glycolysis This process, which occurs in RBCs, is the only way for the cells to metabolize glucose. Glycolysis occurs in two phases. In the preparatory phase, on the left, two ATP molecules are consumed. During the payoff phase, on the right, four ATP molecules are produced, resulting in a net gain of two ATP molecules per glucose molecule consumed.
- Figure 2.2 ATP Release From MS RBCs (From Letourneau et al.) ATP release was measured from RBCs subjected to flow. The average ATP release from the healthy RBCs was  $138 \pm 21$  nM. An increase to  $375 \pm 51$  nM was seen for RBCs obtained from MS patients. The error is reported as standard error of the mean for 11 controls and 18 MS samples. The values are statistically different at a value of p < 0.001.
- Figure 2.3 Proposed mechanism of ATP release from RBCs and subsequent NO production It has been proposed that G-protein coupled receptor (GPCR), cyclic adenosine monophosphate (cAMP), and the cystic fibrosis transmembrane conductance regulation (CFTR) protein are all required for the release of ATP by mechanical deformation, though how the ATP leaves the cell remains in question. In this proposed mechanism, the binding of ATP to the P2Y receptor on the endothelial cell results in the activation NOS and the production of NO.

Figure 2.4 – Photolithography – In order to perform rapid fabrication using PDMS, a reusable master is needed. This can be prepared through photolithography. In this process, a clean silicon wafer is coated with SU-8 photoresist. After pre-baking the wafer, a mask is placed over the photoresist with the desired features. The wafer is then exposed to UV light. After a post-bake, the wafer is soaked in developer to removed unpolymerized photoresist. The result is a wafer with raised features that can be repeatedly used as a mold for PDMS.

Figure 2.5 – Soft Lithography – Through this process, the layers of the microfluidic device were created. The polymer and curing agent were mixed in 20:1 and 5:1 ratios in separate plastic cups and degassed by vacuum. The 20:1 mixture was poured over the channel portion of the master and baked at 75°C for 12 minutes. The 5:1 mixture was then pour wafer the entire master and bake for another 12 minutes at the same temperature. The PDMS was then removed from the master. The second layer of the microfluidic device was prepared using the same steps with an unpatterned silicon master.

Figure 2.6 – Microfluidic Device – A) The microfluidic device layers are diagramed. A polycarbonate membrane separated the bottom layer, containing the channels, and the top layer, patterned with wells. B) A photograph of a completed microfluidic device. C) A diagram of the cross section of a well. bPAECs are adhered to the membrane in the well. The porous membrane separates the bPAECs from the channel through which the RBCs are pumped.

Figure 2.7 – Measurement of ATP Release – Estradiol (E2) or estriol (E3) were added to PSS, immediately followed by RBCs to make a 7% RBC solution. When  $\text{Zn}^{2+}$  bound to C-peptide was used, the  $\text{Zn}^{2+}$  and C-peptide were added to the vial first and allowed to incubate for 2-3 minutes before the addition of PSS. After a two hour incubation, a 200  $\mu\text{L}$  sample was transferred into a cuvette. 100  $\mu\text{L}$  of the luciferin/luciferase solution was added and the cuvette was lightly shaken. The cuvette was placed in a dark box over a PMT and at 15 seconds the luminescence was measured.

Figure 2.8 – DAF-FM DA – DAF-FM DA crosses the cell membrane. Esterases then transform the probe to DAF-FM, which loses its cell permeability. The DAF-FM then reacts with NO, producing a benzotiazol derivative that is fluorescent at the above excitation and emission.

Figure 2.9 – Flowing RBCs Through the Device – Pictured above, the RBC solutions were pumped at the rate of 0.1  $\mu$ L/min through the underlying microfluidic channels for 30 minutes. Each well was imaged before and after using an Olympus MVX fluorescence macroscope, fitted with a mercury-arc lamp and a fluoroscien isothiocyanate (FITC) filter

cube having excitation and emission wavelengths of 470 and 525 nm, respectively.

51

Figure 2.10 – The Effect of Estradiol on RBC ATP Release - Compared to RBCs with the absence of estradiol, the RBC-derived ATP for RBCs treated with 0.5  $\mu$ M estradiol was reduced to 76 ± 7% of the value of the untreated cells. The amount of ATP released decreased with increasing concentration of estradiol; for the 1  $\mu$ M and 1.5  $\mu$ M estradiol solutions, the RBC-derived ATP was reduced to 62 ± 7% and 56 ± 6%, respectively. Error is shown as standard deviation for N = 4 rabbits. The asterisks denote a statistically significant difference from untreated RBCs at p < 0.05.

Figure 2.11 – Estradiol (E2) Decreases ATP Release at Physiological Concentrations – incubating the RBCs with 30 nM estradiol reduces the chemiluminescence in response to ATP release to  $74 \pm 4\%$ , which is statistically equivalent to the decrease in the amount of chemiluminescence seen with 0.5  $\mu$ M estradiol, but at a more physiologically relevant concentration of the hormone. Error is standard deviation for N = 4 rabbits. The asterisk denotes the decrease, as compared to untreated RBCs, is statistically significant at p < 0.02.

Figure 2.12 – The Effect of Estriol (E3) on RBC-derived ATP – Estriol decreases the chemiluminescence due to ATP at physiologically relevant concentrations. 30 nM of estriol reduced the ATP release to 70  $\pm$  11% of that of RBCs alone. The RBCs incubated with 0.5  $\mu$ M and 1.0  $\mu$ M had their ATP release reduced to 69  $\pm$  13% and 62  $\pm$  11%, respectively. Error is shown as standard deviation for N = 4 rabbits, and the asterisk denotes a statistically significant decrease at p < 0.05

Figure 2.13 – The Effect of Estrogen on ATP Release Stimulated By  $Zn^{2+}$  bound to C-peptide – Note that the concentrations of estradiol and estriol are not same looking at the bars left to right in an attempt to compare the data sets. In both sets of results the  $Zn^{2+}$  bound to C-peptide resulted in an increase in chemiluminescence to more than double that seen for RBCs alone. For estradiol (E2), a significant decrease in the ATP release, as compared to RBCs and 10 nM  $Zn^{2+}$ -C-peptide, to  $76 \pm 15\%$  and  $61 \pm 24\%$  was observed for the 0.75  $\mu$ M and 1.5  $\mu$ M samples, respectively. For estriol (E3), the statistically significant decreases were seen for the 0.5  $\mu$ M and 1.0  $\mu$ M samples. They were decreased to  $73 \pm 17\%$  and  $61 \pm 13\%$ , respectively. Error is standard deviation for N = 5 rabbits for estradiol and N = 4 rabbits for estriol. The asterisk denotes the significant increase of ATP release with 10 nM  $Zn^{2+}$  bound to C-peptide at p < 0.0005. The # denotes a decrease as compared to 10 nM  $Zn^{2+}$ -C-peptide at p < 0.05.

Figure 2.14 – Fluorescence Intensity Images – DAF-FM reacts with NO in bPAECs resulting in fluorescence than can be photographed with a CCD camera and the pixel intensity can be measured. As seen above, when RBCs incubated with estradiol (E2) are

flowed beneath wells containing bPAECs, the NO production of those cells is lower. This is due to the decrease in RBC-derived ATP, stimulating NO production in bPAECs. 59

Figure 2.15 – Normalize Fluorescence Intensity – The data in this figure shows the normalized, background subtracted emission. As shown, the emission decreases with RBCs incubated in buffer containing estradiol. In this case, the estradiol is actually able to reduce the NO production to 43  $\pm$  0.1% of that of untreated RBCs. The emission intensity begins to increase with again with increasing concentration of estradiol, although a significant increase in emission, in comparison to RBCs alone, is not measure until the estradiol levels reach approximately 2  $\mu$ M. At this value, the fluorescence intensity is 13  $\pm$  4% higher than the untreated RBCs. The next highest concentration, 1.5  $\mu$ M, is not significantly different from the untreated RBCs. Error is shown as standard deviation for N = 4 rabbits and the asterisk denotes a significant difference from untreated RBCs at p < 0.05.

Figure 2.16 – Washed and Unwashed RBCs – There was a marked decrease in NO production in the bPAECs, denoted by the decrease in fluorescent emission, when the RBCs are pre-incubated with estradiol. RBCs that have been washed to removed excess estradiol do not result in a statistically significant increase in NO production. The black bars represent the data from the previous figure and are included for comparison. The grey bars show that the estradiol is able to decrease the NO production in bPAECs, as detected by fluorescence intensity. The NO production was decreased to  $59 \pm 7\%$  with 10 nM estradiol, and this decrease remained statistically constant across the range of concentrations, down to  $51 \pm 5\%$  that of the NO production of bPAECs exposed to untreated RBCs, seen at 2.0  $\mu$ M. Error is reported as standard deviation for N = 4 rabbits. The asterisks denote a significant difference from untreated RBCs (black bar) and the # denote a significant decrease from untreated RBCs (grey bar).

Figure 3.1 – Proinsulin – This basic diagram shows the role of C-peptide in the structure of insulin, as well as the amino acid sequence of C-peptide. The acidic residues have been colored purple. When the C-peptide is cleaved from proinsulin, the A and B chains remain, forming insulin.

Figure 3.2 – Insulin Packaging and Release – Insulin is first synthesize as preproinsulin in the cytosol before being uptaken into the rough endoplasmic reticulum where the signal peptide is cleaved to form proinsulin. It is then transported to the Golgi apparatus where it is subsequently packaged into vesicles. C-peptide is cleaved from proinsulin during this process. At the same time,  $Zn^{2+}$  ions are entering the vesicle through ZnT8, a  $Zn^{2+}$  transporter in the vesicle membrane. This  $Zn^{2+}$  is involved in the creation of proinsulin hexamers, consisting of six proinsulin and two  $Zn^{2+}$ . After C-peptide is removed, the  $Zn^{2+}$ -insulin complex becomes less soluble and is stored in the vesicles in a crystalline form. Insulin is released from the  $\beta$ -cells in response to blood glucose levels,

and the vesicles undergo exocytosis. When this occurs, insulin and C-peptide are released in equimolar amounts and Zn<sup>2+</sup> is present as well.

Figure 3.3 – Radiolabeled  ${\rm Zn}^{2+}$  Assays –  ${\rm ^{65}Zn^{2+}}$  and the peptide were incubated together in pure water for three minutes to ensure peptide activation. PSS was then added to the mixture, immediately followed by the addition of the appropriate volume of RBCs to prepare 1 mL samples with a 7% hematocrit. Following a one hour incubation samples were centrifuged and the supernatant was collected. In some of the experiments, the RBCs were then washed three times and lysed with bleach. In a 96-well plate, 200  $\mu$ L of supernatant or lysate solution was combined with 100  $\mu$ L of scintillation cocktail. The amount of radioactivity in each sample was then determined using a 1450 Microbeta Plus liquid scintillation counter.

Figure  $3.4 - {}^{65}Zn^{2+}$  Remaining in the Supernatent after Incubation with RBCs – For each set of bars, when C-peptide was also added, it was added in a 1:1 ratio with  ${}^{65}Zn^{2+}$ . As is evident from the data,  ${}^{65}Zn^{2+}$  alone, black bars, does not interact with the RBC. However, with the exception of the 1 nM concentration, when  ${}^{65}Zn^{2+}$  bound to C-peptide is incubated with the RBCs, grey bars, significantly less  ${}^{65}Zn^{2+}$  is found in the supernatant. Error is represented as standard deviation for N = 7 humans. The asterisk represents p < 0.05.

Figure 3.5 – C-Peptide and  $Zn^{2+}$  on the RBC – The data on the left shows the amount of C-peptide interaction with the RBC. Comparing to the data on the right, showing the amount of  $^{65}Zn^{2+}$  recovered from RBC lysate, it is evident that C-peptide and  $Zn^{2+}$  interaction with the RBC in a 1:1 ratio. For both binding curves, saturation seems to begin around 10 picomoles of added  $Zn^{2+}$  bound to C-peptide and results in a maximum of 2.64  $\pm$  1.03 picomoles of C-peptide and 2.96  $\pm$  0.17 picomoles of  $^{65}Zn^{2+}$  interacting with the RBC when 20 picomoles of  $Zn^{2+}$ -activated C-peptide have been added. Within error, this shows that  $Zn^{2+}$  and C-peptide interact with the RBC in a 1:1 manner. Error is shown as standard deviation for N = 4 humans for C-peptide and N = 5 for  $Zn^{2+}$ .

Figure 3.6 – Saturation Curve – After total and specific binding (circles and triangle, respectively) were found, the non-specific binding (squares) was calculated. Comparable to the C-peptide binding, the amount of specifically bound  $Zn^{2+}$  is 1.85  $\pm$  0.53 picomoles for 20 picomoles of added  $^{65}Zn^{2+}$  bound to C-peptide. This data shows that  $Zn^{2+}$ , or  $Zn^{2+}$  bound to C-peptide, is interacting with a receptor on the RBC. The error is shown as standard deviation for N = 7 humans for 2, 5, 10, 20 and 40 picomoles, N = 4 humans for 80 picomoles, and N = 5 humans for 100 picomoles.

Figure 3.7 – C-Peptide and  $Zn^{2+}$  in the Supernatent – The data on the left shows that whether or not 20 nM C-peptide is bound to 20 nM  $Zn^{2+}$ , statistically the same amount is found to be interacting with the RBC. However, when  $Zn^{2+}$  alone is added to an RBC solution, all of it is found in the supernatant after incubation. When  $Zn^{2+}$  is introduced to the sample as 20 nM  $Zn^{2+}$  bound to C-peptide, significantly less  $Zn^{2+}$  was found in the supernatant, meaning it is interacting with the RBC, but only when added to the sample bound to C-peptide. Error is standard deviation for N = 4 humans for C-peptide and N = 5 humans for  $Zn^{2+}$ . The asterisk denotes p < 0.01 as compared to  $Zn^{2+}$  added alone.

Figure 3.8 – Effect of Mutant, Ratios, and BSA on  $Zn^{2+}$  Interaction with RBCs – The mutation in E27A prevents  $^{65}Zn^{2+}$  interaction with the RBC in the presences of BSA (black bars). Also, in normal PSS, only the 1:1  $^{65}Zn^{2+}$  to C-peptide ratio was able to delivery any  $^{65}Zn^{2+}$  to the RBC. When the experiments were repeated using a BSA-free PSS, (grey bars) both peptides are able to deliver  $Zn^{2+}$  to the RBC, regardless of ratio. However, C-peptide is able to deliver roughly double the amount of  $Zn^{2+}$  as compared to the mutant. The error is standard deviation for N = 4 humans. The asterisk represents p < 0.05 and the pound sign represents p < 0.001 as compared to 1:1 ratio of  $Zn^{2+}$  bound to C-peptide.

Figure 3.9 – Hypothesis of  $Zn^{2+}$  Binding to C-peptide and a Mutant – Results showing the loss of  $Zn^{2+}$  interaction with the RBC with higher  $Zn^{2+}$  to C-peptide ratios led to the hypothesis that multiple  $Zn^{2+}$  ions may be binding to the C-peptide in those cases. Then, upon addition of serum albumin containing PSS, the  $Zn^{2+}$  may be removed from the peptide by the albumin because of its high binding affinity. It is believed that the  $Zn^{2+}$  may bind to the E27A peptide, however there is no folding, and the  $Zn^{2+}$  ions are easily removed by the BSA. This hypothesis is related to the data in figure 3.8.

Figure 4.1 – Determination of ATP Release from MS Patient RBCs in Response to Flow – RBCs were diluted to a 7% hematocrit and pumped through tubing, one syringe containing the sample and the other containing luciferin/luciferase. Solutions were pumped, at 6.7  $\mu$ L/min, through 50  $\mu$ m internal diameter microbore tubing. The solutions met at a mixing T-junction and the combined stream was pumped through an additional segment of 75  $\mu$ m internal diameter tubing, with a portion of the polyimide coating removed, over a PMT in a light excluding box. This allowed for the chemiluminescence resulting from the reaction of ATP with luciferin/luciferase to be detected.

Figure 4.2 – Determining C-peptide Interaction with the RBCs of MS Patients using Enzyme-Linked Immunosorbent Assay – The interaction between Zn<sup>2+</sup> bound to C-peptide and RBCs was studying using solutions containing 7% RBCs and 20 nM each of Zn<sup>2+</sup> and C-peptide. Samples were prepared by mixing the appropriate volumes of Zn<sup>2+</sup> and C-peptide in water for several minutes before adding PSS, immediately followed by the RBC of either MS patients or healthy controls. Following a three hour incubation at 37°C, the samples were centrifuged at 500g for four minutes and the C-peptide remaining in the supernatant was measured using an ELISA.

Figure 4.3 – ATP Release from RBCs of MS Patients – The results from the ATP release studies show that the ATP release from the RBCs of MS patients was found to be an average of  $344.7 \pm 46.8$  nM where the average release from healthy controls was  $132.1 \pm 14.1$  nM. When the RBCs of the MS patients were incubated with a CFTR inhibitor, glybenclamide, the ATP release is decreased back down below the amount of the healthy controls, to a level of  $65.3 \pm 11.6$  nM, showing that the increase in ATP release of the flowing RBCs of MS patients is not the result of RBC lysis. The error is reported as standard error of the mean, for N = 19 MS patients, 10 healthy controls and 12 glybenclamide inhibitions. The asterisk represents p < 0.001.

Figure 4.4 – Basal Levels of  $Zn^{2+}$  in the RBCs of MS Patients – The basal amount of  $Zn^{2+}$  in the RBCs of the MS patients was found to be 41.8  $\pm$  1.7  $\mu$ g of  $Zn^{2+}$ /g Hb, which is a 27% increase of the basal levels of  $Zn^{2+}$  of the RBCs of healthy controls, 32.9  $\pm$  2.2  $\mu$ g of  $Zn^{2+}$ /g Hb. The error is reported as standard error of the mean for N = 21 MS patients and 11 healthy controls. The asterisk represents p < 0.01 as compared to the control sample.

Figure  $4.5 - {}^{65}\text{Zn}^{2+}$  interaction with the RBCs of MS Patients – The amount of  ${}^{65}\text{Zn}^{2+}$  that is able to interact with the RBCs of MS patients is significantly higher, at a value of  $3.61 \pm 0.22$  picomoles, than that of healthy controls, at a value of  $2.26 \pm 0.24$  picomoles. The amount of C-peptide interaction with the RBC correlates to this very well, as shown in figure 4.6. The error is reported as standard error of the mean for N = 22 MS patients and 11 healthy controls. The asterisk represents p < 0.001 as compared to the control samples.

Figure 4.6 – C-peptide Interaction with the RBCs of MS Patients – Correlating to the data in figure 4.5, it can be seen that the amount of C-peptide interacting with the RBCs is very similar to the amount of  $^{65}$ Zn $^{2+}$ . 3.61 ± 0.18 picomoles of C-peptide interacted with the RBCs of MS patients, while only 2.43 ± 0.20 picomoles interacted with the RBCs of healthy controls. The error is reported as standard error of the mean for N = 12 MS

patients and 6 healthy controls. The asterisk represents p < 0.001 as compared to the control sample.

Figure 4.7 – Glucose Uptake into the RBCs of MS Patients – It should be noted that the x-axis does not start at zero, so while there are differences, they are not as extreme as they seem. Comparing the untreated RBCs (black) of the MS patients and those of the healthy control, no significant difference was seen in the amount of glucose uptake. However, when the RBCs were stimulated by  $Zn^{2+}$  bound to C-peptide (grey), those from the MS patients took in  $6.0 \pm 0.01\%$  more glucose than those of the healthy controls. While this seems like a small increase, it is a statistically significant one. The error is reported as standard error of the mean for N = 22 MS patient RBC samples and 11 healthy control RBC samples. The asterisk represents p < 0.001 and the pound sign represents p < 0.01.

Figure 4.8 – The Difference in  $^{65}$ Zn $^{2+}$  interaction with the RBCs of Male and Female MS Patients – There is a significant difference in the amount of  $^{65}$ Zn $^{2+}$  interaction with the RBC between male (black bars) and female (white bars) patients with MS that is not seen in healthy controls. The highest amount of  $^{65}$ Zn $^{2+}$  interacting with the RBC s is seen in male MS patients at a level of  $4.16 \pm 0.18$  picomoles. The error is shown as standard error of the mean for N = 6 male MS patients, 3 male healthy controls, 16 female MS patients, and 8 female healthy controls. The \* represents p < 0.001. 138

Figure 5.1 – The Effect of Estriol (E3) on ATP Release from the RBCs of MS Patients – Flow based studies were performed on one sample of RBCs from an MS patient with the addition of 30 and 500 nM estriol. Without estriol, the RBCs from the MS patient released 208.1 nM ATP, while the healthy control released 103.9 nM. When incubated for a half hour with 30 or 500 nM estriol, the ATP release dropped to 59.1 and 21.6 nM, respectively. N = 1.

# **Chapter 1 – Introduction**

# 1.1 Multiple Sclerosis

Multiple Sclerosis (MS) is a disease of the central nervous system (CNS) that affects over 400,000 people in the United States and 2.1 million people worldwide. Although the disease was first described in 1868, by Jean-Martin Charcot, and much is known about MS, it remains difficult to diagnose and the cause remains undetermined. MS can affect people in different ways, but the hallmark feature of the disease is the break down of the myelin sheath, a layer of lipids and proteins that covers the axon of nerve cells. When demyelination occurs, characteristic lesions form and nerve signals are slowed. This causes a variety of neurological complications, including difficulties with vision, motor skills, coordination and cognition.

MS has long been considered to be an autoimmune disease. Patients are typically diagnosed between the ages of 20 and 30, though up to 10% of patients develop symptoms before reaching adulthood. Women are diagnosed with more than twice the frequency of men, and though Caucasians are twice as likely to be affected as any other race, MS does occur in most ethnic groups. There have been several studies suggesting a correlation between geographic location and disease prevalence, with incidences of the disease increasing with distance from the equator.

While MS is not hereditary, there is an increase familial risk, suggesting some genetic component to the disease. There is a 20-40 fold increase of instance MS if a first-degree relative has the disease and a 300 fold increase if a genetically identical twin has the disease. This suggests a genetic factor in the disease development, but with only one identical twin often being affected, it can be assumed that genetics are not the only factor involved. Because of the varied courses in the disease, it can be difficult to predict how and when the disease will worsen for an individual patient. Neurological problems generally develop after 10-15 years, with the majority of patients losing their ability to walk by 15 years post-diagnosis. Although the disease is debilitating, most people with MS have a normal life expectancy. There have been several treatments developed to slow down the disease progression or manage symptoms, but there is currently no cure for MS. 1

An important feature of MS is the breakdown of the blood brain barrier (BBB). The BBB is the inner lining of the capillaries in the brain, made up of endothelial cells that form highly organized tight junctions to create a selectively permeable barrier. The destruction of this barrier is seen early in the course of MS, occurring before the appearance of lesions. These lesions have been found to contain nitric oxide (NO), which is a facet of MS that has been investigated at some length.

In addition to the NO in the lesions, it has been reported that elevated levels of nitrite and nitrate have been measured in the cerebral spinal fluid (CSF), serum, and urine of

MS patients. <sup>8</sup> Interestingly, Boje et al. found that NO may have a role in the change in BBB permeability. <sup>9</sup> The reaction of the NO radical with superoxide forms peroxynitrite, which has been shown to have a disruptive effect on cerebral capillaries. Other NO redox products have been shown to have similar effects, but the mechanism remains undefined.

### 1.2 Classification, Diagnosis, and Treatment of MS

There are four basic types of MS, each with a different disease progression. The most common form of MS is relapse-remitting, characterized by periods of exacerbated symptoms, such as vision problems or difficulty with motor skills, with returns to normal health in between. As the disease progresses, many patients are diagnosed with secondary-progressive MS. This form is also characterized by relapses, however after some years there is a steady worsening of overall neurological function between the attacks. More rare forms of MS include primary-progressive MS, where there is a steady worsening over time with no acute attacks, and progressive-relapsing MS, which starts out like primary-progressive MS, but exacerbations of the condition are also seen. <sup>1</sup>

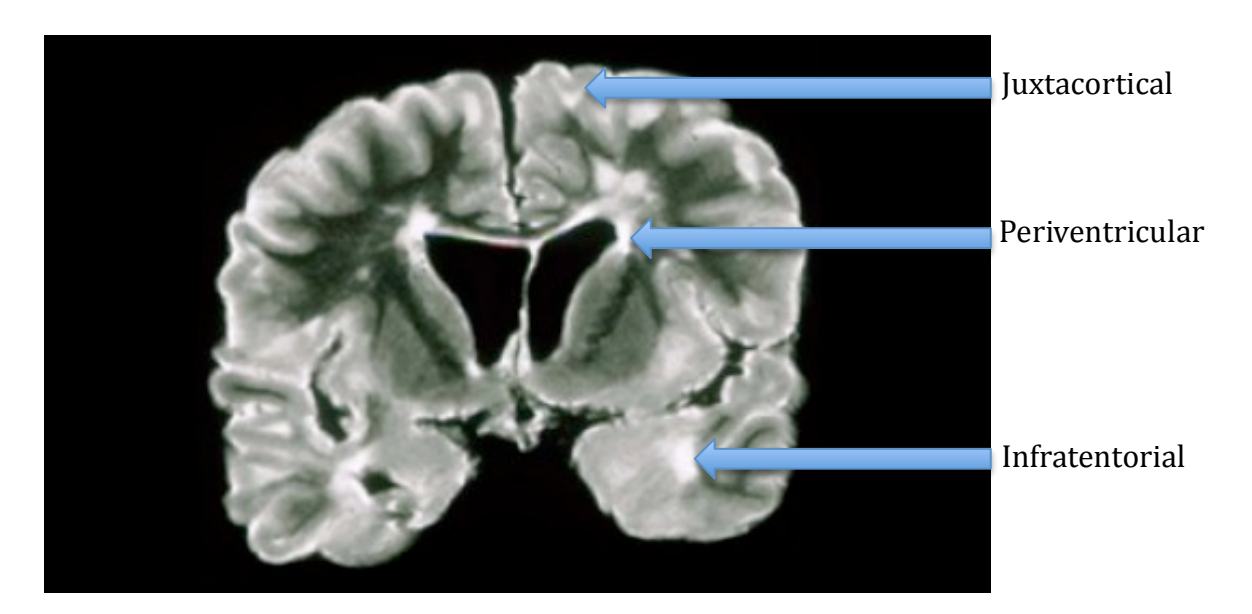
It is the nature of MS that the disease does not present the same way across all patients. This makes the diagnosis of MS slow and difficult. Diagnosis requires meeting a specific set of criteria and can take months or, in some cases, years. Before confirmed diagnosis, most patients present with a clinically isolated syndrome (CIS). CIS is defined

as an isolated event that affects one area of the CNS, in patients with no history of demyelinating events. The event is characterized as a neurological episode that is acute, lasts at least 24 hours and is assumed to be demyelinating. The most common types of CIS are optic neuritis or complications with the CNS. While nearly 90% of MS patients were originally diagnosed with CIS, not all patients diagnosed with CIS will go on to develop the disease. <sup>10</sup>

The diagnostic criteria for MS has been adapted and changed several times in keeping with current disease knowledge and imaging technologies. For a clinically definite diagnosis of MS, most criteria require the characteristic lesions to be separated in both space and time and any alternative diagnoses to be eliminated. The current diagnostic criteria were first described by McDonald et al. in 2001 and were revised in 2005 and 2010. To show dissemination in space, magnetic resonance imaging (MRI) must show at least one lesion in two of the four following areas of the CNS: periventricular, juxtacortical, infratentorial and spinal cord. Examples of these can be seen in figure 1.1. The viewing of these lesions does not require any MRI contrast media. However, for the demonstration of dissemination in time, gadolinium enhancing may be used. The presence of gadolinium enhancement denotes BBB breakdown and has been

consistently found in new lesions in MS patients. <sup>14</sup> Therefore, dissemination in time

requires a new non-enhanced lesion and/or a new gadolinium-enhanced lesion on a



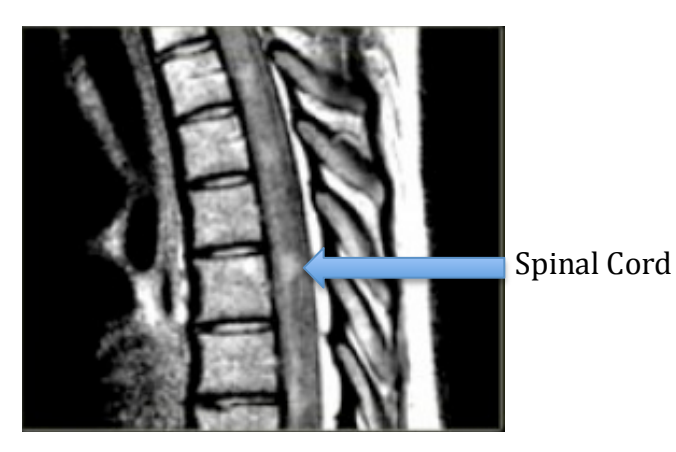


**Figure 1.1 – Common Lesions in MS –** The diagnosis of MS requires lesions to be found in two of the four following areas of the CNS: juxtacortical, periventricular, infratentorial, and the spinal cord. Above are MRI images of lesions in these regions of the brain, as well as in the spinal cord. For interpretation of the references to color in this and all other figures, the reader is referred to the electronic version of this dissertation.

later MRI or the presence of both non-enhanced and enhanced lesions simultaneously. 13

In 2005, criteria were added for diagnosis with progression from the onset, as is seem in primary-progressive and progressive-relapsing forms of the disease. These criteria were revised in 2010 and diagnosis now requires one year of disease progression, plus two of three of the following: at least one lesion in at least one of characteristic part of the brain (periventricular, juxtacortical or infretentorial), at least 2 lesions in the spinal cord, or CSF that tests positive for immunoglobulin G (IgG).

There is a great need for the discovery of biomarkers in MS. Ideally, diagnosis and treatment would be possible while the patients are in the early stages of CIS. This would potentially allow for a better quality of life both in the short term and over longer periods of time, if disease slowing treatments are effective. While the search for an MS biomarker has been ongoing for nearly a century, <sup>15</sup> there is still no biomarker used clinically. <sup>16</sup> Ideal biomarkers are ones that can be objectively measure and evaluated as indicators of biological processes or drug response. <sup>17</sup>

There are four proposed biomarker categories for MS: diagnostic biomarkers, predictive biomarkers, process-specific biomarkers and treatment-related biomarkers. These are discussed at length in chapter 4. <sup>18</sup> Currently, the only potential biomarker used clinically is IgG, an indicator of immune response that, while it is associated with MS, it is

not specific enough to be considered as a true biomarker for the disease. There have been other recent findings in the field of MS biomarkers, however, like IgG, most use invasive CSF testing. The CSF is traditionally believed to be the most likely source of an MS biomarker because of the proximity to the inflammation and lesions in the CNS, though this may not be the case, as CSF is collected through a lumbar puncture in the lower back and may not accurately reflect inflammatory markers in the brain regions were most MS lesions occur. <sup>19</sup>

Although there is still no cure for MS, there are treatments available that will alter the course of the disease, slowing the rate of disability, as well as drugs for symptom management to help patients cope. The first drug for the treatment of MS was approved by the US Food and Drug Administration (FDA) in 1993. Since then, nine drugs have been approved by the FDA for treatment. A complete list of FDA approved MS drugs, their dosage and effects can be seen in table 1.1.

Four of the nine drugs, including the first, Betaseron (IFN- $\beta$ -1b), are in a family of drugs known as interferons (IFNs). In 1996, the second IFN drug, Avonex (IFN- $\beta$ -1a) was approved, followed by Rebif (IFN- $\beta$ -1a) in 2002 and Extavia (IFN- $\beta$ -1b) in 2009. These medications all function similarly, differing in dosage, effectiveness, and side effects. For use in treatment, IFNs are manufactured using recombinant DNA, but IFNs are also naturally present in humans. Their role is complex and not completely understood, but

Drug	Year	Туре	Dosing	Effects	Side Effects
Aubagio <sup>63</sup>	2012	Pyrimidine synthesis inhibitor: reduces proliferation of immune cells	One tablet per day	Reduced relapse rates, fewer new and active lesions	Severe liver toxicity
Avonex <sup>20</sup>	1996	INF-β-1a*	Intra- muscular injection Once per week	Reduced risk of disability progression, fewer exacerbations	heart problems, depression, seizures
Betaseron 20 Extavia	1993 2009	INF-β-1b*	Sub- cutaneous injection Every other day	Stops the increase in total lesion area	Flu-like symptoms, injection site necrosis
Copaxone <sup>24</sup>	1996	Polymer of amino acids, shifts the immune effect to be less inflammatory	Sub- cutaneous injection Every day	Decrease in annual relapse rates, decrease in new lesions	Chest tightness, heart palpitations,
Gilenya <sup>25</sup>	2010	Sphingosine-1- phosphate receptor modulator, prevents lymphocytes from leaving nodes	One capsule per day	Reduced relapse rate, reduced lesion activity	Decreased heart rate, swelling of the eye, liver toxicity
Novantrone <sup>64</sup>	2000	Antineoplastic, intercalates in the DNA, suppresses T and B cells and macrophages	Intravenous Every 3 months	Delays time to relapse and disability progression, reduced lesions	Cardio- toxicity, increased leukemia risk
Rebif <sup>20</sup>	2002	INF-β-1a*	Sub- cutaneous injection Three times per week	Lower relapse rate, prolonged time to first relapse, delay in progression	Depression, liver toxicity, seizures
Tysabri <sup>65,66</sup>	2006	Monoclonal antibody: Lessens movement of immune cells across the BBB	Intravenous Once per month	Reduced risk of disability progression, fewer relapses	Increased risk of leukemia and serious infection

Table 1.1: Medications used in MS. \*IFNs inhibit the proliferation of T cells, decreases the production of proinflammatory cytokines<sup>23</sup>

it is known that they are involved in modulating the immune system. <sup>21,22</sup> In the treatment of MS, INF- $\beta$  has been shown to inhibit the proliferation of T cells, which have a variety of functions in vivo, including regulating the immune system, as well as decrease the production of proinflammatory cytokines. <sup>23</sup>

In 1996, the first non-IFN MS drug was approved by the FDA; Copaxone (glatiramer acetate) has since become the most prescribed single drug for the treatment of MS. This random polymer of the four amino acids found in myelin basic protein (MBP) (glutamic acid, lysine, alanine, and tyrosine) was originally intended for use to mimic MBP in the investigation of its ability to cause irritation and swelling in the brain, but was found to have positive, rather than negative, effects. Now, it is believed to result in a shift in the characteristics of the immune system from being dominated by the proinflammatory T-helper-1 cells to the less harmful T-helper-2 cells. The mechanism for this is not well understood, and there may be more immune effects than first realized. All of the previously mentioned drugs, as well as Novantrone (mitoxantrone) and Tysabri (natalizumab) are dosed by injection or intravenously.

In 2010, the first oral MS medication was FDA approved. Gilenya (fingolimod) has been shown to reduce relapse rate and lesion activity with a capsule medication that is taken once per day. Gilenya is a receptor modulator that prevents lymphocytes from leaving nodes and crossing the BBB, reducing inflammatory damage to nerve cells; however, it can have serious cardiac side effects. Two years later, in 2012, a second oral

medication, Aubagio (teriflunomide), was approved by the FDA. This drug also works by interaction with the immune system, reducing the proliferation of certain types of immune cells. This decreases the number of new lesions and reduces relapse rates. While this drug is new to the market at the time of writing, the treatment has been well tolerated with few adverse reactions. <sup>26</sup>

While disease-modifying treatments have been used, with varying success, to alter the course of the disease, patients still experience exacerbations, or relapses, of MS. The most common agent used in these cases is steroid therapy. 20 Not all exacerbations require treatment, but if the symptoms are impacting a patient's ability to function, the most commonly prescribed steroid treatment for MS is glucocorticosteroids (GCS) with prednisone, methylprednisone and dexamethasone being the top three of that group. Steroids are believed to impact MS through modulation of the immune system, reducing both lymphocyte and pro-inflammatory cytokine levels. 27 GCSs shorten the duration of exacerbations, and it has been suggested that there may be long-term benefits as well, though there has been some question of the validity of the studies leading to those conclusions. 28 High dose steroids, like those used to treat MS are often associated with serious side effects, such as depression, weight gain, insomnia, moodiness, and However, when used for MS treatment, steroids are generally administered in short pulses and are well tolerated with only mild side effects reported.<sup>28</sup>

# 1.3 Animal Model of MS

In 1933, in order to more effectively study MS, an animal model, experimental autoimmune encephalomyelitis (EAE), was developed. Although there are limitations to using EAE as an MS model, including the inability of EAE to mimic all types of MS, <sup>29</sup> it has proven to be a valuable tool in MS research since its development began. Discovered initially as a side effect of the rabies vaccine, it was subsequently found that a series of injections containing neural tissue would induce an autoimmune response in a large variety of animals, including primates and rodents. It has been found that EAE can be induced with crude brain extract and whole myelin, as well as with isolated antigens: myelin basic protein (MBP), proteolipid protein (PLP) or myelin oligodendrocyte glycoprotein (MOG), or by using synthetic peptides.

The antigens are generally injected along with complete Freund's adjuvant and pertussis toxin, to increase the immune response. Clinical signs of EAE are generally seen 8-14 days after induction, and the progression of the disease is measured using a clinical disease scale from 0-5, with 0 representing no clinical signs and 5 representing total paralysis or death. This animal model is often used for preliminary investigations of disease modifying drugs, including several that will be discussed in greater detail presently.

# 1.4 Adenosine Triphosphate and Nitric Oxide

Recently, a small scale study by the Spence group revealed that the red blood cells (RBCs) from MS patients release nearly three times the amount of adenosine triphosphate (ATP), in response to shear stress, than RBCs from healthy controls. <sup>32</sup> Importantly, ATP release from RBCs is known to increase as the cell deformability increases and it has been reported that RBCs obtained from MS patients have properties that would suggest an increase in deformability. The release of ATP from RBCs results in the stimulation of NO synthesis in endothelial cells. <sup>33,34</sup> As mentioned previously, MS patients have elevated levels of nitrite and nitrate in their CSF, serum, and urine, and the lesions that occur as a result of demyelination have been reported to have increased levels of NO. <sup>8</sup>

Sprague et al. have shown that the mechanical deformation experienced by circulating RBC results in ATP release.<sup>33</sup> While the exact mechanism for this release is not fully known, a G-protein coupled receptor (GPCR),<sup>35</sup> cyclic adenosine monophosphate (cAMP),<sup>36</sup> and the cystic fibrosis transmembrane conductance regulator (CFTR) protein<sup>37</sup> have all been implicated in this process. It is expected that the increase in ATP release from RBCs would lead to a subsequent increase in NO production in endothelial cells because ATP is a stimulus of NO production in endothelial cells.<sup>33,34</sup> In this

construct, the binding of ATP to the P2Y receptor on the endothelial cell results in the activation of nitric oxide synthase (NOS) and the production of NO. A schematic of the proposed mechanism can be seen in figure 1.2.

Recently, receptors for ATP have been found to have a role in MS. <sup>39,40</sup> Several studies investigated the role that the ATP receptor, P2X7, plays in MS. The P2X7 receptor is a purinergic ligand-gated cation channel receptor that is activated by ATP. This receptor is found mainly on immune cells both in the peripheral and central nervous systems, though it has been found on neurons as well as oligodendrocytes. <sup>39</sup> Low doses of ATP reversibly open the channel to small cations, such as Na<sup>+</sup> and Ca<sup>2+</sup>, while prolonged or repeated stimulation with higher levels of ATP will increase the pore size to accommodate larger molecules with masses in the range of 100s of Daltons. As a result of the increased permeability, high extracellular concentrations of ATP have a cytotoxic effect on some cells. <sup>41</sup>

Matute et al. showed that the activation of P2X7 has cytotoxic effects on oligodendrocytes both in vivo and in vitro, and the lesions formed in mice as a result are very similar to those found in MS. In addition, they found that there was a significant increase in the levels of P2X7 in both the optic nerve and axonal tract of MS patients, suggesting an increase vulnerability of the oligodendrocytes. Feinstein et al. have investigated the effects of a P2X7 deficiency on EAE. P2X7 deficient mice were four

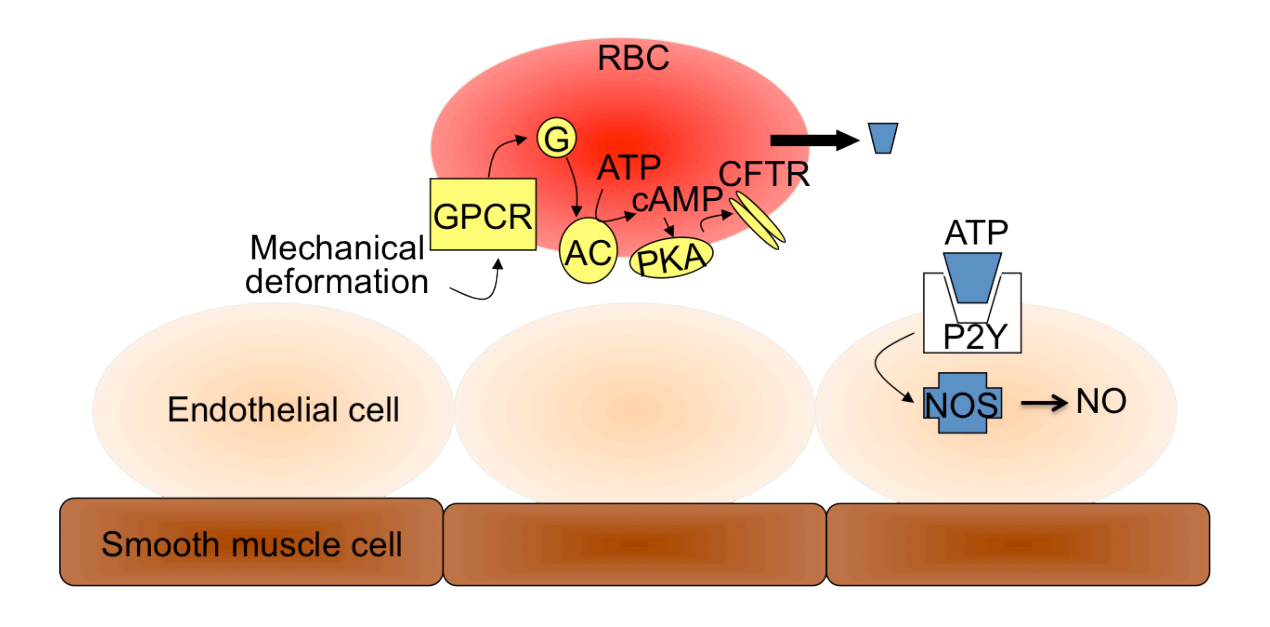


**Figure 1.2 – Proposed mechanism of ATP release from RBCs and subsequent NO production** – It has been proposed that G-protein coupled receptor (GPCR), <sup>35</sup> cyclic adenosine monophosphate (cAMP), <sup>36</sup> and the cystic fibrosis transmembrane conductance regulation (CFTR) protein <sup>67</sup> are all required for the release of ATP by mechanical deformation, though how the ATP leaves the cell remains in question. In this proposed mechanism, the binding of ATP to the P2Y receptor on the endothelial cell results in the activation NOS and the production of NO.

times less likely to suffer from the effects of EAE than normal control mice.<sup>40</sup> Interestingly, the P2X7 deficient mice still had increased levels of cytokine production, resulting from an immune response. This suggests that these mice lack an initiation event in the development of EAE, which points to a role of P2X7 in this disease, as well as in MS.

RBCs lack mitochondria, and therefore the only source of ATP is glycolysis. Because of this, it is expected that the altered ATP release in the RBCs of MS patients would be accompanied by abnormal glucose metabolism. In 1966, Raczkiewicz and Leyko showed that MS patients had a significant increase in the ATP content of their RBCs after an intake of 50 g of glucose, in comparison to their ATP content while fasting. Such an increase was not seen in healthy controls. More recently, Regenold et al. noted an increase in glucose metabolism outside of the mitochondria in the CSF of MS patients. This is significant when considering the lack of mitochondria in RBCs and the increase in ATP release seen from the RBCs of MS patients. Mitochondrial dysfunction in MS patients may be leading to increase glucose metabolism in the RBC.

# 1.5 Pregnancy and Estrogens in MS

While there are treatments for MS, there are still no concrete explanations for the exacerbations and ameliorations of the disease. Additionally, MS is more prevalent in females than males in a ratio between 2:1 and 3:1, varying by region.<sup>44</sup> The sex

discrepancy is seen in the development of EAE in certain strains of mice as well. While women are affected more than twice as often as men, they tend to have slower disease courses, resulting in a longer time between disease onset and certain disability levels. Men with MS, on average, have a shorter time before relapse-remitting MS becomes secondary progressive MS and a greater amount of neurological damage, seen in the form of brain cell death.

Research has been conducted in several areas, such as genetics, environmental factors, and hormones, in an attempt to explain the sex differences. Genetically, it has been suggested that there may be a protective effect found on the Y chromosome or a promoting effect on the X gene, where females would be doubly exposed. In the past 60 years, there has been an increase in the ratio of female to male diagnoses, with an increase in female diagnoses being credited with the change. Because of the social changes that have taken place over the past six decades affecting the role of women in the home and workplace, it has been proposed that the increase may be the result of environmental factors. Some factors that have been suggested for further epidemiological study include: occupation, obesity, dietary habits, birth control and later childbirth. The sex differences in MS, as well as anecdotal patient experiences led to the study of pregnancy and sex hormones, the role they play in the disease, and their potential use as therapeutics.

Up until the 1960s, women with MS were advised not to conceive, as pregnancy was thought to worsen the disease. In 1998, a pregnancy in MS (PRIMS) study investigated the number of relapses during each trimester before, during and after pregnancy. <sup>49</sup> It was found that the number of relapses was decreased during pregnancy, especially in the third trimester, and a spike in relapses was often seen in the first trimester postpartum.

It has been suggested that this trend corresponds to the levels of sex steroids, such as estradiol and estriol, that are present during pregnancy. When the levels are at their highest, the relapse rates are at their lowest. Levels of these hormones dramatically decrease after delivery, and a corresponding spike in relapse rates is seen. There is currently an on-going clinical trail, the Prevention of Post-Partum Relapses with Progestin and Estradiol in Multiple Sclerosis (POPART'MUS) trial, aimed at ameliorating these relapses. After delivery, women with MS are treated with estradiol and high doses of progestin and are monitored for three months. 44,50

Since PRIMS, several studies have looked at the effects of estrogens on MS, as well as on the animal model EAE. <sup>51-53</sup> Jansson et al. investigated the effects of castration of female mice on disease onset, as well as the effect of long term treatment with pregnancy levels of estradiol and estriol. <sup>51</sup> It was found that both estrogens delayed the onset of EAE, though estriol did so at a more physiologically relevant concentration

and for a longer time. Results from studies looking at the MS relapse rates in pregnancy, as well as the study done by Jansson et al. have lead to a Phase I clinical trial treating women with MS with the pregnancy hormone estriol. Although this was a small scale trial involving only 10 women, it showed promising results. All 10 patients had a decrease in size and number of lesions while being treated with estriol. When treatment ceased, lesion levels returned to their pretreatment state within three months. Once treatment was reinstated, there was again a decrease in the size and number of lesions.

The results of this study led Palaszynski et al. to investigate the effectiveness of estriol treatment on EAE in male mice. This study showed that both male and female mice pretreated with estriol showed no clinical signs of EAE for up to thirty days after MOG injections, suggesting that estriol may be a beneficial treatment for both sexes. In addition, there are currently large scale clinical trials looking at the effects of estriol alone, as well as the hormone used in conjunction with Copaxone. 54,55

It is currently thought that estrogens may ameliorate MS through a shift in immune response from T helper 1 (Th1) cells to T helper 2 (Th2) cells. However, as seen in figure 1.3, estradiol and estriol have similar structure to dehydroxyepiandosterone (DHEA), a precursor for both molecules. It has previously been shown by the Spence group that DHEA attenuates ATP release from healthy rabbit RBCs. This suggests the

**Figure 1.3 – Steroid structures –** Dehydroxyepiandosterone (DHEA) is a precursor of both estradiol and estriol, and all three steroids have similar structures leading to the hypothesis that the estrogens will have a similar effect on the ATP release from the RBC as that of DHEA.

potential for a similar effect on the RBC with both estrogen and estriol. A reduction in ATP release from RBCs would lead to a decrease in NO production of endothelial cells. This is contrary to much of the current literature, <sup>57,58</sup> which reports stimulation of NO production in endothelial cells in response to estrogens. It is interesting to note, however, that previous studies showing the stimulation of NO production by estrogens were not performed in the presence of RBCs. <sup>58</sup>

#### 1.6 Zinc and MS

The idea of altered zinc status in MS has been proposed since the late 1970s, <sup>59</sup> but the data associating zinc and MS has been generally overlooked by MS researchers with only a handful of reports on the subject in the past four decades. Interestingly, there have been several studies done on clusters of MS patients, meaning areas where there are higher than normal rates of MS diagnosis. In many of these areas, it was found that there was an issue with zinc contamination of some type, either in the soil and water, or from zinc smelters. <sup>60-62</sup>

In addition, the RBCs of MS patients have been found to have increases in the zinc levels, even without being part of an MS cluster. The level of zinc in the RBC was found to be significantly higher in MS patients than that of healthy controls, as well as being higher than the level in patients with other neurological impairments or inflammatory diseases. It is interesting to note that the serum zinc levels did not differ between these

groups, suggesting the increase in RBC zinc levels is not a result of defective zinc absorption or individual nutrition.  $^{59}$ 

In 1983, Dore-Duffy et al. proposed that the increase in RBC zinc levels may be an indication of an increase affinity of zinc-carrier protein complexes to surface receptors on the RBCs, or the RBCs from MS patients have an increased number of receptors for these proteins. Thirty years later, the work presented here furthers those proposals and answers some questions to the underlying mechanism of the etiology of MS. Data here will show support for the hypothesis that an increase of zinc delivery to the RBC results in an increase in glucose uptake into the cell. From this, the release of ATP at three times the level of controls results in an increase in the amount of NO produced in endothelial cells, potentially leading to BBB breakdown and disease progression in MS.

REFERENCES

#### REFERENCES

- 1 Cook, S. D. (Taylor & Francis, New York, 2006).
- Gorman, M., Healy, B., Polgar-Turcsanyi, M. & Chitnis, T. Relapses are more frequent in pediatric-onset than adult-onset multiple sclerosis. *Multiple Sclerosis* **14**, S66-S66 (2008).
- Vukusic, S. & Confavreux, C. Pregnancy and multiple sclerosis: the children of PRIMS. *Clinical neurology and neurosurgery* **108**, 266-270 (2006).
- 4 Handel, A., Giovannoni, G., Ebers, G. & Ramagopalan, S. Environmental factors and their timing in adult-onset multiple sclerosis. *Nature Reviews Neurology* **6**, 156-166 (2010).
- Pugliatti, M., Sotgiu, S. & Rosati, G. The worldwide prevalence of multiple sclerosis. *Clinical Neurology and Neurosurgery* **104**, 182-191 (2002).
- Sadovnick, A. D., Dyment, D. A., Ebers, G. C. & Risch, N. J. Evidence for genetic basis of multiple sclerosis. *Lancet* **347**, 1728-1730 (1996).
- 7 Minagar, A. & Alexander, J. S. Blood-brain barrier disruption in multiple sclerosis. *Multiple Sclerosis* **9**, 540-549 (2003).
- 8 Smith, K. J. & Lassmann, H. The role of nitric oxide in multiple sclerosis. *Lancet Neurology* **1**, 232-241 (2002).
- 9 Boje, K. M. K. & Lakhman, S. S. Nitric oxide redox species exert differential permeability effects on the blood-brain barrier. *Journal of Pharmacology and Experimental Therapeutics* **293**, 545-550 (2000).
- Dalton, C. M., Brex, P. A., Miszkiel, K. A., Hickman, S. J., MacManus, D. G., Plant G. T., Thompson A. J. & Miller D. H. Application of the new McDonald criteria to patients with clinically isolated syndromes suggestive of multiple sclerosis. *Annals of Neurology* **52**, 47-53 (2002).
- McDonald, W. I., Compston, A., Edan, G., Goodkin, D., Hartung, H. P., Lublin, F. D., McFarland, H. F., Paty, D. W., Polman, C. H., Reingold, S. C., Sandberg-Wollheim, M., Sibley, W., Thompson, A., van den Noort, S., Weinshenker, B. Y. & Wolinsky, J. S. Recommended diagnostic criteria for multiple sclerosis: Guidelines from the International Panel on the Diagnosis of Multiple Sclerosis. *Annals of Neurology* 50, 121-127 (2001).

- Polman, C. H., Reingold, S. C., Edan, G., Filippi, M., Hartung, H. P., Kappos, L., Lublin, F. D., Metz, L. M., McFarland, H. F., O'Connor, P. W., Sandberg-Wollheim, M., Thompson, A. J., Weinshenker, B. G. & Wolinsky, J. S. Diagnostic criteria for multiple sclerosis: 2005 Revisions to the "McDonald Criteria". *Annals of Neurology* 58, 840-846 (2005).
- Polman, C. H., Reingold, S. C., Banwell, B., Clanet, M., Cohen, J. A., Filippi, M., Fujihara, K., Havrdova, E., Hutchinson, M., Kappos, L., Lublin, F. D., Montalban, X., O'Connor, P., Sandberg-Wollheim, M., Thompson, A. J., Waubant, E., Weinshenker, B. & Wolinsky, J. S. Diagnostic Criteria for Multiple Sclerosis: 2010 Revisions to the McDonald Criteria. *Annals of Neurology* **69**, 292-302 (2011).
- Kermode, A. G., Thompson, A. J., Tofts, P., MacManus, D. G., Kendall, B. E., Kingsley, D. P., Moseley, I. F., Rudge, P. & McDonald, W. I. Breakdown of the blood-brain-barrier precedes symptoms and other MRI signs of new lesions in multiple sclerosis pathogeneic and clinical implications. *Brain* 113, 1477-1489 (1990).
- Awad, A., Hemmer, B., Hartung, H. P., Kieseier, B., Bennett, J. L. & Stuve, O. Analyses of cerebrospinal fluid in the diagnosis and monitoring of multiple sclerosis. *Journal of Neuroimmunology* **219**, 1-7 (2010).
- Avsar, T., Korkmaz, D., Tütüncü, M., Demirci, N. O., Saip, S., Kamasak, M., Siva, A. & Turanli, E. T. Protein biomarkers for multiple sclerosis: semi-quantitative analysis of cerebrospinal fluid candidate protein biomarkers in different forms of multiple sclerosis. *Multiple Sclerosis Journal* **18**, 1081-1091 (2012).
- Biomarkers Definitions Working Group. Biomarkers and surrogate endpoints: Preferred definitions and conceptual framework. *Clinical Pharmacology & Therapeutics* **69**, 89-95 (2001).
- 18 Comabella, M. & Khoury, S. J. in *Multiple Sclerosis: Diagnosis and Therapy* (ed Howard L. Weiner) Ch. 2, 26-55 (John Wiley& Sons, 2012).
- Bielekova, B. & Martin, R. Development of biomarkers in multiple sclerosis. *Brain* **127** (2004).
- Stankiewicz, J. M. & Khoury, S. J. in *Multiple Sclerosis: Diagnosis and Therapy* (ed Howard L. Weiner) Ch. 8, 183-212 (John Wiley & Sons, 2012).
- Zhang, J., Hutton, G. & Zang, Y. A comparison of the mechanisms of action of interferon beta and glatiramer acetate in the treatment of multiple sclerosis. *Clinical Therapeutics* **24**, 1998-2021 (2002).

- Tremlett, H., Yoshida, E. & Oger, J. Liver injury associated with the betainterferons for MS - A comparison between the three products. *Neurology* **62**, 628-631 (2004).
- Yong, V., Chabot, S., Stuve, O. & Williams, G. Interferon beta in the treatment of multiple sclerosis Mechanisms of action. *Neurology* **51**, 682-689 (1998).
- Farina, C., Weber, M., Meinl, E., Wekerle, H. & Hohlfeld, R. Glatiramer acetate in multiple sclerosis: update on potential mechanisms of action. *Lancet Neurology* **4**, 567-575 (2005).
- Kappos, L., Radue, E. W., O'Connor, P., Polman, C., Hohlfeld, R., Calabresi, P., Selmaj, K., Agoropoulou, C., Leyk, M., Zhang-Auberson, L. & Burtin, P. A Placebo-Controlled Trial of Oral Fingolimod in Relapsing Multiple Sclerosis. *New England Journal of Medicine* **362**, 387-401 (2010).
- O'Connor, P. W., Li, D., Freedman, M. S., Bar-Or, A., Rice, G. P., Confavreux, C., Paty, D. W., Stewart, J. A. & Scheyer R. A Phase II study of the safety and efficacy of teriflunomide in multiple sclerosis with relapses. *Neurology* **66**, 894-900 (2006).
- Burton, J., O'Connor, P., Hohol, M. & Beyene, J. Oral versus Intravenous Steroids for Treatment of Relapses in Multiple Sclerosis. *Cochrane Database of Systematic Reviews* **8**, No. CD006921 (2009).
- Andersson, P. & Goodkin, D. Glucocorticosteroid therapy for multiple sclerosis: A critical review. *Journal of the Neurological Sciences* **160**, 16-25 (1998).
- Gold, R., Linington, C. & Lassmann, H. Understanding pathogenesis and therapy of multiple sclerosis via animal models: 70 years of merits and culprits in experimental autoimmune encephalomyelitis research. *Brain* **129**, 1953-1971 (2006).
- Lavi, E. & Constantinescu, C. S. Experimental models of multiple sclerosis. (Springer, 2005).
- 31 Hjelmstrom, P., Juedes, A. E., Fjell, J. & Ruddle, N. H. B-cell-deficient mice develop experimental allergic encephalomyelitis with demyelination after myelin oligodendrocyte glycoprotein sensitization. *Journal of immunology* **161**, 4480-4483 (1998).
- Letourneau, S., Hernandez, L., Faris, A. N. & Spence, D. M. Evaluating the effects of estradiol on endothelial nitric oxide stimulated by erythrocyte-derived ATP

- using a microfluidic approach. *Analytical & Bioanalytical Chemistry* **379**, 3369-3375 (2010).
- Sprague, R. S., Ellsworth, M. L., Stephenson, A. H. & Lonigro, A. J. ATP: the red blood cell link to NO and local control of the pulmonary circulation. *American Journal of Physiology* **271**, H2717-2722 (1996).
- Oblak, T. D., Root, P. & Spence, D. M. Fluorescence monitoring of ATP-stimulated, endothelium-derived nitric oxide production in channels of a poly(dimethylsiloxane)-based microfluidic device. *Analytical Chemistry* **78**, 3193-3197 (2006).
- Olearczyk, J. J., Stephenson, A. H., Lonigro, A. J. & Sprague, R. S. Heterotrimeric G protein G(i) is involved in a signal transduction pathway for ATP release from erythrocytes. *American Journal of Physiology-Heart and Circulatory Physiology* **286**, H940-H945 (2004).
- Sprague, R. S., Ellsworth, M. L., Stephenson, A. H. & Lonigro, A. J. Participation of cAMP in a signal-transduction pathway relating erythrocyte deformation to ATP release. *American Journal of Physiology Cell Physiology* **281**, C1158-C1164 (2001).
- Sprague, R. S., Ellsworth, M. L., Stephenson, A. H., Kleinhenz, M. E. & Lonigro, A. J. Deformation-induced ATP release from red blood cells requires CFTR activity. American Journal of Physiology - Heart and Circulatory Physiology 44, H1726-H1732 (1998).
- Sprague, R. S., Olearczyk, J. J., Spence, D. M., Stephenson, A. H., Sprung, R. W. & Lonigro, A. J. Extracellular ATP signaling in the rabbit lung: erythrocytes as determinants of vascular resistance. *American Journal of Physiology-Heart and Circulatory Physiology* **285**, H693-H700 (2003).
- Matute, C., Torre, I., Pérez-Cerdá, F., Pérez-Samartín, A., Alberdi, E., Etxebarria, E., Arranz, A. M., Ravid, R., Rodríguez-Antigüedad, A., Sánchez-Gómez, M. & Domercq, M. P2X7 receptor blockade prevents ATP excitotoxicity in oligodendrocytes and ameliorates experimental autoimmune encephalomyelitis. *Journal of Neuroscience* **27**, 9525-9533 (2007).
- Sharp, A. J., Polak, P. E., Simonini, V., Lin, S. X., Richardson, J. C., Bongarzone, E. R. & Feinstein, D. L. P2X7 deficiency suppresses development of experimental autoimmune encephalomyelitis. *Journal of Neuroinflammation* **5**, (2008).
- Adinolfi, E., Pizzirani, C., Idzko, M., Panther, E., Norgauer, J., Di Virgilio, F. & Ferrari, D. P2X7 receptor: Death or life? *Purinergic Signal* **1**, 219-227 (2005).

- Raczkiew, J. & Leyko, W. Adenine Nucleotide Content of Erythrocytes of Multiple Sclerosis Patients. *Clinica Chimica Acta* **14**, 408-409 (1966).
- Regenold, W. T., Phatak, P., Makley, M. J., Stone, R. D. & Kling, M. A. Cerebrospinal fluid evidence of increased extra-mitochondrial glucose metabolism implicates mitochondrial dysfunction in multiple sclerosis disease progression. *Journal of the Neurological Sciences* **275**, 106-112 (2008).
- Voskuhl, R. & Gold, S. Sex-related factors in multiple sclerosis susceptibility and progression. *Nature Reviews Neurology* **8**, 255-263 (2012).
- Papenfuss, T. L., Rogers, C. J., Gienapp, I., Yurrita, M., McClain, M., Damico, N., Valo, J., Song, F. & Whitacre, C. C. Sex differences in experimental autoimmune encephalomyelitis in multiple murine strains. *Journal of Neuroimmunology* **150**, 59-69 (2004).
- 46 Confavreux, C., Vukusic, S. & Adeleine, P. Early clinical predictors and progression of irreversible disability in multiple sclerosis: an amnesic process. *Brain* **126**, 770-782 (2003).
- 47 Koch-Henriksen, N. & Sorensen, P. The changing demographic pattern of multiple sclerosis epidemiology. *Lancet Neurology* **9**, 520-532 (2010).
- Orton, S. M., Herrera, B. M., Yee, I. M., Valdar, W., Ramagopalan, S. V., Sadovnick, A. D. & Ebers, G. C. Sex ratio of multiple sclerosis in Canada: a longitudinal study. *Lancet Neurology* **5**, 932-936 (2006).
- 49 Confavreux, C., Hutchinson, M., Hours, M. M., Cortinovis-Tourniaire, P. & Moreau, T. Rate of pregnancy-related relapse in multiple sclerosis. *New England Journal of Medicine* **339**, 285-291 (1998).
- Vukusic, S., Ionescu, I., El-Etr, M., Schumacher, M., Baulieu, E. E., Cornu, C. & Confavreux, C. The Prevention of Post-Partum Relapses with Progestin and Estradiol in Multiple Sclerosis (POPART'MUS) trial: Rationale, objectives and state of advancement. *Journal of the Neurological Sciences* **286**, 114-118 (2009).
- Jansson, L., Olsson, T. & Holmdahl, R. Estrogen induces a potent suppression of experimental autoimmune encephalomyelitis and collagen-induced arthritis in mice. *Journal of Neuroimmunology* **53**, 203-207 (1994).
- Palaszynski, K. M., Liu, H., Loo, K. K. & Voskuhl, R. R. Estriol treatment ameliorates disease in males with experimental autoimmune encephalomyelitis:

- implications for multiple sclerosis. *Journal of Neuroimmunology* **149**, 84-89 (2004).
- Sicotte, N. L., Liva, S. M., Klutch, R., Pfeiffer, P., Bouvier, S., Odesa, S., Wu, T. C. & Voskuhl, R. R. Treatment of multiple sclerosis with the pregnancy hormone estriol. *Annals of Neurology* **52**, 421-428 (2002).
- 54 http://clinicaltrials.gov/ct2/show/NCT00451204 (US National Library of Medicine, 2012).
- 55 http://clinicaltrials.gov/show/NCT01466114 (US National Library of Medicine).
- Subasinghe, W. & Spence, D. M. Simultaneous determination of cell aging and ATP release from erythrocytes and its implications in type 2 diabetes. *Analytica Chimica Acta* **618**, 227-233 (2008).
- Jaubert, A. M., Mehebik-Mojaat, N., Lacasa, D., Sabourault, D., Giudicelli, Y. & Ribière, C. Nongenomic estrogen effects on nitric oxide synthase activity in rat adipocytes. *Endocrinology* **148**, 2444-2452 (2007).
- Scott, P.-A., Tremblay, A., Brochu, M. & St-Louis, J. Vasorelaxant action of 17-beta-estradiol in rat uterine arteries: Role of nitric oxide synthases and estrogen receptors. *American Journal of Physiology* **293**, H3713-H3719 (2007).
- Dore-Duffy, P., Catalanotto, F., Donaldson, J. O., Ostrom, K. M. & Testa, M. A. Zinc in Multiple-Sclerosis. *Annals of Neurology* **14**, 450-454 (1983).
- Henry, J. P., Williamson, D. M., Schiffer, R., Wagner, L., Shire, J. & Garabedian, M. Investigation of a cluster of multiple sclerosis in two elementary school cohorts. *Journal of Environmental Health* **69**, 34-38 (2007).
- Schiffer, R. B., McDermott, M. P. & Copley, C. A multiple sclerosis cluster associated with a small, north-central Illinois community. *Archives of Environmental Health* **56**, 389-395 (2001).
- Stein, E. C., Schiffer, R. B., Hall, W. J. & Young, N. Multiple sclerosis and the workplace Report of an industry-based cluster. *Neurology* **37**, 1672-1677 (1987).
- Goodin, D. S., Frohman, E. M., Garmany, G. P., Halper, J., Likosky, W. H., Lublin, F. D., Silberberg, D. H., Stuart, W. H. & van den Noort, S. Disease modifying therapies in multiple sclerosis Report of the Therapeutics and Technology Assessment Subcommittee of the American Academy of Neurology and the MS Council for Clinical Practice Guidelines. *Neurology* 58, 169-178 (2002).

- Marriott, J., Miyasaki, J., Gronseth, G. & O'Connor, P. Evidence Report: The efficacy and safety of mitoxantrone (Novantrone) in the treatment of multiple sclerosis Report of the Therapeutics and Technology Assessment Subcommittee of the American Academy of Neurology. *Neurology* **74**, 1463-1470 (2010).
- Miller, D. H., Khan, O. A., Sheremata, W. A., Blumhardt, L. D., Rice, G. P., Libonati, M. A., Willmer-Hulme, A. J., Dalton, C. M., Miszkiel, K. A. & O'Connor, P. W. A controlled trial of natalizumab for relapsing multiple sclerosis. *New England Journal of Medicine* **348**, 15-23, (2003).
- 66 Kleinschmidt-DeMasters, B. & Tyler, K. Progressive multifocal leukoencephalopathy, natalizumab, and multiple sclerosis Reply. *New England Journal of Medicine* **353**, 1745-1745 (2005).
- Sprague, R. S., Ellsworth, M. L., Stephenson, A. H., Kleinhenz, M. E. & Lonigro, A. J. Deformation-induced ATP release from red blood cells requires CFTR activity. *American Journal of Physiology* 275, H1726-1732 (1998).
- Sprague, R. S., Ellsworth, M. L., Stephenson, A. H. & Lonigro, A. J. ATP: The red blood cell link to NO and local control of the pulmonary circulation. *American Journal of Physiology-Heart and Circulatory Physiology* **271**, H2717-H2722 (1996).

# Chapter 2 – The Effect on Estrogen on Endothelial Nitric Oxide Stimulation via Red Blood Cell Derived Adenosine Triphosphate

# 2.1 Red Blood Cell Derived ATP and NO Stimulation

## 2.1.1 Red Blood Cell Glycolysis

Human blood is made up of plasma and three different cell types: leukocytes, also known as white blood cells, platelets and erythrocytes, also known as red blood cells (RBCs). RBCs are the most common type of blood cell and account for 35-45% of total blood volume. The cells are produced in bone marrow through the process of erythropoiesis and have an average life span of 120 days. Oxygen from the lungs binds to hemoglobin in the RBC and is delivered throughout the body. This was originally thought to be the sole purpose of these cells; however, in 1976, Dean et al. found that RBCs contain large pools of adenosine triphosphate (ATP). In 1992, Bergfeld et al. showed that the ATP is released from RBCs in response to hypoxia, and Ellsworth et al. later suggested this mechanism is a contributor to the regulation of vascular tone.

Stemming from these discoveries, in 1996, Sprague et al. found that RBCs release ATP in response to mechanical deformation, such as that experienced by the cells as they travel through the vascular system and are exposed to shear stress. Additionally, it was shown that the ATP released could then stimulate nitric oxide synthesis in other cell types. RBCs are anucleated cells, containing neither a nucleus nor cellular organelles.

This allows for their small disk shape. The lack of mitochondria causes the RBC to produce ATP through the process of glycolysis, making glucose the only energy source for the cell. <sup>1</sup>

The first step in glycolysis is glucose uptake into the RBC. This occurs through facilitated diffusion. Glucose is a polar molecule and therefore does not diffuse through the hydrophobic membranes of RBCs. As a result, it is necessary for carrier molecules to transport glucose across the membrane and into the cell. The glucose transport proteins (GLUT) were numbered in chronological order as they were discovered, with the major protein on RBCs being the first of the 13 discovered thus far. GLUT1 is 10-20% of the total RBC membrane protein, but is also found in astrocytes, cardiac muscle and blood-tissue barriers, such as the BBB. GLUT1 spans the plasma membrane with 12 transmembrane domains. These hydrophobic domains are  $\alpha$ -helical in nature and in total are comprised of nearly 500 amino acids.

In a healthy individual, RBCs, in total, consume around 20 grams of glucose per day, resulting in about 10% of the total glucose metabolism in the body. Once the glucose has entered the cell, 90% is metabolized through the process of glycolysis. Glycolysis literally translates to "carbohydrate splitting" and is the way in which glucose is broken down into lactate. This 10-step process can be seen in figure 2.1. Glycolysis occurs in two phases, the preparatory phase and the payoff phase. During the preparatory phase, there is an investment of two ATP molecules for every glucose molecule. In the pay off

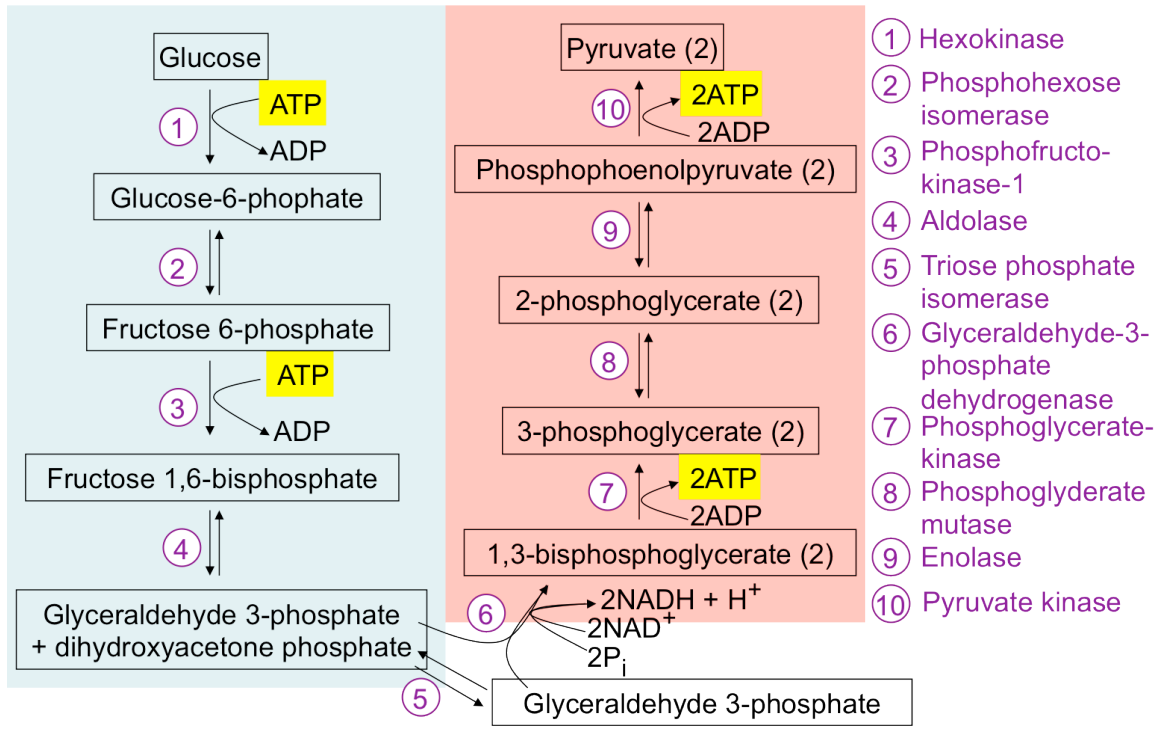


**Figure 2.1 – Glycolysis –** This process, which occurs in RBCs, is the only way for the cells to metabolize glucose. Glycolysis occurs in two phases. In the preparatory phase, on the left, two ATP molecules are consumed. During the payoff phase, on the right, four ATP molecules are produced, resulting in a net gain of two ATP molecules per glucose molecule consumed.

phase, four molecules of adenosine diphosphate (ADP) are converted to ATP, resulting in a net gain of two ATP for the breakdown of each glucose molecule. The ATP conserves some of the energy from the glucose molecule. This method of glucose metabolism occurs under anaerobic conditions, despite the RBC carrying oxygen, and results in far less ATP than glucose breakdown until aerobic conditions. <sup>9</sup>

## 2.1.2 ATP Release and NO Stimulation

As discussed previously, ATP is released from the RBC in response to several different stimuli in the local environment, including lowering of pH, hypoxia, changes in osmotic pressure, and mechanical deformation. ATP is believed to cross the plasma membrane with the aid of an ion channel, assumed to be the cystic fibrosis transmembrane conductance regulator (CFTR). It has not yet been determined if ATP is released through the channel of CFTR itself, or if CFTR is regulating another ion channel in the cell membrane through which ATP is released. Abnormal ATP release from RBCs has been associated with cystic fibrosis, pulmonary hypertension, diabetes, and multiple sclerosis (MS).

While at Wayne State University, the Spence group preformed a small scale study using RBCs from 18 MS patients and 11 controls. The RBC ATP release was measured using a capillary-based flow system described previously.  $^{17}$  Briefly, as RBCs pass through 50  $\mu$ m

internal diameter tubing, they experience shear stress and release ATP, which reacts with a luciferin/luciferase mixture. The resulting chemiluminescence from the samples and standards can be measured with a photomultiplier tube (PMT), and the amount of ATP can be quantified. The resulting data are shown in figure 2.2. The average release of ATP from the RBCs of MS patients was  $375 \pm 51$  nM, almost three times higher than the  $138 \pm 21$  nM from the RBCs of healthy controls.  $^{16}$ 

When released from the RBC, ATP can stimulate nitric oxide (NO) production in endothelial cells through binding to the purinergic receptor, P2Y. This stimulates endothelial nitric oxide synthase (eNOS) which converts L-arginine to L-citrulline with NO as the byproduct, as shown in figure 2.3. In 1987, NO was identified as the endothelium-derived relaxing factor and it is now well established as a determinant in the control of vasodilation. Because of this, NO production is often thought of as a positive event. However, in many autoimmune disease, NO is believed to contribute to immune response and tissue destruction. NO and its metabolites, such as nitrite and nitrate, are found at higher than normal levels in the cerebral spinal fluid (CSF) and urine of MS patients, as compared to healthy controls. In addition, NO and its metabolites are found in the lesions formed from the characteristic demyelination.

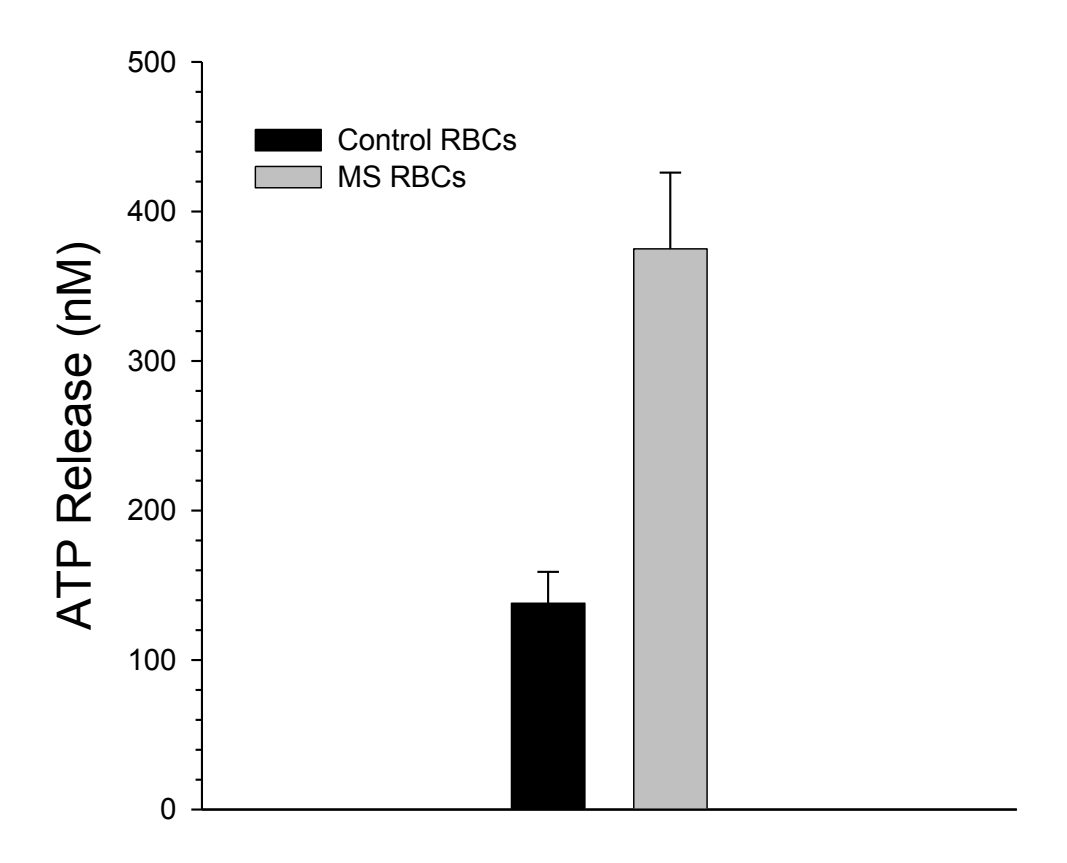
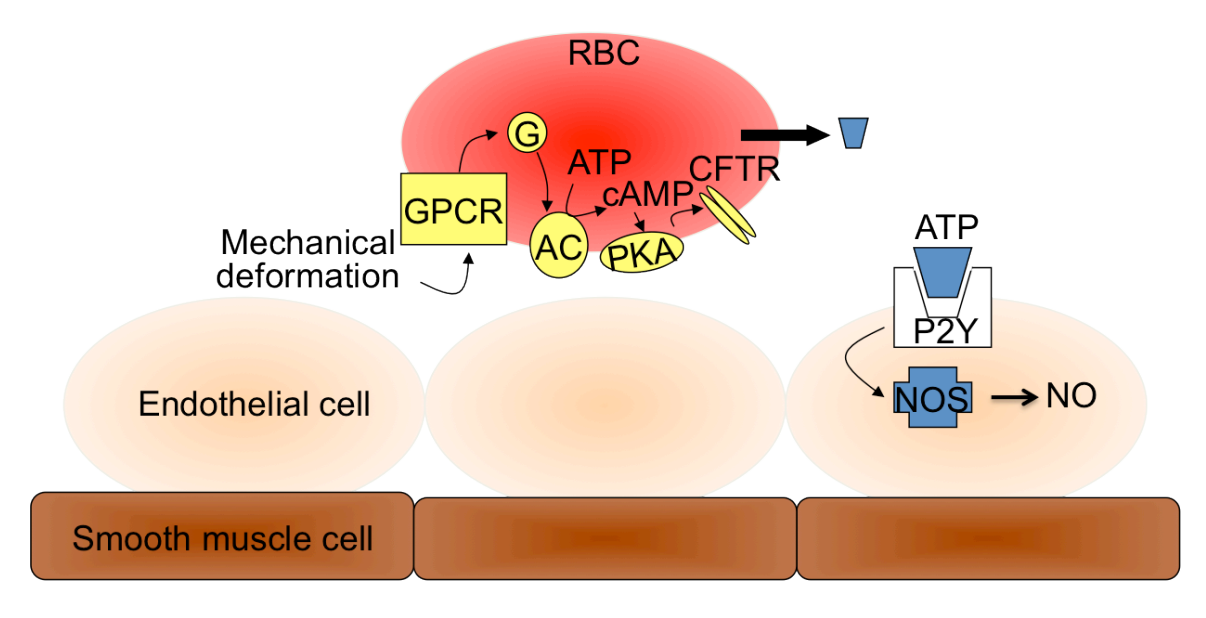


Figure 2.2 – ATP Release From MS RBCs (From Letourneau et al.)  $^{16}$  – ATP release was measured from RBCs subjected to flow. The average ATP release from the healthy RBCs was 138  $\pm$  21 nM. An increase to 375  $\pm$  51 nM was seen for RBCs obtained from MS patients. The error is reported as standard error of the mean for 11 controls and 18 MS samples. The values are statistically different at a value of p < 0.001.



**Figure 2.3 – Proposed mechanism of ATP release from RBCs and subsequent NO production –** It has been proposed that G-protein coupled receptor (GPCR), <sup>49</sup> cyclic adenosine monophosphate (cAMP), <sup>50</sup> and the cystic fibrosis transmembrane conductance regulation (CFTR) protein <sup>11</sup> are all required for the release of ATP by mechanical deformation, though how the ATP leaves the cell remains in question. In this proposed mechanism, the binding of ATP to the P2Y receptor on the endothelial cell results in the activation NOS and the production of NO. <sup>5</sup>

# 2.1.3 Estrogen and MS

As previously discussed, reports in the literature have described a decrease in relapses during the second and third trimesters of pregnancy in women with MS.<sup>21</sup> This decrease in relapse rate correlates with the increase of estrogens in pregnant women. The mechanism for this is not completely understood, but as a result of these observations, estrogens, specifically estradiol and estriol have been extensively studied. Voskuhl et al. have reported that increased estrogen levels in murine EAE, due to either pregnancy or subcutaneous estrogen-containing pellets, have a protective effect on the severity of the EAE.<sup>22</sup> These results are intriguing in light of reports that substances such as estradiol and estriol have the ability to stimulate NO production in certain cell types. It would seem that an increase in estrogens would be detrimental, rather than protective, to MS-like complications.<sup>23,24</sup>

Additionally, as mentioned above, CFTR is necessary for the deformation-induced release of ATP from the RBC. There have been several reports of the ability of estrogen to inhibit CFTR in various cell types, including pancreatic epithelial cells<sup>25</sup> and lung epithelial cells. Singh et al. showed that estrogens interact directly with CFTR and the acute effect of this interaction is the inhibition of CFTR. Since CFTR is required for ATP release, RBC-derived ATP is elevated in MS patients, and estrogen has been shown to

ameliorate the disease, it is hypothesized that estrogen may have its effect on MS through this inhibition pathway.

In order to investigate the interaction between the RBCs, releasing ATP, and endothelial cells, producing NO, these cells needed to be in close contact to each other as they would be in vivo. A microfluidic device has previously been used in the Spence group for this purpose. This device uses microfluidic channels, through which RBCs are pumped, below a membrane that has endothelial cells immobilized on it. Having the RBCs able to interact with an endothelial layer, as it would in vivo, enables for more accurate measurements that take into account cell-to-cell communication. This device will be further described in the next section.

#### 2.2 Microfluidic Devices

Microfluidics is the science of systems able to process and manipulate low volumes of fluids using devices having channels with dimensions of up to hundreds micrometers. Many devices handle volumes in the low microliter range, with some able to handle volumes as low as the single digit nanoliter range. The field of microfluidics began with applications in analysis, however, over time, the technology has spread to areas of synthesis, biophysics and fuel cells as well. <sup>29</sup>

Although microfluidic devices can be fabricated from many different materials, one of the most common and well established for rapid prototyping is poly(dimethylsiloxane) (PDMS). Through the use of soft lithography, these devices can be made quickly and repeatedly through the use of a master. Typically made through photolithography, a master has raised features that will create recesses in the PDMS for the channels. The use of a variety of software programs to create the mask for the master results in the ability to make microfluidic devices in a variety of different configurations. To create the master, photoresist is coated onto a silicon wafer. The mask is then placed over the wafer and exposed to ultraviolet light. The photoresist polymerizes, creating the features. The excess is then washed away. This process is shown in figure 2.4.

In 2007, Genes et al. reported an in vitro model of the microvasculature using a PDMS microfluidic device. By using a two-layer device separated by a membrane, RBCs flowing in a channel on the bottom can be in contact with endothelial cells cultured on the membrane in wells of the top layer. This enables the device to closely mimic the in vivo conditions where cells are able to affect one another through cell signaling methods. Although devices enabling cell-to-cell communication had been previously reported, 32,33 this device was the first to incorporate separated components of blood circulation on a microfluidic device. This device enabled ATP released from RBCs as a result of shear stress to interact with the endothelial cells immobilized above the membrane. The resultant NO production can be measured with a fluorescent probe. By increasing the ATP release from RBCs by using a chemical stimulus, the NO production was seen to increase as well. Therefore, the device was able to show production of NO,

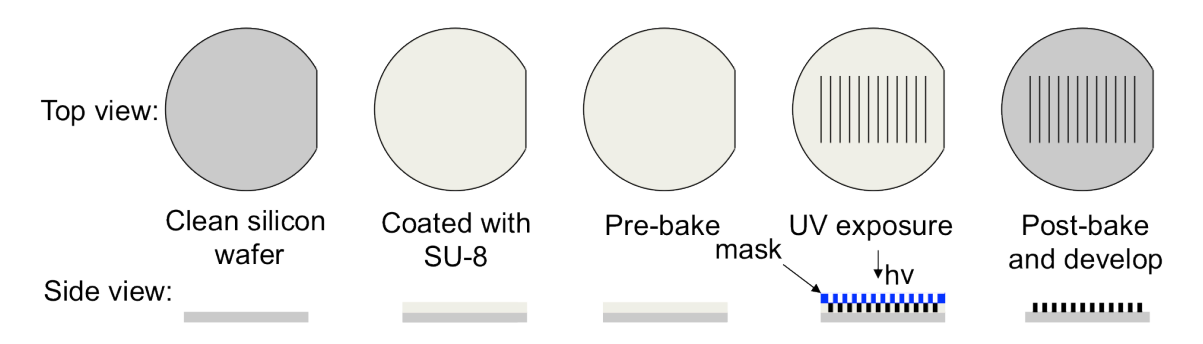


**Figure 2.4 – Photolithography –** In order to perform rapid fabrication using PDMS, a reusable master is needed. This can be prepared through photolithography. In this process, a clean silicon wafer is coated with SU-8 photoresist. After pre-baking the wafer, a mask is placed over the photoresist with the desired features. The wafer is then exposed to UV light. After a post-bake, the wafer is soaked in developer to removed unpolymerized photoresist. The result is a wafer with raised features that can be repeatedly used as a mold for PDMS.

in this case, occurs as a result of cell-to-cell communication between the RBCs and endothelial cells.  $^{28,34}$ 

Knowing that the RBCs of MS patients release an increased amount of ATP, and the protective influence of estrogens in the disease, the first step in this research was to investigate the effect of estrogens, specifically estradiol and estriol, on the ATP release from healthy RBCs. The previously mentioned microfluidic device was used to determine the effect of the estrogen-induced decrease in RBC-derived ATP on the NO production of endothelial cells. The proximity of the RBCs to the endothelial cells in a microvascular mimic is key to the understanding the effects of estrogen in the blood stream.

# 2.3 Experimental

#### 2.3.1 Collection and Purification of Rabbit RBCs

RBCs used in these studies were obtained from male New Zealand white rabbits between 2.0 and 2.5 kg. The rabbits were anesthetized using ketamine, 8 mg/kg, intramuscular, and xylazine, 1 mg/kg, intramuscular, followed by pentobarbital sodium, 15 mg/kg, intravenously. A cannula was placed in the rabbit trachea for ventilation with room air at a rate of 20 breaths/min. Prior to exsanguination, 500 units of heparin were administered using a catheter placed in the carotid artery. The exsanguination was performed through the same catheter, and approximately 80 mL of whole blood were collected from each rabbit.

The whole blood was then centrifuged at 500g for 10 min at 25°C, and the plasma was removed and retained for other experimentation. The remaining RBCs were then resuspended and washed three times in physiological salt solution (PSS) containing, in mM, 4.7 KCl (Fisher Scientific, Fair Lawn, NJ), 2.0 CaCl<sub>2</sub> (Fisher Scientific), 140.5 NaCl (Columbus Chemical Industries, Columbus, WI), 12 MgSO<sub>4</sub> (Fisher Scientific), 21.0 tris(hydroxymethylaminomethane) (Invitrogen, Carlsbad, CA), 5.6 glucose (Sigma, St. Louis, MO), and 5% bovine serum solution (Sigma) at a final pH of 7.4, adjusted with hydrochloric acid. The hematocrit of the RBCs was measured using a CritSpin© analyzer.

# 2.3.2 Preparation of Regents

Purified water with 18.2 M $\Omega$  resistance was used for all experiments. Estradiol (Sigma) stock solutions were prepared by first dissolving 2 mg in 1 mL dimethyl sulfoxide (DMSO) (EMD Chemicals, Gibbstown, NJ) to make a 7.3 mM solution. Two 1:100 serial dilutions were performed in PSS to make 73  $\mu$ M and 0.73  $\mu$ M solutions. Estriol (Sigma) stock solutions were prepared by dissolving 2 mg in 1 mL DMSO, resulting in a 3.5 mM solution. Two 1:100 serial dilutions were performed in PSS to make 35  $\mu$ M and 0.35  $\mu$ M solutions. Zn<sup>2+</sup> stock solution was prepared by dissolving Zinc (II) chloride (Jade Scientific, Canton, MI) in purified water and diluted to 400 nM.

Crude C-peptide (Genscript, Piscataway, NJ) was purified using reverse-phase high performance liquid chromatography (RP-HPLC) and dried. The purified C-peptide was dissolved in purified water and diluted to a 400 nM working solution. When Zn<sup>2+</sup>, bound to C-peptide was added to samples, the Zn<sup>2+</sup> and C-peptide solutions were mixed in water before the addition of any other components or buffers. 5 mL samples of 7% RBCs were prepared with varying concentrations of estradiol or estriol by adding the hormone to the appropriate volume of PSS, followed by the addition of the RBCs for a 30 minute incubation. For some experiments, these samples were then centrifuged at 500g at 25°C for 5 minutes, then washed twice by resuspending the cells in PSS and centrifuging at 500g at 25°C for 3 minutes.

# 2.3.3 Preparation of Microfluidic Device

The microfluidic device used in these studies was comprised of two individual PDMS (Dow Corning, Midland, MI) layers sealed around a 0.6 micrometer pore size polycarbonate membrane (GE Water & Process Technologies, Feasterville-Trevose, PA). The channel layer was fabricated by pouring a degassed, 20:1 mixture of Sylguard 184 PDMS elastomer and curing agent onto a silicon master with 12 raised-feature channels wth the dimensions: 200  $\mu$ m wide x 100  $\mu$ m deep x 3 cm long. After curing for 12 min at 75°C, a degassed 5:1 mixture of the elastomer and curing agent was poured over the master. This layer was then cured an additional 12 min at 75°C prior to removal from the master. Inlet holes were punched at one end of each channel using a 20 gauge luer

stub adapter, and the PDMS at other end of the channel was cut and removed to allow for the exit of waste.

A degassed 20:1 PDMS mixture was also poured onto an unpatterned silicon wafer and cured for 15 minutes at 75°C. This can be seen in figure 2.5. After removal from the wafer, 36 holes were punched in a 3 x 12 array, using an  $1/8^{th}$  inch hole punch. The layers were then aligned around the polycarbonate membrane, with three wells lined up on each channel, and cured for an additional 45 min to seal them. This design is similar to that described previously by the Spence group  $^{34,35}$  and can be seen in figure 2.6.

## 2.3.4 Chemiluminesce Detection of ATP Release from RBCs

In these experiments, the ATP release from the RBC was measured in a static system. This was performed using the chemiluminescent reaction of ATP and a solution of luciferin/luciferase was prepared by dissolving 2 mg luciferin (Gold Biotechology, St. Louis, MO) in 5 mL DDW, and transferring this to a vial containing 100 mg of luciferase (Sigma). To detect the chemiluminescence, a photomultiplier tube (PMT) was used as a transducer. 100  $\mu$ L of sample, prepared as described in section 2.4.2, and 100  $\mu$ L of luciferin/luciferase were pipetted into a plastic cuvette and mixed. The measurement was taken 15 seconds after the addition of the luciferin/luciferase mixture by placing the cuvette over the PMT. All samples were measured in triplicate. A diagram of this set up can be seen in figure 2.7.

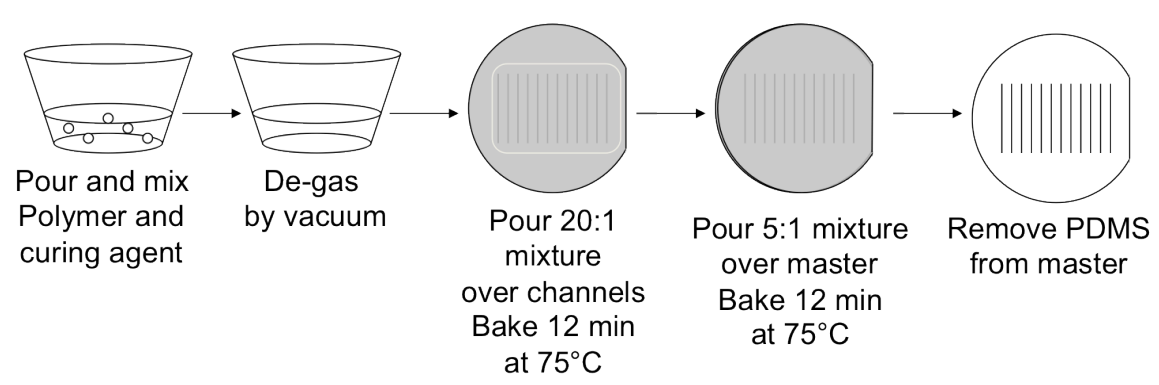


**Figure 2.5 – Soft Lithography –** Through this process, the layers of the microfluidic device were created. The polymer and curing agent were mixed in 20:1 and 5:1 ratios in separate plastic cups and degassed by vacuum. The 20:1 mixture was poured over the channel portion of the master and baked at 75°C for 12 minutes. The 5:1 mixture was then pour wafer the entire master and bake for another 12 minutes at the same temperature. The PDMS was then removed from the master. The second layer of the microfluidic device was prepared using the same steps with an unpatterned silicon master.

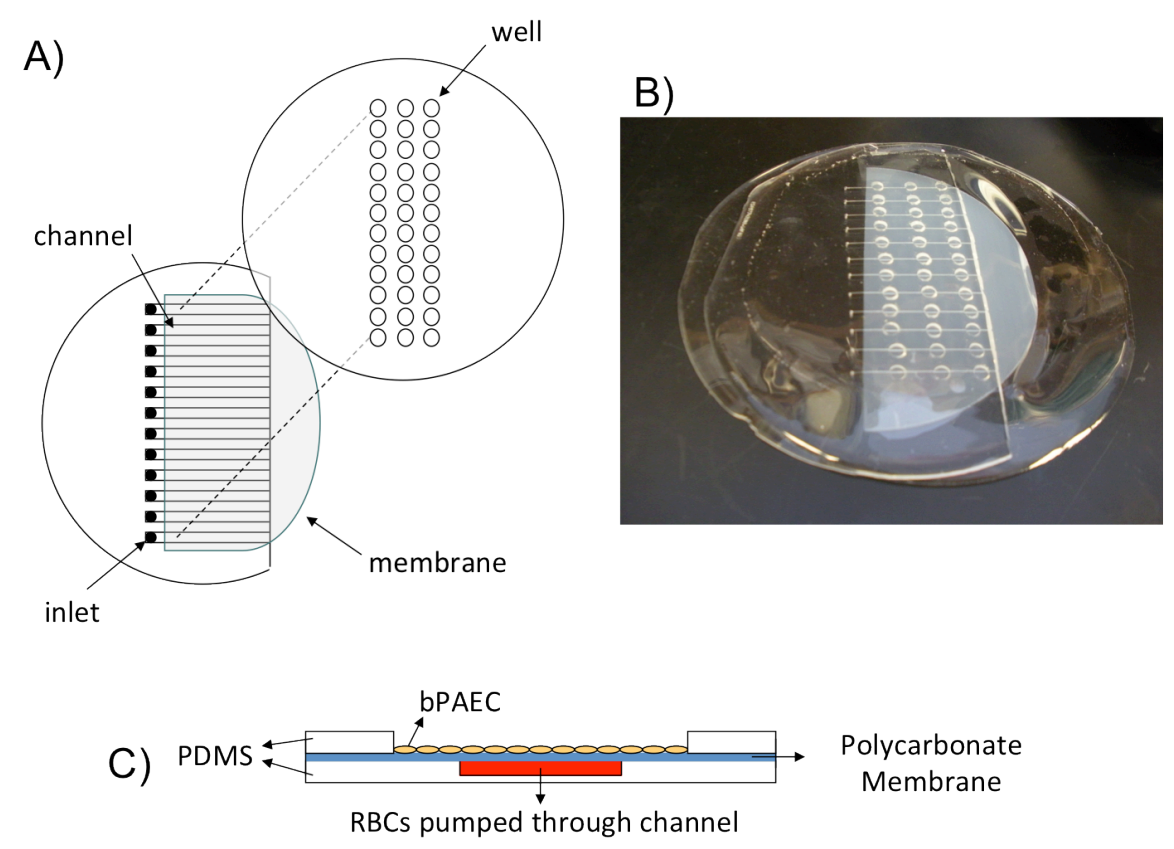


**Figure 2.6 – Microfluidic Device –** A) The microfluidic device layers are diagramed. A polycarbonate membrane separated the bottom layer, containing the channels, and the top layer, patterned with wells. B) A photograph of a completed microfluidic device. C) A diagram of the cross section of a well. bPAECs are adhered to the membrane in the well. The porous membrane separates the bPAECs from the channel through which the RBCs are pumped.

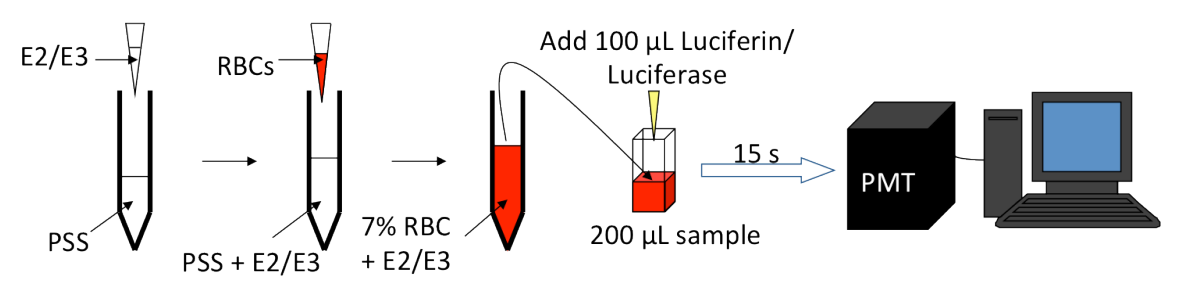


Figure 2.7 – Measurement of ATP Release – Estradiol (E2) or estriol (E3) were added to PSS, immediately followed by RBCs to make a 7% RBC solution. When  $\text{Zn}^{2+}$  bound to C-peptide was used, the  $\text{Zn}^{2+}$  and C-peptide were added to the vial first and allowed to incubate for 2-3 minutes before the addition of PSS. After a two hour incubation, a 200  $\mu\text{L}$  sample was transferred into a cuvette. 100  $\mu\text{L}$  of the luciferin/luciferase solution was added and the cuvette was lightly shaken. The cuvette was placed in a dark box over a PMT and at 15 seconds the luminescence was measured.

# 2.3.5 Adhering Cells to a Microfluidic Device and Fluorescence Determination of NO

For the purpose of these studies, a confluent layer of bovine pulmonary artery endothelial cells (bPAECs) was required in each well. For the cells to adhere to the membrane,  $10~\mu L$  of a  $100~\mu g/m L$  fibronectin solution were pipetted into each well and allowed to dry. The device was then sterilized under ultraviolet (UV) light for 15 minutes. The bPAECs were harvested from a T-75 culture flask containing a confluent monolayer of these cells. The flask was first washed with 7 mL of 4-(2-hydroxyethyl)-1-piperazineethanesufonic acid (HEPES) solution for 2 minutes. After aspirating off the HEPES, 5 mL of a trypsin solution was allowed to incubate on the cells for 2 minutes, followed by the addition of 9 mL of trypsin neutralizing solution. Pipetting and scraping were used to fully remove the cells from the surface of the flask so they were suspended in solution.

The suspension was removed to a 15 mL centrifuge tube and was then centrifuged at 1500g for 5 minutes at 25°C. Following centrifugation, the supernatant was aspirated off, leaving a pellet of cells that were then resuspended in 1 mL of endothelial growth media to ensure a homogeneous solution. Next, 10  $\mu$ L of this solution were then pipetted into each well of the device and allowed to incubate for 1 hour at 37°C and 5%  $CO_2$ . After incubation, the media solution on the cells was changed by carefully removing the solution and adding 10  $\mu$ L of media to each well. This was followed by an additional 2 hour incubation.

After the cells had become immobilized on the membrane, the media was removed from the wells and replaced with 10  $\mu$ L of a 5 mM L-arginine solution in Hank's Balanced Salt Solution (HBSS) to ensure sufficient substrate for the production of NO. Following a 30 minute incubation at 37°C and 5% CO<sub>2</sub>, the solution was removed and replaced with 10  $\mu$ L of 100  $\mu$ M 4-amino-5-methylamino-2',7'-difluorofluoroescien diacetate (DAF-FM DA), a fluorescent probe for detecting intracellular NO, pictured in figure 2.8, for a 30 minute incubation. DAF-FM DA is able to cross the cell membrane. Once inside, esterases transform the probe to DAF-FM, which loses its cell permeability. The DAF-FM then fluorescently reacts with NO. From the time DAF-FM DA was introduced to the cells until the end of the experiment, the device was kept in the dark. After the 30 minute incubation, the excess DAF-FM DA solution was removed and replaced with 10  $\mu$ L of HBSS per well.

In these experiments, the device was used to monitor the intracellular NO production of the bPAECs as ATP diffused through the membrane from samples with RBCs and varying concentrations of estradiol that were pumped at the rate of 0.1  $\mu$ L/min through the underlying microfluidic channels for 30 minutes. Each well was imaged immediately before and after using an Olympus MVX fluorescence macroscope, fitted with a mercury-arc lamp and a fluoroscien isothiocyanate (FITC) filter cube having excitation and emission wavelengths of 470 and 525 nm, respectively. This set up can be seen in figure 2.9. The pixel intensity of each well was measured and background subtracted.

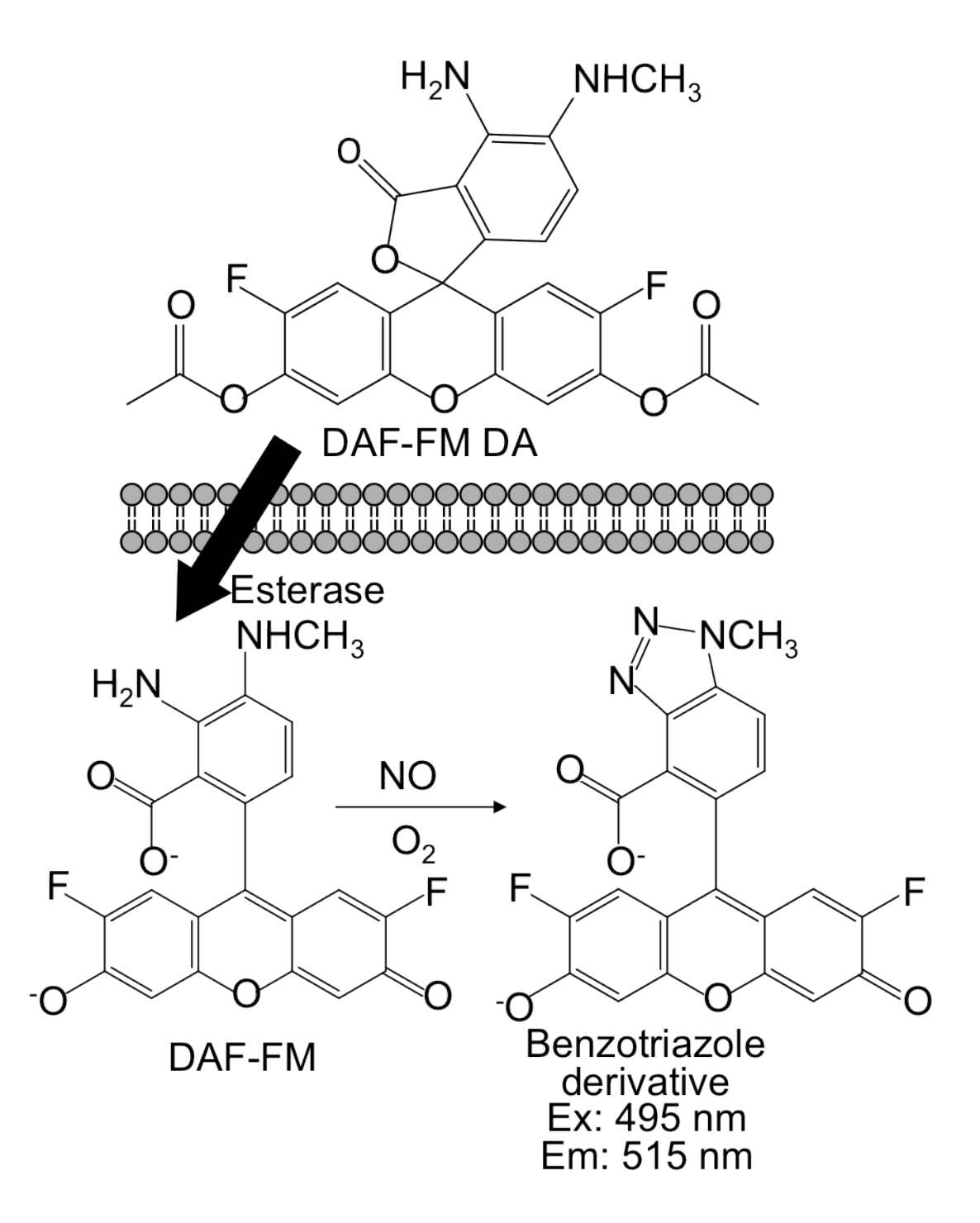


**Figure 2.8 – DAF-FM DA –** DAF-FM DA crosses the cell membrane. Esterases then transform the probe to DAF-FM, which loses its cell permeability. The DAF-FM then reacts with NO, producing a benzotiazol derivative that is fluorescent at the above excitation and emission.



Figure 2.9 – Flowing RBCs Through the Device – Pictured above, the RBC solutions were pumped at the rate of 0.1  $\mu$ L/min through the underlying microfluidic channels for 30 minutes. Each well was imaged before and after using an Olympus MVX fluorescence macroscope, fitted with a mercury-arc lamp and a fluoroscien isothiocyanate (FITC) filter cube having excitation and emission wavelengths of 470 and 525 nm, respectively.

This value is directly dependent on the concentration of NO produced within the bPAECs.

## 2.4 Results

In figure 2.10, it is shown that there is a significant decrease in the ATP release from RBCs when the cells are pre-incubated with estradiol. When compared to RBCs with the absence of estradiol, the RBC-derived ATP for RBCs treated with 0.5  $\mu$ M estradiol was reduced to 76  $\pm$  7% the value of the untreated cells. The amount of ATP released decreased with increasing concentration of estradiol; for the 1  $\mu$ M and 1.5  $\mu$ M estradiol solutions, the RBC-derived ATP was reduced to 62  $\pm$  7% and 56  $\pm$  6%, respectively.

Accounting for the number of RBCs in the sample, the levels of estradiol originally tested were higher than those found in vivo. Adjusting for the reduced concentration of RBCs in the samples, the average equivalent levels of estradiol in healthy women are 32 pM normally and up to 90 nM in late pregnancy. For estriol these values are 7 nM normally, 30 nM in early pregnancy, and up to 0.5  $\mu$ M in late pregnancy. With this knowledge, the study was repeated using lower concentrations of estradiol and also with estriol.

As shown in figure 2.11, incubating the RBCs with 30 nM estradiol reduces the chemiluminescence in response to ATP release to 74  $\pm$  4%, which is statistically equivalent to the decrease in the amount of chemiluminescence seen with 0.5  $\mu$ M

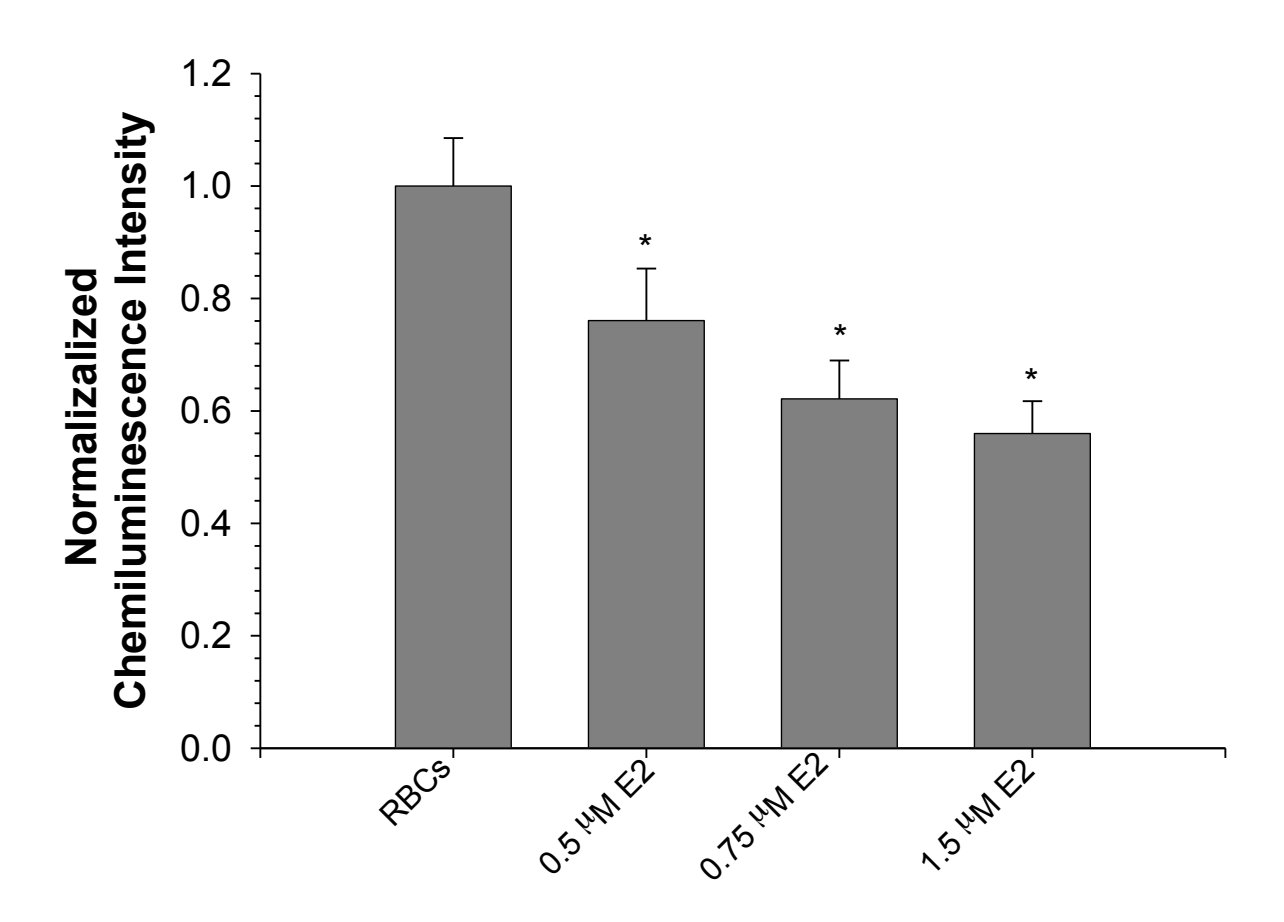


**Figure 2.10 – The Effect of Estradiol on RBC ATP Release** - Compared to RBCs with the absence of estradiol, the RBC-derived ATP for RBCs treated with 0.5  $\mu$ M estradiol was reduced to 76 ± 7% of the value of the untreated cells. The amount of ATP released decreased with increasing concentration of estradiol; for the 1  $\mu$ M and 1.5  $\mu$ M estradiol solutions, the RBC-derived ATP was reduced to 62 ± 7% and 56 ± 6%, respectively. Error is shown as standard deviation for N = 4 rabbits. The asterisks denote a statistically significant difference from untreated RBCs at p < 0.05.

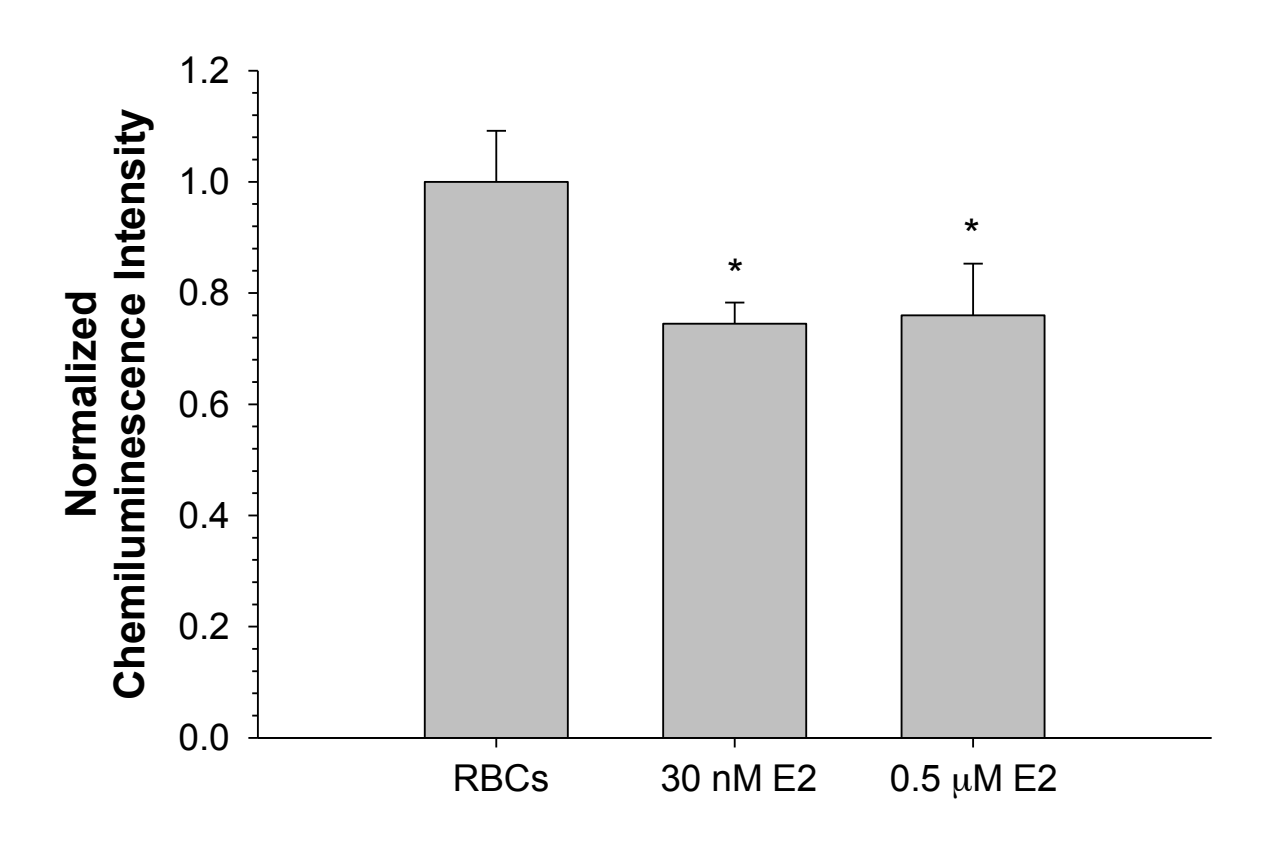
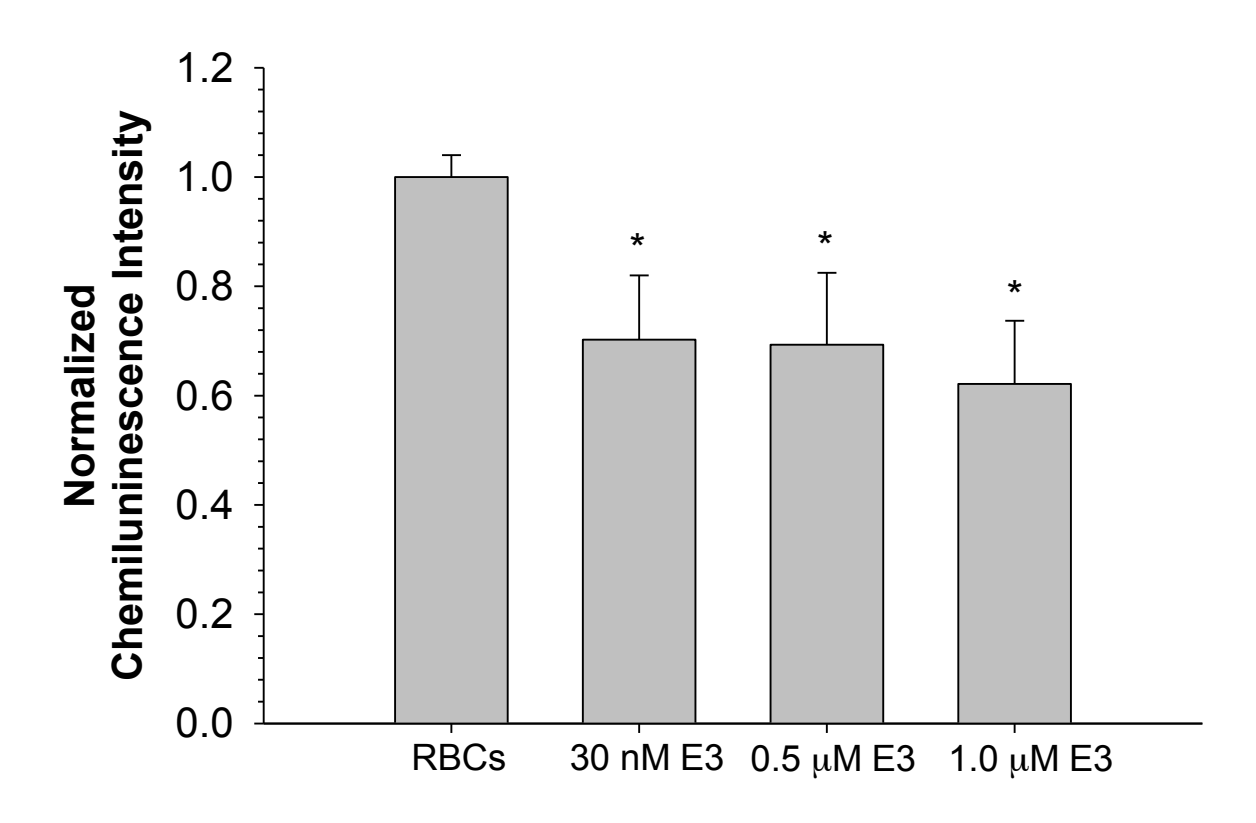


Figure 2.11 – Estradiol (E2) Decreases ATP Release at Physiological Concentrations – incubating the RBCs with 30 nM estradiol reduces the chemiluminescence in response to ATP release to 74  $\pm$  4%, which is statistically equivalent to the decrease in the amount of chemiluminescence seen with 0.5  $\mu M$  estradiol, but at a more physiologically relevant concentration of the hormone. Error is standard deviation for N = 4 rabbits. The asterisk denotes the decrease, as compared to untreated RBCs, is statistically significant at p < 0.02.

estradiol, but at a more physiologically relevant concentration of the hormone. In figure 2.12, the data shows the ability of estriol to decrease the chemiluminescence due to ATP release to an even greater degree at physiologically relevant concentrations. 30 nM of estriol reduced the ATP release to 70  $\pm$  11% of that of RBCs alone. The RBCs incubated with 0.5  $\mu$ M and 1.0  $\mu$ M had their ATP release reduced to 69  $\pm$  13% and 62  $\pm$  11%, respectively.

Additionally,  $Zn^{2+}$  bound to C-peptide was used as a stimulus of ATP release. The estrogens were then used to attenuate this increase. In figure 2.13, the increase in ATP release as a result of the Zn<sup>2+</sup> bound to C-peptide and the subsequent decrease with the addition of both estrogens can be seen. It is important to note that the concentrations of estradiol and estriol are not the same looking at the bars left to right in an attempt to compare the data sets. In both sets of results the Zn<sup>2+</sup> bound to C-peptide resulted in an increase in chemiluminescence to more than double that seen for RBCs alone. For estradiol, a significant decrease in the ATP release, as compared to RBCs and 10 nM  $^{2+}$  bound to C-peptide, to 76 ± 15% and 61 ± 24% was observed for the 0.75  $\mu$ M and 1.5 µM samples, respectively. For estriol, the statistically significant decreases were seen for the 0.5  $\mu$ M and 1.0  $\mu$ M samples. They were decreased to 73  $\pm$  17% and 61  $\pm$ 13%, respectively. While neither hormone was able to bring the ATP release back to basal levels, it is significant that decreases were seen, even when an ATP stimulus was present.



**Figure 2.12 – The Effect of Estriol (E3) on RBC-derived ATP –** Estriol decreases the chemiluminescence due to ATP at physiologically relevant concentrations. 30 nM of estriol reduced the ATP release to  $70 \pm 11\%$  of that of RBCs alone. The RBCs incubated with 0.5  $\mu$ M and 1.0  $\mu$ M had their ATP release reduced to 69  $\pm$  13% and 62  $\pm$  11%, respectively. Error is shown as standard deviation for N = 4 rabbits, and the asterisk denotes a statistically significant decrease at p < 0.05

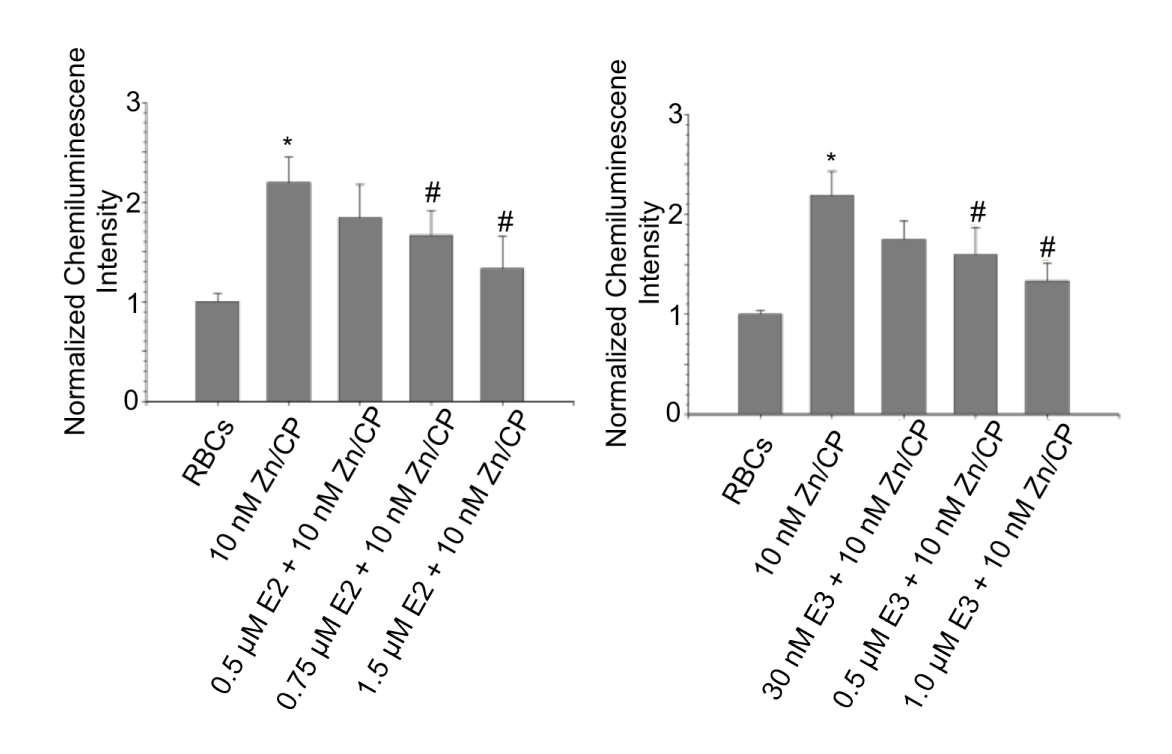
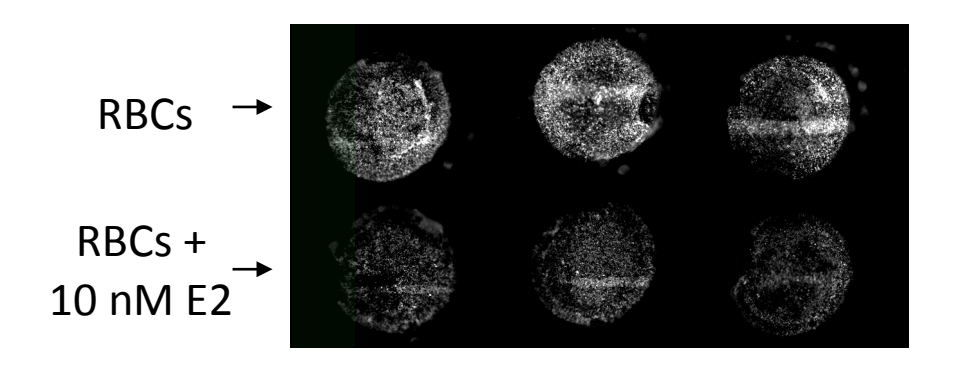


Figure 2.13 – The Effect of Estrogen on ATP Release Stimulated By  $Zn^{2+}$  bound to C-peptide – Note that the concentrations of estradiol and estriol are not same looking at the bars left to right in an attempt to compare the data sets. In both sets of results the  $Zn^{2+}$  bound to C-peptide resulted in an increase in chemiluminescence to more than double that seen for RBCs alone. For estradiol (E2), a significant decrease in the ATP release, as compared to RBCs and 10 nM  $Zn^{2+}$ -C-peptide, to  $76 \pm 15\%$  and  $61 \pm 24\%$  was observed for the 0.75  $\mu$ M and 1.5  $\mu$ M samples, respectively. For estriol (E3), the statistically significant decreases were seen for the 0.5  $\mu$ M and 1.0  $\mu$ M samples. They were decreased to  $73 \pm 17\%$  and  $61 \pm 13\%$ , respectively. Error is standard deviation for N = 5 rabbits for estradiol and N = 4 rabbits for estriol. The asterisk denotes the significant increase of ATP release with 10 nM  $Zn^{2+}$  bound to C-peptide at p < 0.0005. The pound sign denotes a decrease as compared to 10 nM  $Zn^{2+}$ -C-peptide at p < 0.05.

In the cell-containing microfluidic device, RBC solutions containing RBCs with and without C-peptide and estradiol are pumped through the channels in the bottom layer of PDMS. As previously discussed, the flow-induced shear stress results in ATP release from the RBCs. This ATP interacts with the bPAECs lining the wells in the top layer of PDMS resulting in NO production that can be measured using DAF-FM DA as a fluorescent probe. Photos were taken with a charge-coupled device (CCD) camera, such as those seen in figure 2.14. The pixel intensity of these images was measured and then background subtracted to account for differences in the number of bPAECs. The numbers were then normalized.

The data in figure 2.15 shows the normalized, background subtracted emission. As shown, the emission decreases with RBCs incubated in buffer containing estradiol in as low a concentration as 10 nM. In this case, the estradiol is actually able to reduce the NO production to  $43 \pm 0.1\%$  of that of untreated RBCs. However, the emission intensity then begins to increase with again with increasing concentration of estradiol, although a significant increase in emission, in comparison to RBCs alone, is not measured until the estradiol levels reach approximately 2  $\mu$ M, a value that is physiologically high, even during pregnancy. At this value, the fluorescence intensity is  $13 \pm 4\%$  higher than the untreated RBCs. The next highest concentration,  $1.5~\mu$ M, is not significantly different from the untreated RBCs.

Estrogen has been found to have nongenomic effects, increasing NO production from eNOS in endothelial cells. <sup>38</sup> Because of this, a second set of data was collected. Before



**Figure 2.14 – Fluorescence Intensity Images –** DAF-FM reacts with NO in bPAECs resulting in fluorescence than can be photographed with a CCD camera and the pixel intensity can be measured. As seen above, when RBCs incubated with estradiol (E2) are flowed beneath wells containing bPAECs, the NO production of those cells is lower. This is due to the decrease in RBC-derived ATP, which stimulates NO production in bPAECs.

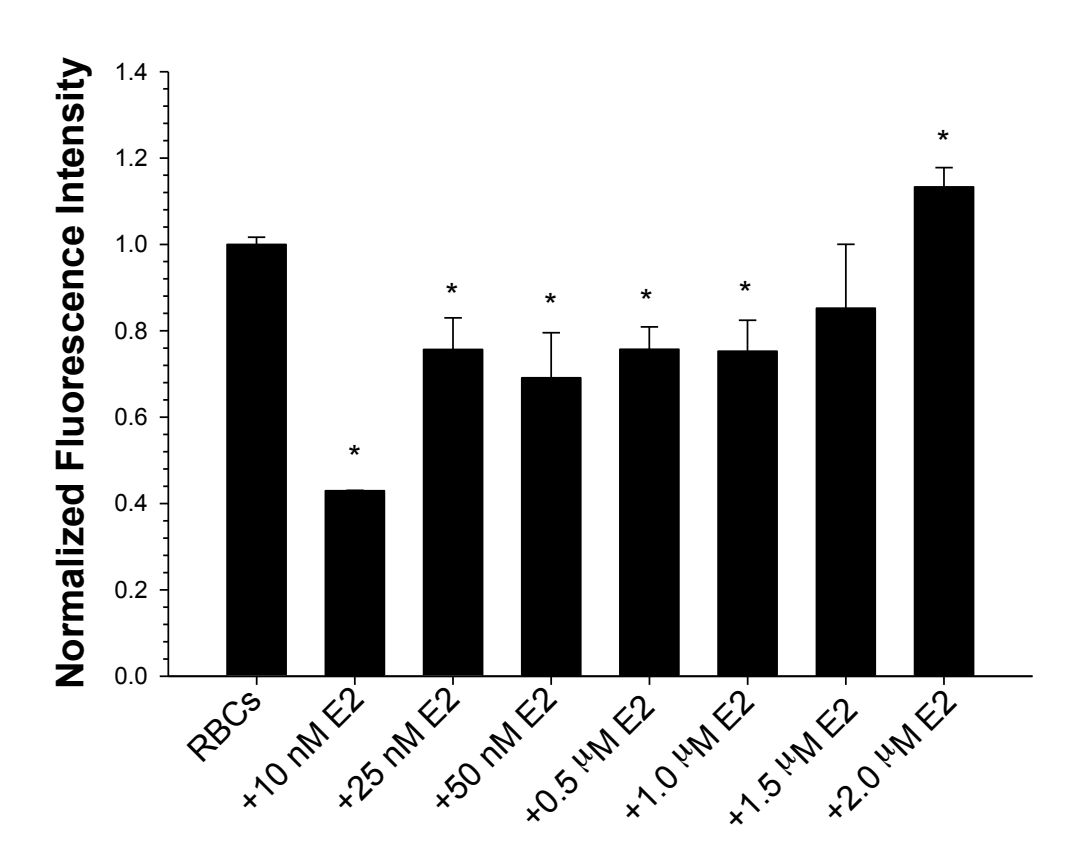


**Figure 2.15 – Normalize Fluorescence Intensity** – The data in this figure shows the normalized, background subtracted emission. As shown, the emission decreases with RBCs incubated in buffer containing estradiol. In this case, the estradiol is actually able to reduce the NO production to  $43 \pm 0.1\%$  of that of untreated RBCs. The emission intensity begins to increase with again with increasing concentration of estradiol, although a significant increase in emission, in comparison to RBCs alone, is not measure until the estradiol levels reach approximately 2  $\mu$ M. At this value, the fluorescence intensity is  $13 \pm 4\%$  higher than the untreated RBCs. The next highest concentration, 1.5  $\mu$ M, is not significantly different from the untreated RBCs. Error is shown as standard deviation for N = 4 rabbits and the asterisk denotes a significant difference from untreated RBCs at p < 0.05.

the RBC samples were pumped through the microfluidic device, they were centrifuged and washed twice with PSS and then resuspended in PSS. As shown in figure 2.16, there was a marked decrease in NO production in the bPAECs, denoted by the decrease in fluorescent emission, when the RBCs were pre-incubated with estradiol. However, the RBCs that have been washed to remove excess estradiol do not result in a statistically significant increase in NO production. The black bars represent the data from the previous figure and are included for comparison. The grey bars show that the estradiol is able to decrease the NO production in bPAECs, as detected by fluorescence intensity. This decrease is the result of a decrease in RBC-derived ATP. The NO production was decreased to  $59 \pm 7\%$  with 10 nM estradiol and this decrease remained statistically constant across the range of concentrations, with the largest decrease, down to  $51 \pm 5\%$  that of the NO production of bPAECs exposed to untreated RBCs, seen at  $2.0 \,\mu\text{M}$ .

Together, these data show that estrogens have the ability to inhibit the release of ATP from RBCs, as well as the subsequent ATP-stimulated NO production in endothelial cells. The estrogens were also able to attenuate the ATP release from RBCs that were previously incubated with Zn<sup>2+</sup>-activated C-peptide, an ATP stimulus. Knowing that patients with MS have higher than normal levels of ATP released from their RBCs, and the ameliorating effects of estrogens on the disease, these data could provide a missing link.

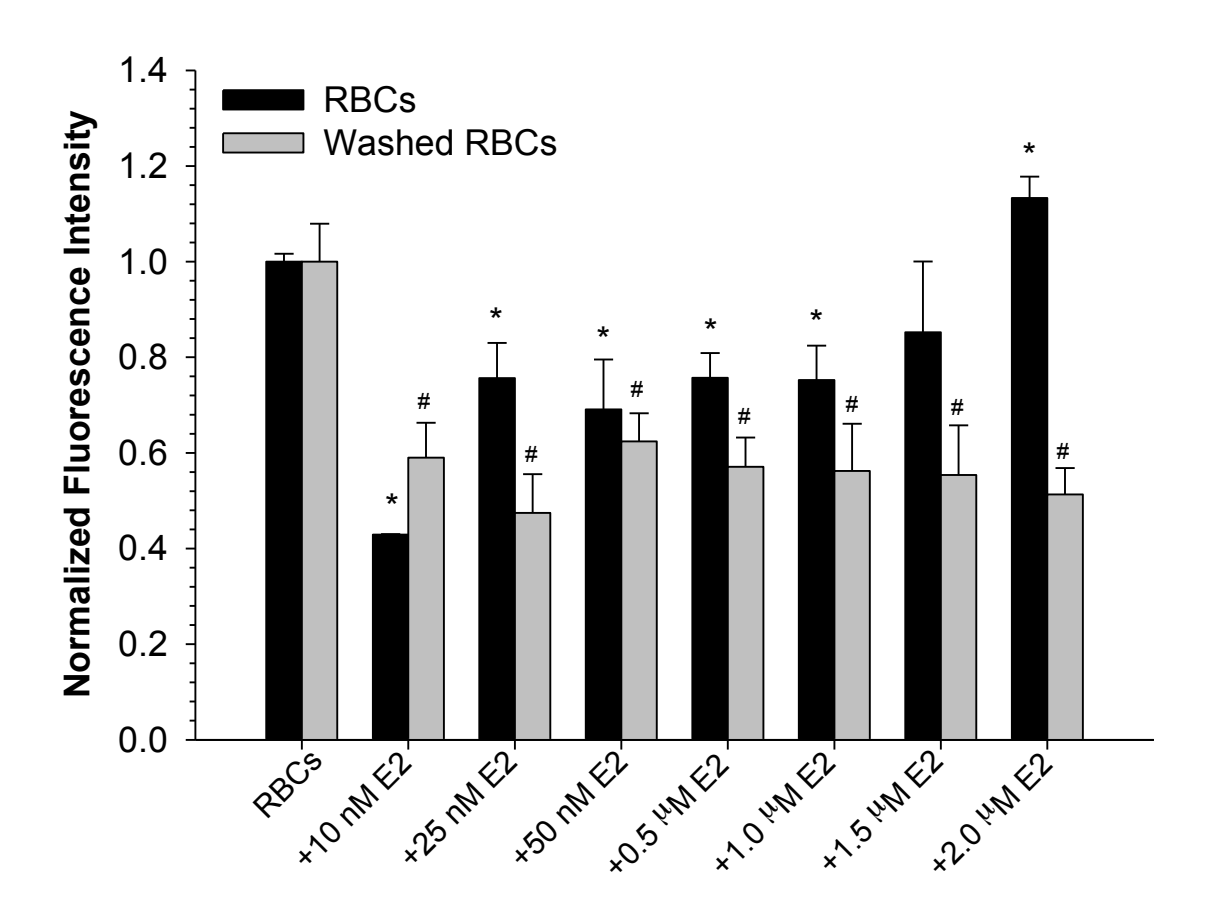


**Figure 2.16 – Washed and Unwashed RBCs** – There was a marked decrease in NO production in the bPAECs, denoted by the decrease in fluorescent emission, when the RBCs are pre-incubated with estradiol. RBCs that have been washed to remove excess estradiol do not result in a statistically significant increase in NO production. The black bars represent the data from the previous figure and are included for comparison. The grey bars show that the estradiol is able to decrease the NO production in bPAECs, as detected by fluorescence intensity. The NO production was decreased to  $59 \pm 7\%$  with 10 nM estradiol, and this decrease remained statistically constant across the range of concentrations, down to  $51 \pm 5\%$  that of the NO production of bPAECs exposed to untreated RBCs, seen at  $2.0 \, \mu\text{M}$ . Error is reported as standard deviation for N = 4 rabbits. The asterisks denote a significant difference from untreated RBCs (black bar) and the pound sounds denote a significant decrease from untreated RBCs (grey bar).

#### 2.5 Discussion

The interaction of RBCs and the availability of NO has proved to be difficult to discern and is heavily debated. There are multiple mechanisms by which the RBCs are involved in the physiological control of NO levels. RBCs have the ability to act as a scavenger and NO carrier through the use of nitroso-thiol groups, releasing this NO in response to stimulus, such as hypoxia. 

39-41 It has also been suggested that the hemoglobin in the RBC reduces nitrate to NO as a nitrite reductase to contribute to NO levels in the blood stream. 

Like the research presented here, others have demonstrated that RBC-derived ATP contributes to an increase in NO levels in response to various stimuli. 

5,28,43,44 ATP has been shown to increase NO production in a variety of cells types, including endothelial cells.

The results in figures 2.10, 2.11, and 2.12, show that estrogens have the ability to decrease the ATP release from RBCs. This was anticipated based on previous studies showing that DHEA attenuated RBC-derived ATP, <sup>45</sup> and the inhibitory effect of estrogen on CFTR that has been seen in other cell types. <sup>25-27</sup> In addition to lowering the levels of ATP release from RBC at a basal state, the estrogens were also effective at decreasing the release from RBCs that had been previously treated with Zn<sup>2+</sup> bound to C-peptide, stimulus of ATP release. As previously mentioned, estrogens have been shown to have a protective effect against EAE, the animal model of MS, and as well as on the disease in

humans. 22,46-48 Coupled with the data from the preliminary study showing that patients with MS have higher than normal amounts of ATP released from their RBCs as compared to healthy controls, 16 this may provide a link to the protective effects of estrogens on MS. Additionally, the increase in ATP release from the RBCs of MS patients may contribute to the increased levels of NO and its products nitrate and nitrite.

RBCs pumped through the channel of the microfluidic device release ATP as a result of shear stress that stimulates the production of NO in bPAECs. The data shown in figure 2.16 shows this NO production was decreased when the RBCs were incubated with estrogens prior to their being flowed through the system. Increasing concentrations of estrogens subsequently increase the amount of NO produced by bBAECs. When the RBCs were washed with PSS to remove excess estrogen prior to their introduction to the microfluidic device, the NO production did not increase significantly with increasing concentrations of estrogens in the RBCs.

Interestingly, other reports have suggested that estrogens stimulate NO production in cells. <sup>23,24</sup> If this was the only factor, it would seem that estrogens should not have the protective effect that is seem in both EAE and MS. The original data, seen in figure 2.15, shows that this may be the case, though the NO production did not increase back to the levels seen in RBCs alone until a superphysiological amount of estradiol was incubated with the RBCs. Previous studies investing the effect of estrogens on NO production in endothelial cells have applied these hormones directly to the cells. <sup>38</sup> This discrepancy in

data shows how important it is to have and use devices that enable cell-to-cell communication. Applied alone to endothelial cells estrogens have different effects than they do in vivo. The interaction of chemicals with blood components and their subsequent effects on other cells is an important part of understanding what is truly happening. Here, the microfluidic device was able to discern between endothelium-derived NO due directly to estradiol and the inhibition of NO production as a result of the decrease in RBC-derived ATP caused by the hormone.

In conclusion, ATP is released from RBCs in response to shear stress. This ATP stimulates NO production in the endothelial cells lining the blood vessels. RBCs from patients with MS release three times the amount of ATP then RBCs from healthy controls. This increase in ATP release may be over-stimulating the NO production in the endothelial cells, and NO is known to be toxic to the BBB. It has been shown that high levels of estrogens, due to pregnancy or drug therapy, can ameliorate MS. The findings here may provide an explanation for the therapeutic effects of estrogens. If estrogens are able to attenuate the excessive release of ATP from the RBCs of MS patients, the amount of NO production would also be decreased, potentially leading to less damage from the disease.

**REFERENCES** 

#### REFERENCES

- Harmening, D. *Clinical Hematology and Fundamentals of Hemostasis*. (F. A. Davis Co, 2009).
- Dean, B. & Perrett, D. Studies on adenine and adenosine metabolims by intact human erythrocytes using high-performance liquid chromatography. *Biochimica Et Biophysica Acta* **437**, 1-15 (1976).
- Bergfeld, G. & Forrester, T. Release of ATP from human erythrocytes in response to a brief period of mypoxia and hypercapnia. *Cardiovascular Research* **26**, 40-47 (1992).
- 4 Ellsworth, M. L., Forrester, T., Ellis, C. G. & Dietrich, H. H. The erythrocyte as a regulator of vascular tone. *American Journal of Physiology-Heart and Circulatory Physiology* **269**, H2155-H2161 (1995).
- Sprague, R. S., Ellsworth, M. L., Stephenson, A. H. & Lonigro, A. J. ATP: The red blood cell link to NO and local control of the pulmonary circulation. *American Journal of Physiology-Heart and Circulatory Physiology* **271**, H2717-H2722 (1996).
- Olson, A. & Pessin, J. Structure, function, and regulation of the mammalian facilitative glucose transporter gene family. *Annual Review of Nutrition* **16**, 235-256 (1996).
- 7 Kasahara, M. & Hinkle, P. Reconsitution and purification of D-glucose transporter from human erythrocytes. *Journal of Biological Chemistry* **252**, 7384-7390 (1977).
- 8 Carruthers, A., DeZutter, J., Ganguly, A. & Devaskar, S. Will the original glucose transporter isoform please stand up! *American Journal of Physiology-Endocrinology and Metabolism* **297**, E836-E848 (2009).
- 9 van Wijk, R. & van Solinge, W. The energy-less red blood cell is lost: erythrocyte enzyme abnormalities of glycolysis. *Blood* **106**, 4034-4042 (2005).
- Light, D., Capes, T., Gronau, R. & Adler, M. Extracellular ATP stimulates volume decrease in Necturus red blood cells. *American Journal of Physiology-Cell Physiology* **277**, C480-C491 (1999).

- Sprague, R. S., Ellsworth, M. L., Stephenson, A. H., Kleinhenz, M. E. & Lonigro, A. J. Deformation-induced ATP release from red blood cells requires CFTR activity. *American Journal of Physiology* **275**, H1726-1732 (1998).
- Reisin, I. L., Prat, A. G., Abraham, E. H., Amara, J. F., Gregory, R. J., Ausiello, D. A. & Cantiello, H. F. The cystic fibrosis transmembrane conductance regulator is a duel ATP and chloride channel. *Journal of Biological Chemistry* **269**, 20584-20591 (1994).
- Sprague, R., Stephenson, A., Ellsworth, M., Keller, C. & Lonigro, A. Impaired release of ATP from red blood cells of humans with primary pulmonary hypertension. *Experimental Biology and Medicine* **226**, 434-439 (2001).
- Sprague, R., Stephenson, A., Bowles, E., Stumpf, M., Ricketts, G. & Lonigro, A. Expression of the heterotrimeric G protein Gi and ATP release are impaired in erythrocytes of humans with diabetes mellitus. *Hypoxia and Exercise* **588**, 207-216 (2006).
- Subasinghe, W. & Spence, D. M. Simultaneous determination of cell aging and ATP release from erythrocytes and its implications in type 2 diabetes. *Analytica Chimica Acta* **618**, 227-233 (2008).
- Letourneau, S., Hernandez, L., Faris, A. N. & Spence, D. M. Evaluating the effects of estradiol on endothelial nitric oxide stimulated by erythrocyte-derived ATP using a microfluidic approach. *Analytical and Bioanalytical Chemistry* **397**, 3369-3375 (2010).
- Sprung, R., Sprague, R. & Spence, D. Determination of ATP release from erythrocytes using microbore tubing as a model of resistance vessels in vivo. Analytical Chemistry **74**, 2274-2278 (2002).
- Palmer, R. M., Ferrige, A. G. & Moncada, S. Nitric oxide release accounts for the biological activity of endothelium-derived relaxing factor. *Nature* **327**, 524-526 (1987).
- 19 Kolb, H. & Kolb-Bachofen, V. Nitric oxide in autoimmune disease: cytotoxic or regulatory mediator? *Immunology Today* **19**, 556-561 (1998).
- Giovannoni, G., Heales, S. J., Land, J. M. & Thompson, E. J. The potential role of nitric oxide in multiple sclerosis. *Multiple Sclerosis* **4**, 212-216 (1998).
- 21 Confavreux, C. et al. Rate of pregnancy-related relapse in multiple sclerosis. New England Journal of Medicine **339**, 285-291 (1998).

- Voskuhl, R. R., Kim, S., Liva, S. M., Dalal, M. A. & Verity, M. A. Estriol ameliorates autoimmune demyelinating disease Implications for multiple sclerosis. *Neurology* **52**, 1230-1238 (1999).
- Jaubert, A. M., Mehebik-Mojaat, N., Lacasa, D., Sabourault, D., Giudicelli, Y. & Ribière C. Nongenomic estrogen effects on nitric oxide synthase activity in rat adipocytes. *Endocrinology* **148**, 2444-2452 (2007).
- Scott, P. A., Tremblay, A., Brochu, M. & St-Louis, J. Vasorelaxant action of 17β-estradiol in rat uterine arteries: role of nitric oxide synthases and estrogen receptors. *American Journal of Physiology* **293**, H3713-H3719 (2007).
- Sweezey, N., Gauthier, C., Gagnon, S., Ferretti, E. & Kopelman, H. Progesterone and estradiol inhibit CFTR-mediated ion transport by pancreatic epithelial cells. American Journal of Physiology-Gastrointestinal and Liver Physiology **271**, G747-G754 (1996).
- Sweezey, N., Ghibu, F. & Gagnon, S. Sex hormones regulate CFTR in developing fetal rat lung epithelial cells. *American Journal of Physiology-Lung Cellular and Molecular Physiology* **272**, L844-L851 (1997).
- Singh, A. K., Schultz, B. D., Katzenellenbogen, J. A., Price, E. M., Bridges, R. J. & Bradbury, N. A. Estrogen inhibition of cystic fibrosis transmembrane conductance regulator-mediated chloride secretion. *Journal of Pharmacology and Experimental Therapeutics* **295**, 195-204 (2000).
- Genes, L. I., N, V. T., Hulvey, M. K., Martin, R. S. & Spence, D. M. Addressing a vascular endothelium array with blood components using underlying microfluidic channels. *Lab on a Chip* **7**, 1256-1259 (2007).
- Whitesides, G. M. The origins and the future of microfluidics. *Nature* **442**, 368-373 (2006).
- Duffy, D., McDonald, J., Schueller, O. & Whitesides, G. Rapid prototyping of microfluidic systems in poly(dimethylsiloxane). *Analytical Chemistry* **70**, 4974-4984 (1998).
- Zhang, J., Tan, K. L., Hong, G. D., Yang, L. J. & Gong, H. Q. Polymerization optimization of SU-8 photoresist and its applications in microfluidic systems and MEMS. *Journal of Micromechanics and Microengineering* **11**, 20-26 (2001).
- Lee, P., Hung, P., Shaw, R., Jan, L. & Lee, L. Microfluidic application-specific integrated device for monitoring direct cell-cell communication via gap junctions between individual cell pairs. *Applied Physics Letters* **86**, No. 223902 (2005).

- Abhyankar, V., Lokuta, M., Huttenlocher, A. & Beebe, D. Characterization of a membrane-based gradient generator for use in cell-signaling studies. *Lab on a Chip* **6**, 389-393 (2006).
- Tolan, N. V., Genes, L. I., Subasinghe, W., Raththagala, M. & Spence, D. M. Personalized Metabolic Assessment of Erythrocytes Using Microfluidic Delivery to an Array of Luminescent Wells. *Analytical Chemistry* **81**, 3102-3108 (2009).
- Genes, L. I., Tolan, N. V., Hulvey, M. K., Martin, R. S. & Spence, D. M. Addressing a vascular endothelium array with blood components using underlying microfluidic channels. *Lab on a Chip* **7**, 1256-1259 (2007).
- Peck, J. D., Hulka, B. S., Poole, C., Savitz, D. A., Baird, D., Richardson & B. E. Steroid hormone levels during pregnancy and incidence of maternal breast cancer. *Cancer Epidemiology Biomarkers & Prevention* **11**, 361-368 (2002).
- 37 Sicotte, N. L., Liva, S. M., Klutch, R., Pfeiffer, P., Bouvier, S., Odesa, S., Wu, T. C. & Voskuhl, R. R. Treatment of multiple sclerosis with the pregnancy hormone estriol. *Annals of Neurology* **52**, 421-428 (2002).
- 38 Chambliss, K. L. & Shaul, P. W. Estrogen modulation of endothelial nitric oxide synthase. *Endocrinology Reviews* **23**, 665-686 (2002).
- Jia, L., Bonaventura, C., Bonaventura, J. & Stamler, J. S. S-Nitrosohemoglobin: a dynamic activity of blood involved in vascular control. *Nature* 380, 221-226 (1996).
- Stamler, J. S., Jia, L., Eu, J. P., McMahon, T. J., Demchenko, I. T., Bonaventura, J., Gernert, K. & Piantadosi, C. A. Blood flow regulation by S-nitrosohemoglobin in the physiological oxygen gradient. *Science* **276**, 2034-2037 (1997).
- 41 Gow, A. J. & Stamler, J. S. Reactions between nitric oxide and haemoglobin under physiological conditions. *Nature* **391**, 169-173 (1998).
- Minneci, P. C., Deans, K. J., Shiva, S., Zhi, H., Banks, S. M., Kern, S., Natanson, C., Solomon, S. B. & Gladwin, M. T. Nitrite reductase activity of hemoglobin as a systemic nitric oxide generator mechanism to detoxify plasma hemoglobin produced during hemolysis. *American Journal of Physiology* 295, H743-H754 (2008).
- Sprague, R. S., Olearczyk, J. J., Spence, D. M., Stephenson, A. H., Sprung, R. W. & Lonigro, A. J. Extracellular ATP signaling in the rabbit lung: erythrocytes as

- determinants of vascular resistance. *American Journal of Physiology-Heart and Circulatory Physiology* **285**, H693-H700 (2003).
- Spence, D. M., Torrence, N. J., Kovarik, M. L. & Martin, R. S. Amperometric determination of nitric oxide derived from pulmonary artery endothelial cells immobilized in a microchip channel. *Analyst* **129**, 995-1000 (2004).
- Spence, D. M. & Subasinghe, W. Simultaneous determination of cell aging and ATP release from erythrocytes and its implications in type 2 diabetes. *Analytica Chimica Acta* **618**, 227-233 (2008).
- Jansson, L., Olsson, T. & Holmdahl, R. Estrogen Induces a Potent Suppression of Experimental Autoimmune Encephalomyelitis and Collagen-Induced Arthritis in Mice. *Journal of Neuroimmunology* **53**, 203-207 (1994).
- Palaszynski, K. M., Liu, H., Loo, K. K. & Voskuhl, R. R. Estriol treatment ameliorates disease in males with experimental autoimmune encephalomyelitis: implications for multiple sclerosis. *Journal of Neuroimmunology* **149**, 84-89 (2004).
- 48 Gold, S. M. & Voskuhl, R. R. Estrogen treatment in multiple sclerosis. *Journal of the Neurological Sciences* **286**, 99-103 (2009).
- Olearczyk, J. J., Stephenson, A. H., Lonigro, A. J. & Sprague, R. S. Heterotrimeric G protein G(i) is involved in a signal transduction pathway for ATP release from erythrocytes. *American Journal of Physiology-Heart and Circulatory Physiology* **286**, H940-H945 (2004).
- Sprague, R. S., Ellsworth, M. L., Stephenson, A. H. & Lonigro, A. J. Participation of cAMP in a signal-transduction pathway relating erythrocyte deformation to ATP release. *American Journal of Physiology-Cell Physiology* **281**, C1158-C1164 (2001).

# Chapter 3 – Delivery of Zn<sup>2+</sup> to the Red Blood Cell by C-peptide

#### 3.1 Diabetes Mellitus

#### 3.1.1 Classifications

The term diabetes mellitus, commonly referred to as diabetes, denotes a group of diseases that result in hyperglycemia through various mechanisms. Hyperglycemia is the term used to describe higher than normal amounts of glucose in the blood plasma. Normally, the blood glucose level falls between 70 and 100 mg/dL, or 3.8 and 5.5 mM. A fasting glucose level above 100 mg/dL is referred to as impaired fasting glucose, and can be a precursor to diabetes. If this level is greater than or equal to 126 mg/dL, or 7 mM, a patient is diagnosed as diabetic. Another way to diagnose diabetes is by using a glucose tolerance test, where 75 grams of glucose are ingested and the blood is tested 2 hours later. If the glucose level is at or above 200 mg/dL, or 11 mM, the diagnosis is confirmed. 2

There are four recognized classifications of diabetes: type 1 and type 2 diabetes, gestational diabetes, and other. The other types of diabetes include any mechanism by which the pancreas becomes damaged or destroyed and hormonal imbalances or genetic defects that alter insulin levels. Type 1 and type 2 diabetes differ by the role of insulin. Type 1 diabetes, also known as juvenile diabetes, is characterized by impaired insulin secretion. Insulin is the hormone necessary for regulating glucose uptake into

cells. As a result, if its secretion is impaired, elevated levels of blood glucose are seen. In type 1 diabetes, the beta cells in the pancreas, responsible for the secretion of insulin are destroyed in an autoimmune process. The cause of this destruction has not been fully elucidated, but is believed to have both environmental and genetic factors and may be caused, in part, by a virus. 3,4

Patients with type 2 diabetes make up about 90% of the diabetic population in the United States.<sup>5</sup> Type 2 diabetics are insulin resistant, meaning that, as compared to normal controls, the same amount of insulin will not be as effective in stimulating glucose uptake and utilization.<sup>6</sup> This resistance eventually causes the beta cells of the pancreas to decrease and eventually stop the production of insulin, although the reason for this is unclear.<sup>7</sup> Type 2 diabetes often develops later in life, generally after the age of 40. While there is a genetic component to the disease susceptibility, environmental factors also play a role. Being overweight or obese has been significantly associated with several aspects of poor health status, including type 2 diabetes. When compared to adults of normal weight, adults who are considered to be extremely obese, with a body mass index of 40 or above, are more than 7 times more likely to have diabetes.<sup>8</sup>

Gestational diabetes mellitus (GDM) is defined as glucose intolerance first recognized during pregnancy. Approximately 4% of pregnancies are complicated by GDM by increasing the risk of high blood pressure and preeclampsia, as well as higher birth

weights and an increase in the number of caesarian delivery. Woman who experience GDM are at a higher risk for the development of type 2 diabetes, with approximately 70% developing the disease within ten years of delivery. 5

The hyperglycemia seen in diabetic patients is associated with a large variety of diabetic The major cause of disability and death in diabetic patients is complications. artherosclerosis, a vascular disease where substances, such as fat and cholesterol, build up on the walls of arteries, forming plaques, which harden them. <sup>10</sup> Some of these plaques are vulnerable, meaning the fibrous cap that separates the plaque from the lining of the artery is likely to rupture. When this happens, a cascade of events occurs and a thrombus is formed that can be lodged in an artery, slowing or preventing blood flow to tissue in a certain area of the body. 11 Additionally, hyperglycemia has been shown to increase oxidative stress in endothelial cells and as a result, nitric oxide (NO) release is decreased. Furthermore, it has been shown that the red blood cells (RBCs) of patients with type 2 diabetes release significantly less adenosine triphosphate (ATP) than those of healthy controls. 12,13 ATP is a known stimulator of NO, as described in chapter 1. NO is a known vasodilator, so the lack of ATP release and vessel dilation add to the vascular complications seen in the disease. <sup>14</sup>

#### 3.1.2 Complications

Complications in the microvascular system lead to a variety of other common diabetic complications, such as retinopathy, neuropathy and nephropathy. Retinopathy is damage to the retina that can cause blindness. In fact, 12% of all new cases of blindness each year are the result of diabetic retinopathy. One of the major factors involved in the decline of retinal function is vascular damage leading to a decrease in blood flow to the area of the eye, which results in a lack of oxygen to the tissue. As a result, there is an increase in neovascular growth factors to promote the proliferation of new blood vessels. While it would seem that new blood vessels would ameliorate the issues, the vessel growth results in an accumulation of fibrous tissue that can distort the retina or even detach the retina, leading to vision loss. 16

In addition to an increase risk of blindness, nearly all patients with diabetes have at least some level of neuropathy, or damage to the nervous system. Although it can occur at any time, the prevalence of neuropathy positively correlates to disease duration and severity, <sup>17</sup> with a more rapid progression seen in patients with type 1 diabetes. <sup>18</sup> Like retinopathy, it is believed that neuropathy is caused in part by abnormal blood flow in the neurovasculature, in addition to direct damage due to hyperglycemia. <sup>19</sup> The previously mentioned decrease in endothelial NO production may also play a role in diabetic neuropathy. The lack of vasodilation may make the occlusion of vessels an even more common event. Neuropathy leads to the loss of sensation and weakness in

the extremities and when seen in combination with other microvascular issues, is the leading cause of non-traumatic amputations in the United States.<sup>20</sup>

Nephropathy affects the kidneys of both type 1 and type 2 diabetic patients, with the former being at a great risk for total renal failure. 21 Combining the types, diabetes is the most common cause of end-stage kidney failure in the United States. <sup>22</sup> In the kidney, there are systems of ducts, tubules, and arteries that make up nephrons. These systems are responsible for filtering the blood and removing the waste as urine. In each nephron there is a capillary referred to as the glomerulus in which the blood pressure is very high. This pressure forces water and solutes out of the blood into the surrounding glomerular capsule, where it is further processed and eventually becomes urine to be excreted from the body. In diabetic patients, nephropathy is characterized by glomerular hyperfiltration. Because of the difficulties in the microvasculature, the pressure in the glomerulus is increased and as a result, albumin, a common protein in blood plasma, is forced out into the urine, causing a condition called albuminuria.  $^{23}$ Additionally, in the early stages of nephropathy, the glomerular basement membranes surrounding the glomerulus, become thicker as a result of upregulated production of the macromolecules, such as collagen, that make up this membrane. The thickening of the glomerular basement membranes also leads to glomerular dysfunction and, eventually, to kidney failure. 24,25

It is important to note that retinopathy, neuropathy, and nephropathy are all at least partially caused by the issues that develop in the microvasculature of diabetic patients. While none of these conditions can be avoided completely, the risk can be lessened by controlling blood sugar through diet, insulin injections, and other pharmaceuticals, depending on the type and severity of the diabetes. <sup>26</sup> If the complications in the microvasculature can be minimized the quality of life for diabetic patients would be much improved.

## 3.2 Insulin and C-Peptide

### 3.2.1 Discovery of Insulin

It is believed that diabetes was first described by the ancient Egyptians over 3000 years ago. In the first century, Aretaeus, a physician in ancient Greece noted that people afflicted with the disease urinated often and therefore used the Greek word diabetes, meaning siphon, to refer to it. Patients of the time did not live long, as there was no treatment. The term diabetes mellitus was not used until the 17<sup>th</sup> century when a British physician, Thomas Willis, noted a sweet taste in the urine of patients with diabetes. The method of diagnosis became tasting the urine of a patient; if it was sweet, the diagnosis was diabetes mellitus. This remained unchanged until the 20<sup>th</sup> century. Despite physician efforts, there remained no treatment for diabetic patients until the early 20<sup>th</sup> century when physicians began using starvation diets, limiting food

to less than 500 calories per day, to combat the disease. Unfortunately, this treatment left patients in very weakened states and it was not uncommon for them to die of starvation. <sup>27,28</sup>

In 1889 Oskar Minkowski and Joseph von Mering removed the pancreas from a dog and the animal developed severe diabetes. Through further testing, they determined that the pancreas produces a substance that is involved in the regulation of blood glucose levels. In 1921, Fredrick Banting and Charles Best discovered that by injecting a crude extract of the pancreas into a dog that had previously had his pancreas removed they were able to ameliorate the symptoms. The dog became healthier and his blood glucose levels dropped. The following year, after Bertram Collip had purified insulin out of the extract, the team had their first human subject. A 14-year-old boy, near death, was successfully treated and lived for an additional 13 years.<sup>28</sup>

#### 3.2.2 Insulin and C-Peptide Production and Release

Since the work of Banting and Best, much has been learned about insulin and its production in the pancreas. The pancreas contains the islets of Langerhans, scattered throughout the organ, comprising 1-2% of total pancreatic mass. There are four different types of islet cells:  $\alpha$ -cells,  $\beta$ -cells,  $\delta$ -cells, and pancreatic polypeptide cells. It is the  $\beta$ -cells that are responsible for the synthesis, storage, and secretion of insulin. <sup>28</sup> Insulin is a 51 amino acid peptide hormone that is made up two chains, A and B, connected by two disulfide bonds. It is first synthesized as preproinsulin in the cytosol

before being taken up into the rough endoplasmic reticulum. After the signal peptide has resulted in the correct relocation of preproinsulin, it is cleaved off to form proinsulin.

Proinsulin consists of the A and B chains that are connected by a third chain, C-peptide, as shown in figure 3.1. Proinsulin is then transported to the Golgi apparatus where it is subsequently packaged into vesicles. C-peptide is cleaved from proinsulin during this process, which is completed in the vesicles. Three enzymes are involved in this process; two endopeptidases and carboxypeptidease H remove C-peptide from proinsulin to create insulin. 30

At the same time the C-peptide is being cleaved from the proinsulin, Zn<sup>2+</sup> ions are entering the vesicle through ZnT8, a Zn<sup>2+</sup> transporter in the vesicle membrane.<sup>31</sup> As a result, the concentration of Zn<sup>2+</sup> in the vesicles approaches millimolar levels.<sup>32</sup> This Zn<sup>2+</sup> is involved in the creation of proinsulin hexamers, consisting of six proinsulin molecules and two Zn<sup>2+</sup> atoms. After C-peptide is removed, the Zn<sup>2+</sup>-insulin complex becomes less soluble and is stored in the vesicles in a crystalline form.<sup>33</sup>

Insulin is released from the  $\beta$ -cells in response to blood glucose levels. When these levels exceed 5.5 mM, as is the case after a healthy individual eats a meal, there is an increase in glucose uptake into the  $\beta$ -cell through a glucose transporter, GLUT2. Inside

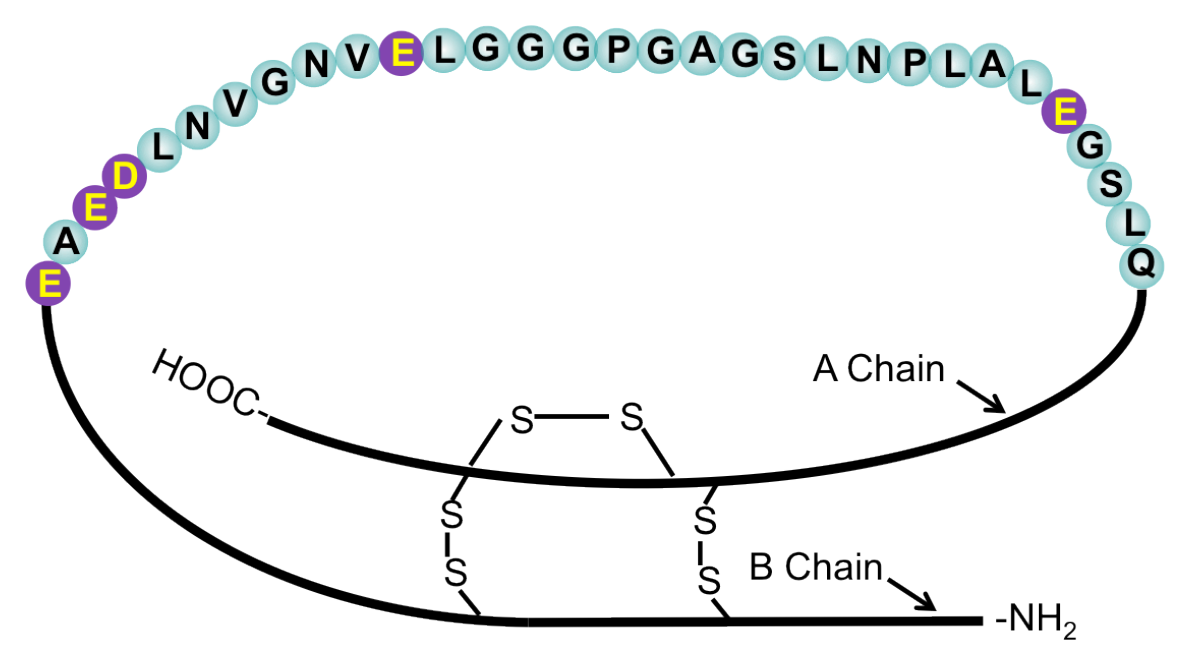


**Figure 3.1 – Proinsulin** – This basic diagram shows the role of C-peptide in the structure of insulin, as well as the amino acid sequence of C-peptide. The acidic residues have been colored purple. When the C-peptide is cleaved from proinsulin, the A and B chains remain, forming insulin.

the  $\beta$ -cell, glucose-6-phosphate is formed through a phosphorylation by glucokinase. <sup>34</sup> As a result of the phosphorylation, the concentration of ATP decreases, as the concentration of adenosine diphosphate (ADP) increases. The change in this ratio closes a potassium ion channel and opens a calcium ion channel; in response to in influx of calcium ions, the vesicles in the  $\beta$ -cells undergo exocytosis. <sup>35-37</sup> A diagram of this can be seen in figure 3.2. It is important to note that when this occurs, insulin and C-peptide are released in equimolar amounts and Zn<sup>2+</sup> is present in as well.

### 3.2.3 Structure of C-peptide

As mentioned in the previous section, C-peptide is produced as a by-product of insulin. C-peptide is a 31 amino acid peptide; the sequence of this peptide has not been conserved evolutionarily, nor is it conserved between species. However, at the carboxyl end of the peptide, the glutamine in the first position and the glutamic acid in the fifth position are conserved in almost 70% of species, and the pentapeptide from this end, EGSLQ, has been shown to elicit 75% of the activity that is seen with the intact peptide. <sup>39</sup>

Pure C-peptide does not have a stable secondary structure in aqueous solution. While it is not physiologically relevant, there is evidence of  $\alpha$ -helices in trifluoroethanol. Circular dichroism (CD) spectroscopy data from the Spence lab, collected by Wathsala Medawala, confirmed that there was no observable secondary structure for pure C-

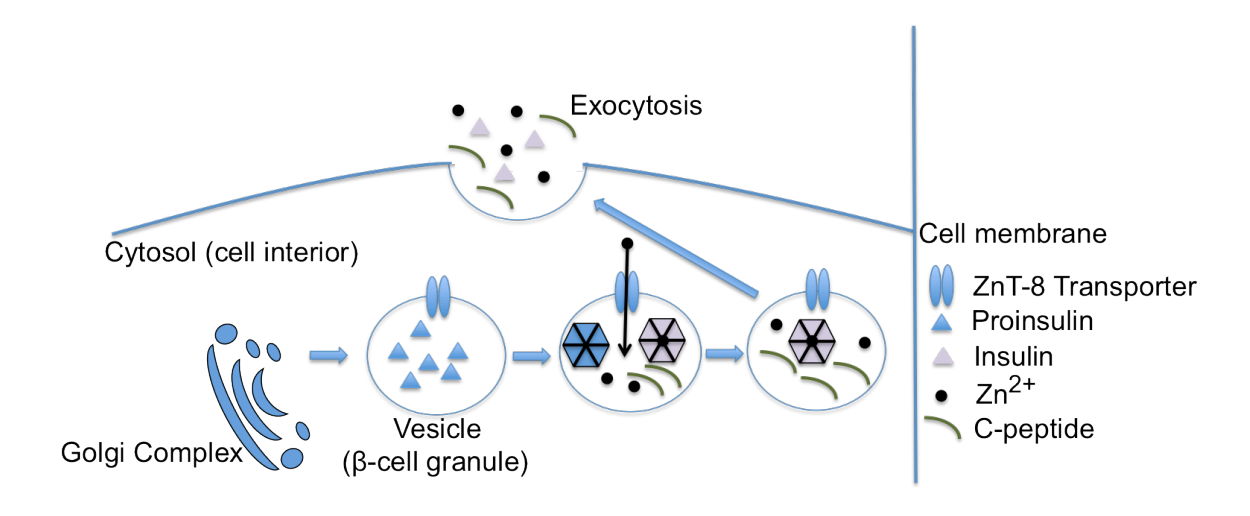


Figure 3.2 – Insulin Packaging and Release – Insulin is first synthesize as preproinsulin in the cytosol before being uptaken into the rough endoplasmic reticulum where the signal peptide is cleaved to form proinsulin. It is then transported to the Golgi apparatus where it is subsequently packaged into vesicles. C-peptide is cleaved from proinsulin during this process. At the same time, Zn  $^{2+}$  ions are entering the vesicle through ZnT8, a Zn  $^{2+}$  transporter in the vesicle membrane. This Zn  $^{2+}$  is involved in the creation of proinsulin hexamers, consisting of six proinsulin and two Zn  $^{2+}$ . After C-peptide is removed, the Zn  $^{2+}$ -insulin complex becomes less soluble and is stored in the vesicles in a crystalline form. Insulin is released from the β-cells in response to blood glucose levels, and the vesicles undergo exocytosis. It is important to note that when this occurs, insulin and C-peptide are released in equimolar amounts and Zn  $^{2+}$  is present as well.

peptide in aqueous solution. However, when Zn<sup>2+</sup> is added in a 1:1 mole ratio with C-peptide, there is a decrease in the minimum on the CD spectra, denoting less randomness and potential folding. Interestingly, when a higher concentration of Zn<sup>2+</sup> is added, the minimum returns to the value for C-peptide alone. 41

To date, no receptor for C-peptide has been found, though studies have shown it binding to several different human cell membranes. While the mechanism of the bioactivity of C-peptide is incompletely understood, there have been physiological effects measured on N<sup>+</sup>/K<sup>+</sup>-ATPase activity, and downstream activation, endothelial NO synthase stimulation, hindse stimulation, hindse activated protein kinase (MAPK) pathway activation, hosphatidylinositol-3-kinase activation, and downstream activation of transcription factors.

#### 3.2.4 Biological Effects of C-Peptide

Originally discovered in 1967, C-peptide was long considered to be biologically inactive. <sup>49</sup> It was widely accepted that it was only required for the proper arrangement of the insulin A and B chains, as shown in figure 3.1. <sup>50</sup> In fact, clinically, C-peptide has only been used as a diagnostic. Because of its longer half-life in blood and its direct correlation to insulin release, C-peptide is used to determine insulin release in diabetic patients. This information is used to discern a diagnosis of diabetes, including type 1 versus type 2, as well as to monitor patient response to pharmaceuticals that stimulate

the secretion of insulin.  $^{51}$  In the past 20 years, however, there has been emerging research showing the C-peptide has other physiological effects,  $^{52,53}$  particularly when bound to  $\mathrm{Zn}^{2+.54}$ 

C-peptide lacks basic residues, but contains five acidic residues: four glutamic acids and one aspartic acid. The result of this is a negatively charged peptide that result in the ability to bind cations, specifically, Zn<sup>2+55</sup> While studies have emerged finding physiological activity of C-peptide, 56-58 there have been reports that this activity is only seen when C-peptide is co-administered with insulin, <sup>59</sup> and the results were often difficult to reproduce. In 2008, Meyer et al. were also able to show that C-peptide increases the ATP release from RBCs; however, a metal ion was necessary for this to occur. During the course of their investigation, it was noted that the C-peptide that had been believed to be pure actually contained metal ions. This impure C-peptide was active when first dissolved in water, but lost activity over the course of hours. The metal ions originally used to produce C-peptide activity were Fe<sup>2+</sup> and Cr<sup>3+</sup>, however, based on the high concentration of  $Zn^{2+}$  in the  $\beta$ -cell where C-peptide is produced, it is predicted that this is the metal activating C-peptide in vivo. <sup>60</sup>

It is the position of this thesis that as a result of presumable pure C-peptide being contaminated with metals, the reproducibility issues with previous results are

explainable. Additionally, in cases where activity is seen only when insulin is co-administered, it is possible that the insulin still contains high amounts of Zn<sup>2+</sup> able to interact with C-peptide. In an in vivo study looking at the effects of C-peptide on glucose metabolism in type 1 diabetics, C-peptide alone increased glucose utilization by 25%. A separate study found that the co-administration of C-peptide and insulin increased glucose metabolism by 66%. Zn<sup>2+</sup> bound to C-peptide has also been shown to increase ATP release from RBCs obtained from a type 1 diabetic rat model back to the level of healthy controls. This effect was not seen in the RBCs from the type 2 diabetic rats unless they were first incubated with metformin, a common pharmaceutical to treat the disease. This has lead to the suggestion that the RBCs of patients with type 2 diabetes are both C-peptide and insulin resistant, and therefore, there is an increased need for the study of the biological effects of C-peptide.

The research presented here uses <sup>65</sup>Zn<sup>2+</sup> and enzyme-linked immunosorbant assays (ELISA) to investigate the transport of Zn<sup>2+</sup> and C-peptide to healthy human RBCs. A mutant form of C-peptide was employed to investigate the importance of the acidic residue in the 27<sup>th</sup> position in the binding of Zn<sup>2+</sup> to the peptide and then subsequent delivery to the RBC. These studies help to more fully understand the effect the Zn<sup>2+</sup> bound to C-peptide has on the metabolism of RBCs.

#### 3.3 Experimental

#### 3.3.1 Preparation of Reagents

Purified water with 18.2 M $\Omega$  resistance was used for all experiments to eliminate metal ion contamination. Crude C-peptide (Genscript, Piscataway, NJ) and its E27A mutant were purified using reverse phase high performance liquid chromatography (RP-HPLC). Fractions were analyzed for purity using liquid chromatography-mass spectrometry (LC-MS) and MS/MS. The fractions containing the pure peptides were lyophilized overnight. The dried product was then weighed to 0.25 mg/vial and stored at -20°C until use. To prepare a stock solution of 8.3  $\mu$ M peptide, one vial of 0.25 mg peptide was thawed and dissolved in 10 mL of deionized water. Usually, this solution can be stored for a month at 4°C. On the day of use, for either C-peptide or the mutant, a working solution of 332 nM was prepared in pure water.

Several of these experiments involved the radioligand <sup>65</sup>Zn<sup>2+</sup> (Perkin Elmer, Boston, MA). Because of the relatively short half-life of this isotope, the concentration of the stock solution was calculated regularly. For use, the stock solution was diluted in water to prepare an 800 nM working solution. Non-radioactive Zn<sup>2+</sup> stock solution was prepared by dissolving Zn<sup>2+</sup> (II) chloride (Jade Scientific, Canton, MI) in purified water and diluted to 800 nM.

RBCs used in these experiments were washed and incubated in physiological salt solution (PSS) containing, in mM, 4.7 KCl (Fisher Scientific, Fair Lawn, NJ), 2.0 CaCl<sub>2</sub> (Fisher Scientific), 140.5 NaCl (Columbus Chemical Industries, Columbus, WI), 12 MgSO<sub>4</sub> (Fisher Scientific), 21.0 tris(hydroxymethylaminomethane) (Invitrogen, Carlsbad, CA), 5.6 glucose (Sigma, St. Louis, MO), and 5% bovine serum solution (Sigma) at a final pH of 7.4, adjusted with hydrochloric acid.

#### 3.3.2 Collection and Preparation of Human RBCs

Following human venipuncture and collection into heparinized vacutainers (BD, Franklin Lakes, NJ), whole blood was centrifuged for 10 minutes at 500g to separate the RBCs from the other blood components. Following the removal of the plasma and buffy coat, the RBCs were washed three times with PSS and centrifuged. After the final washing, the supernatant was removed and the hematocrit of the RBCs was measured using a CritSpin© analyzer.

# 3.3.3 Radiolabeled Zn<sup>2+</sup> Assays for Determination of the Amount of Zn<sup>2+</sup> Interacting with the RBC

The amount of  $Zn^{2+}$  interacting with the RBC in the presence of C-peptide or the mutant was determined using the radioligand  $^{65}Zn^{2+}$ . First,  $^{65}Zn^{2+}$  and the peptide were incubated in pure water for three minutes to ensure peptide activation. PSS was then added to the mixture, immediately followed by the addition of the appropriate volume

of RBCs to prepare 1 mL samples with a 7% hematocrit. Following a one hour incubation at 37°C, samples were centrifuged at 500g for four minutes and the supernatant was collected. In some of the experiments, the RBCs were then washed three times and lysed with bleach. For the saturation experiments, the RBCs were incubated a second time in PSS containing 100 µM Zn<sup>2+</sup> to displace the specifically bound  $^{65}$ Zn<sup>2+</sup>. After a one-hour incubation, the samples were centrifuged at 500q for 4 minutes and the supernatant was removed and the amount of radioactivity in the sample was measured. In a 96-well plate, 200 μL of supernatant or lysate solution were combined with 100 µL of scintillation cocktail (optiphase supermix, Perkin Elmer, Waltham, MA). The amount of radioactivity in each sample was then determined using a 1450 Microbeta Plus liquid scintillation counter (Wallac, Turku, Finland). A diagram of the experimental set-up can be seen in figure 3.3. Comparing to a set of  $^{65}$ Zn $^{2+}$ standards prepared in RBC supernatant or lysate, the concentration of  $^{65}\mathrm{Zn}^{2+}$  in each sample was quantified. In the case of the supernatant, knowing the amount of  $^{65}\mathrm{Zn}^{2+}$ added to the original RBC sample and how much was left in the supernatant, the amount of <sup>65</sup>Zn interacting with the RBCs was determined by subtraction.

#### 3.4 Results

Figure 3.4 shows the results of the first study involving <sup>65</sup>Zn<sup>2+</sup> interacting with human RBCs in the presence and absence of C-peptide. Because of previous studies showing an

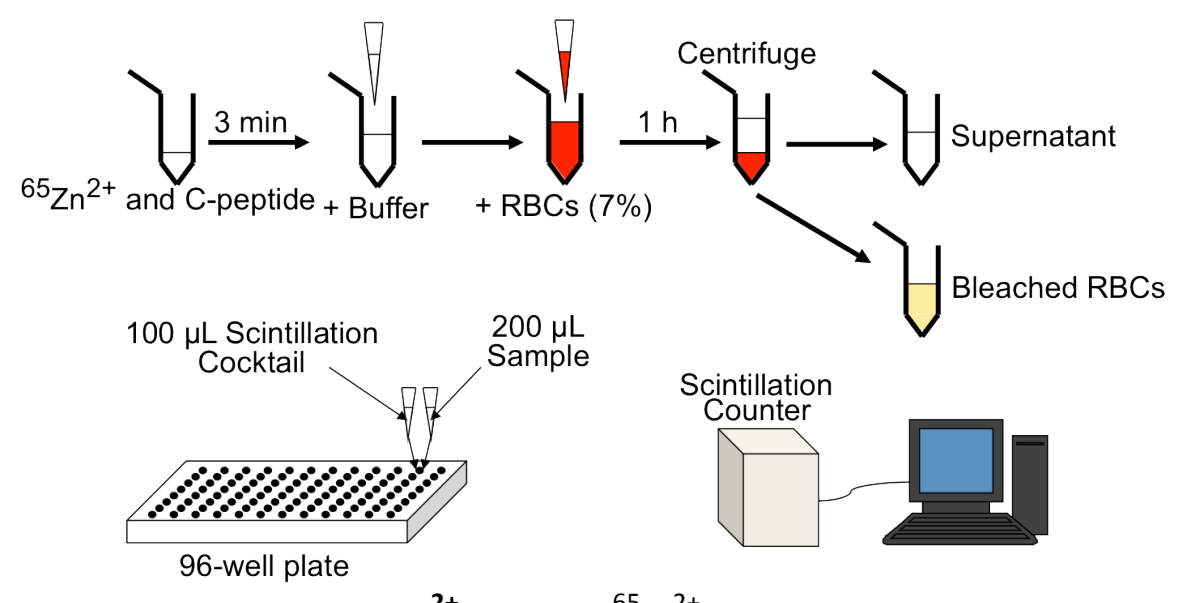


**Figure 3.3 – Radiolabeled Zn**<sup>2+</sup> **Assays** – <sup>65</sup>Zn<sup>2+</sup> and the peptide were incubated together in pure water for three minutes to ensure peptide activation. PSS was then added to the mixture, immediately followed by the addition of the appropriate volume of RBCs to prepare 1 mL samples with a 7% hematocrit. Following a one hour incubation samples were centrifuged and the supernatant was collected. In some of the experiments, the RBCs were then washed three times and lysed with bleach. In a 96-well plate, 200 μL of supernatant or lysate solution was combined with 100 μL of scintillation cocktail. The amount of radioactivity in each sample was then determined using a 1450 Microbeta Plus liquid scintillation counter.

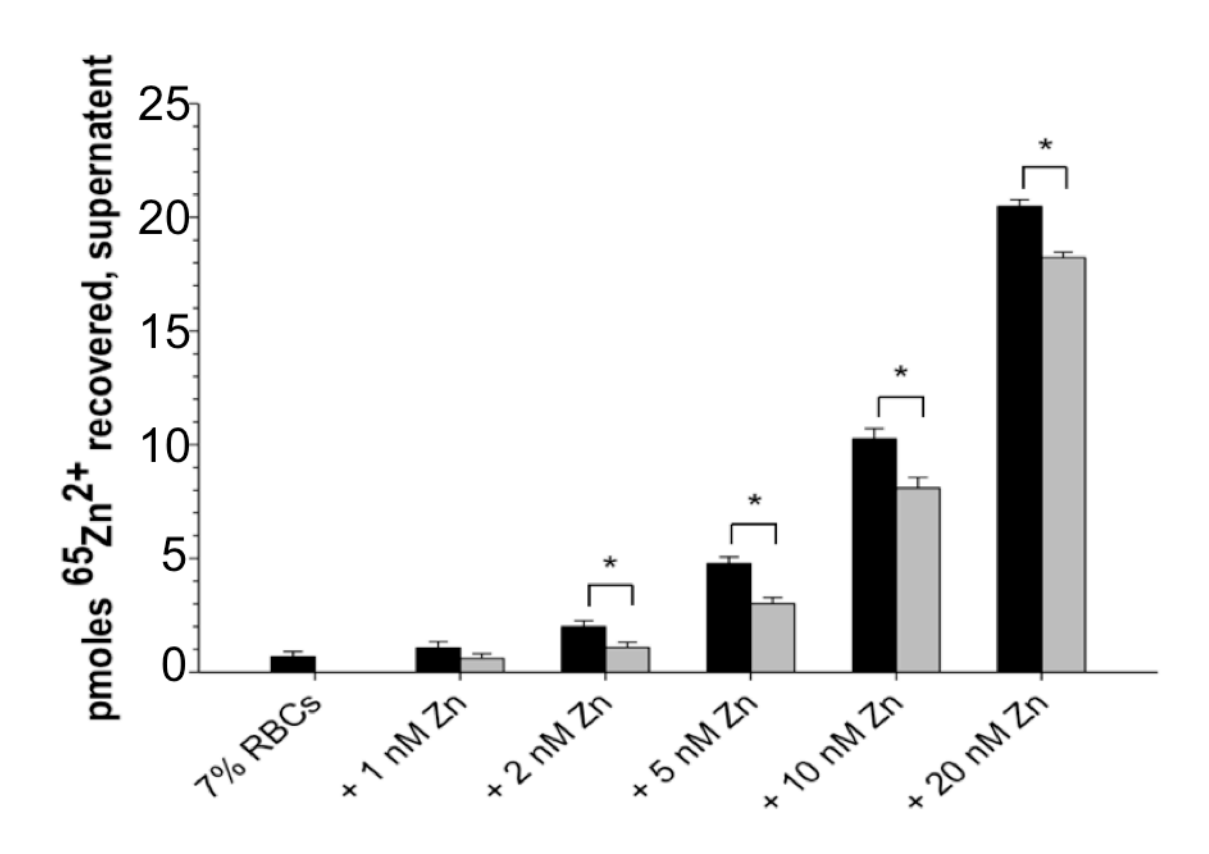


Figure 3.4 –  $^{65}$ Zn <sup>2+</sup> Remaining in the Supernatent after Incubation with RBCs – For each set of bars, when C-peptide was also added, it was added in a 1:1 ratio with  $^{65}$ Zn <sup>2+</sup>. As is evident from the data,  $^{65}$ Zn <sup>2+</sup> alone, black bars, does not interact with the RBC. However, with the exception of the 1 nM concentration, when  $^{65}$ Zn <sup>2+</sup> bound to C-peptide is incubated with the RBCs, grey bars, significantly less  $^{65}$ Zn <sup>2+</sup> is found in the supernatant. Error is represented as standard deviation for N = 7 humans. The asterisk represents p < 0.05.

increase in ATP release from RBCs incubated with  $Zn^{2+}$  bound to C-peptide,  $^{60}$  it was thought that there may be an increase interaction of  $^{65}Zn^{2+}$  with the RBC. Prior to these studies, by investigating the amount of  $Zn^{2+}$  measured in the supernatant and that remaining on the RBCs, it was determined that all of the  $^{65}Zn^{2+}$  could be accounted for. Using the supernatant saves time and increases sensitivity, so for the majority of the studies, the  $^{65}Zn^{2+}$  was measured only in the supernatant. For each set of bars, when C-peptide was also added, it was added in a 1:1 ratio with  $^{65}Zn^{2+}$ . As is evident from the data,  $^{65}Zn^{2+}$  alone does not interact with the RBC. However, with the exception of the 1 nM concentration, when  $^{65}Zn^{2+}$  bound to C-peptide is incubated with the RBCs, significantly less  $^{65}Zn^{2+}$  is found in the supernatant.

For comparison with the amount of C-peptide interacting with the RBC,  $^{65}$ Zn $^{2+}$  was also measured on the RBC directly. Figure 3.5 shows a correlation between the amount of  $^{65}$ Zn $^{2+}$  and the amount of C-peptide interacting with the RBC. On the left, data collected by Wathsala Medawala using an enzyme-linked immunosorbent assay (ELISA) to find the amount of C-peptide interaction with the RBC is shown. Comparing this data to the data on the right showing the amount of  $^{65}$ Zn $^{2+}$  recovered from RBC lysate, it is evident that C-peptide and Zn $^{2+}$  interaction with the RBC in a 1:1 ratio. For both

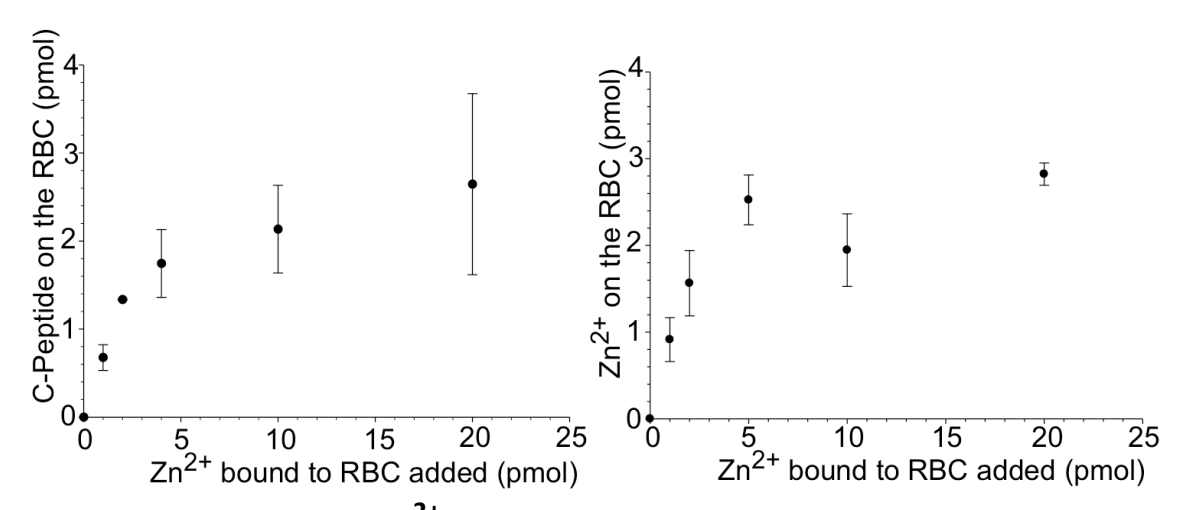
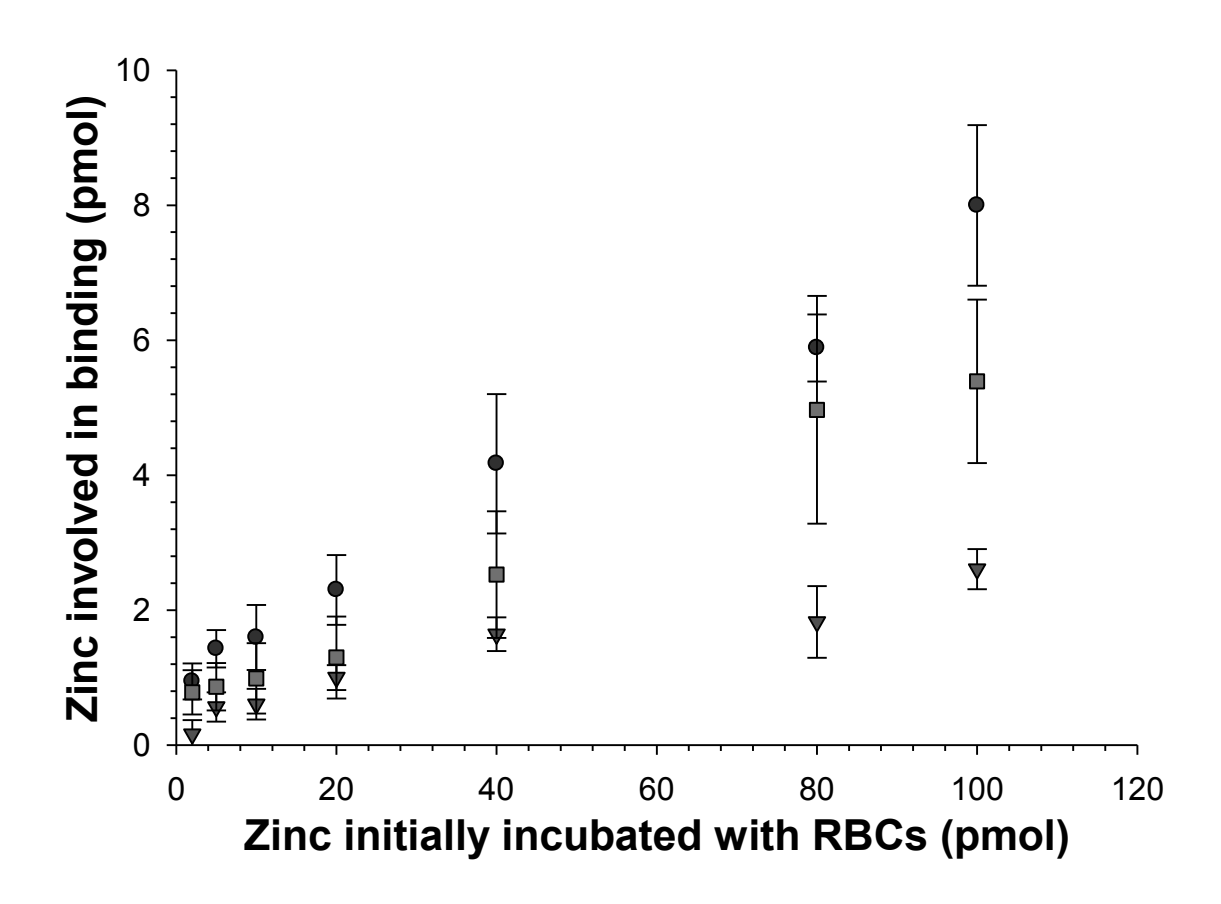


Figure 3.5 – C-Peptide and  $Zn^{2+}$  on the RBC – The data on the left shows the amount of C-peptide interaction with the RBC. Comparing to the data on the right, showing the amount of  $^{65}Zn^{2+}$  recovered from RBC lysate, it is evident that C-peptide and  $Zn^{2+}$  interaction with the RBC in a 1:1 ratio. For both binding curves, saturation seems to begin around 10 picomoles of added  $Zn^{2+}$  bound to C-peptide and results in a maximum of 2.64  $\pm$  1.03 picomoles of C-peptide and 2.96  $\pm$  0.17 picomoles of  $^{65}Zn^{2+}$  interacting with the RBC when 20 picomoles of  $Zn^{2+}$ -activated C-peptide have been added. Within error, this shows that  $Zn^{2+}$  and C-peptide interact with the RBC in a 1:1 manner. Error is shown as standard deviation for N = 4 humans for C-peptide and N = 5 for  $Zn^{2+}$ .

binding curves, saturation seems to begin around 10 picomoles of added  $Zn^{2+}$  bound to C-peptide and results in a maximum of 2.64  $\pm$  1.03 picomoles of C-peptide and 2.96  $\pm$  0.17 picomoles of  $^{65}Zn^{2+}$  interacting with the RBC when 20 picomoles of  $Zn^{2+}$ -activated C-peptide have been added. Within error, this shows that  $Zn^{2+}$  and C-peptide interact with the RBC in a 1:1 ratio. Experiments examining different  $Zn^{2+}$  to C-peptide ratios will be discussed later.

It was noted during experimentation that with increased amounts of  $Zn^{2+}$ -activated C-peptide, up to 100 picomoles, an increased amount of  $^{65}Zn^{2+}$  was observed interacting with the RBCs, while the amount of C-peptide remained relatively stable, under 3 picomole. To discern if this increased amount of  $^{65}Zn^{2+}$  was the result of non-specific binding, where the binding is not the result of a unique arrangement of the binding partner, a saturation study was completed. RBCs were first incubated with various concentrations of  $^{65}Zn^{2+}$ -activated C-peptide, after the supernatant was removed and measured for excess  $^{65}Zn^{2+}$ , the RBCs were incubated a second time with normal  $Zn^{2+}$ -activated C-peptide at a concentration 10 times greater than the highest concentration of  $^{65}Zn^{2+}$  bound to C-peptide. The non-radioactive competitor displaces only the  $^{65}Zn^{2+}$  that had been specifically bound. The non-specific binding can then be calculated through simple subtraction. The results of this can be seen in figure 3.6. From this, it



**Figure 3.6 – Saturation Curve** – After total and specific binding (circles and triangle, respectively) were found, the non-specific binding (squares) was calculated. Comparable to the C-peptide binding, the amount of specifically bound  $Z_1^{2+}$  is  $1.85 \pm 0.53$  picomoles for 20 picomoles of added  $Z_1^{2+}$  bound to C-peptide. This data shows that  $Z_1^{2+}$ , or  $Z_1^{2+}$  bound to C-peptide, is interacting with a receptor on the RBC. The error is shown as standard deviation for N = 7 humans for 2, 5, 10, 20 and 40 picomoles, N = 4 humans for 80 picomoles, and N = 5 humans for 100 picomoles.

can be seen that there was non-specific binding occurring, and comparable to the C-peptide binding, the amount of specifically bound  $Zn^{2+}$  is 1.85  $\pm$  0.53 picomoles for 20 picomoles of added  $^{65}Zn^{2+}$  bound to C-peptide. This data also shows that  $Zn^{2+}$ , or  $Zn^{2+}$  bound to C-peptide, is interacting with a receptor on the RBC.

Additionally, Wathsala Medawala investigated the amount of C-peptide interacting with the RBC with and without  $Zn^{2+}$ , to compare to data collected showing the interaction of  $Zn^{2+}$  with the RBC with and without C-peptide. In figure 3.7, the data shows that whether or not C-peptide is activated by  $Zn^{2+}$ , statistically the same amount is found to be interacting with the RBC. However, when  $Zn^{2+}$  alone is added to an RBC solution, all of it is found in the supernatant after incubation. When  $Zn^{2+}$  is introduced to the sample as  $Zn^{2+}$  bound to C-peptide, significantly less  $Zn^{2+}$  was found in the supernatant, meaning it is interacting with the RBC, but only when added to the sample as  $Zn^{2+}$  bound to C-peptide. This is significant as it was previously thought that  $Zn^{2+}$  was helping C-peptide interact with the RBC, when in fact, C-peptide is carrying  $Zn^{2+}$  to the RBC.

The binding of Zn<sup>2+</sup> to C-peptide and several mutants been studied using mass spectrometry<sup>66</sup> and CD spectroscopy.<sup>41</sup> One of the mutants, called E27A, had the glutamic acid in position 27 switched for an alanine. Wild type C-peptide was found to

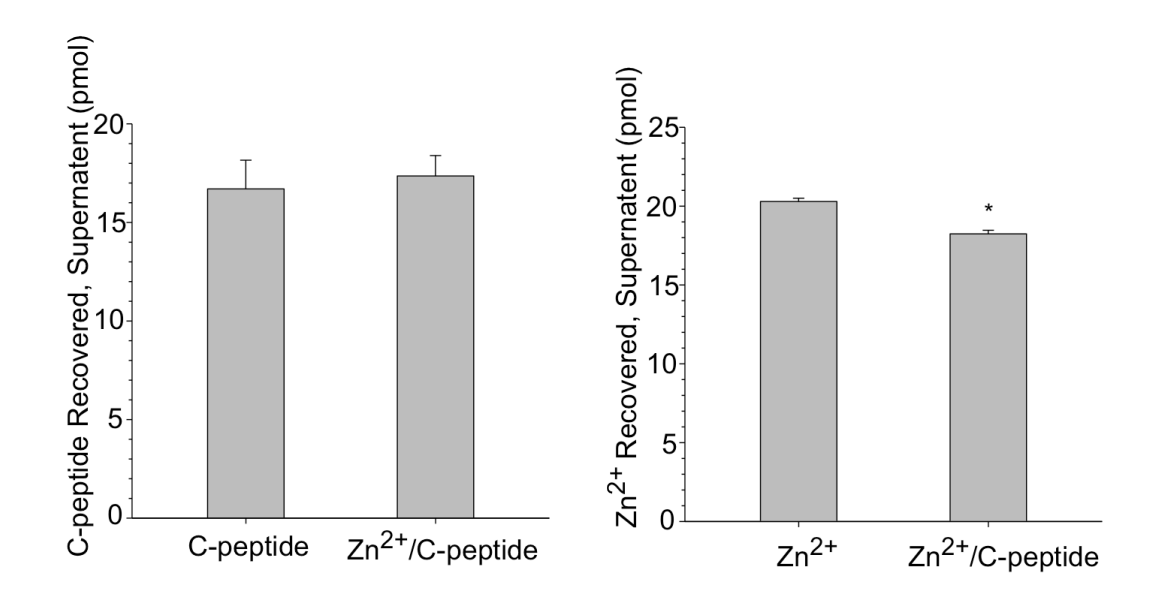


Figure 3.7 – C-Peptide and  $Zn^{2+}$  in the Supernatent – The data on the left shows that whether or not 20 nM C-peptide is bound to 20 nM  $Zn^{2+}$ , statistically the same amount is found to be interacting with the RBC. However, when  $Zn^{2+}$  alone is added to an RBC solution, all of it is found in the supernatant after incubation. When  $Zn^{2+}$  is introduced to the sample as 20 nM  $Zn^{2+}$  bound to C-peptide, significantly less  $Zn^{2+}$  was found in the supernatant, meaning it is interacting with the RBC, but only when added to the sample bound to C-peptide. Error is standard deviation for  $Zn^{2+}$  humans for C-peptide and  $Zn^{2+}$  The asterisk denotes  $Zn^{2+}$  added alone.

bind to Zn<sup>2+</sup> in a 1:1 ratio, while E27A was able to bind four Zn<sup>2+</sup> ions per molecule. This suggests that C-peptide would have a more closed structure when bound to Zn<sup>2+</sup>, and E27A would have an open structure. Figure 3.8 shows the effect this would have on  $Zn^{2+}$  delivery to the RBC. The mutation in E27A prevents  $^{65}Zn^{2+}$  interaction with the RBC when the experimental conditions are kept the same.  $^{65}\mathrm{Zn}^{2+}$  and the peptides were added in a 1:1 ratio. Because binding studies suggested that E27A has the ability to bind  $Zn^{2+}$ , other ratios of  $^{65}Zn^{2+}$  to peptide were investigated for  $Zn^{2+}$  delivery to the RBC. In normal PSS, shown by the black bars, only the 1:1 ratio of  $^{65}$ Zn $^{2+}$  to C-peptide ratio was able to delivery any  $^{65}$ Zn $^{2+}$  to the RBC. One of the components of PSS, bovine serum albumin (BSA), is known to bind  $Zn^{2+67}$  and if the  $^{65}Zn^{2+}$  ions bound to the E27A are not bound tightly, they would be easily removed by the BSA. Therefore, the experiments were repeated using a BSA-free PSS. They grey bars of figure 3.8 show both peptides are able to deliver Zn<sup>2+</sup> to the RBC, regardless of ratio. However, Cpeptide is able to deliver rough double the amount of  $Zn^{2+}$  as compared to the mutant.

## 3.5 Discussion

The major finding of this research is the evidence of C-Peptide being a Zn<sup>2+</sup> carrier to the RBC. It was already known that C-peptide will increase the ATP release from RBCs

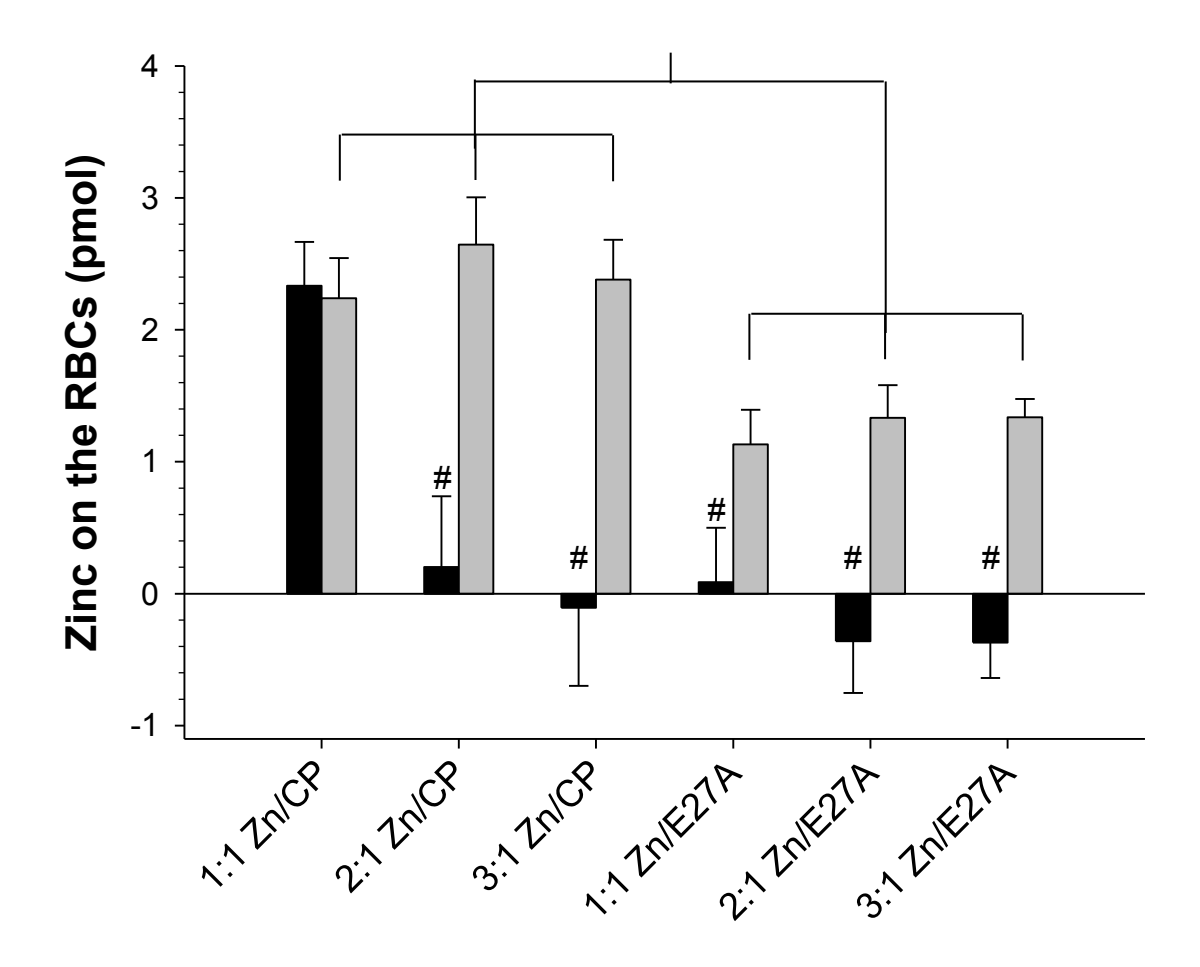


Figure 3.8 – Effect of Mutant, Ratios, and BSA on  $Zn^{2+}$  Interaction with RBCs – The mutation in E27A prevents  $^{65}Zn^{2+}$  interaction with the RBC in the presences of BSA (black bars). Also, in normal PSS, only the 1:1  $^{65}Zn^{2+}$  to C-peptide ratio was able to delivery any  $^{65}Zn^{2+}$  to the RBC. When the experiments were repeated using a BSA-free PSS, (grey bars) both peptides are able to deliver  $Zn^{2+}$  to the RBC, regardless of ratio. However, C-peptide is able to deliver roughly double the amount of  $Zn^{2+}$  as compared to the mutant. The error is standard deviation for N = 4 humans. The asterisk represents p < 0.05 and the pound sign represents p < 0.001 as compared to 1:1 ratio of  $Zn^{2+}$  bound to C-peptide.

only when previously activated by  $Zn^{2+}.60$  Studies completed by Watshsala Medawala have previously shown that C-peptide does in fact bind to  $Zn^{2+}$  in a 1:1 manner. It was the expectation that C-peptide would need  $Zn^{2+}$  to interact with the RBC, however, it was found that it is  $Zn^{2+}$  that needs C-peptide for RBC interaction. Figure 3.4 shows the interaction of  $Zn^{2+}$  with the RBC at different concentrations, and from this, it is evident that  $Zn^{2+}$  will not interact with the RBC without the presence of C-peptide. Mimicking in vivo conditions, the RBCs were suspended in PSS containing BSA. Because of known BSA and  $Zn^{2+}$  binding, it is not surprising that  $Zn^{2+}$  in the solution is unable to reach the RBC on its own.

Upon further investigation, it was found that after incubation with  $Zn^{2+}$  bound to C-peptide, the amount of  $Zn^{2+}$  interacting with the RBC and the amount of C-peptide interaction with the RBC were relatively equivalent with approximately 2 picomoles of each interacting with the RBC, as seen in figure 3.5. Since the C-peptide and  $Zn^{2+}$  are acting together, it is reasonable for the saturation of the RBCs to occur in a 10 nM solution of  $Zn^{2+}$  bound to C-peptide, as the levels of C-peptide are typically in the single digit nanomolar level in vivo.

Because of the specific and non-specific binding seen in figure 3.6, it is believed that the Zn<sup>2+</sup> is binding to a receptor on the RBC. While there is currently no known receptor for C-peptide, it is known that Zn<sup>2+</sup> has an effect on glucose transport in certain cell types that is believed to be mediated through GLUT1, 68 the major glucose transporter in RBCs. With the increase in RBC-derived ATP after incubation with Zn<sup>2+</sup> bound to Cpeptide, it is believe that there will also be an increase in glucose uptake into the RBC, as glycolysis is the only means the cell has to produce ATP. Therefore, it would be logical for the mechanism of increase to begin with GLUT1. Additionally, acute oral Zn<sup>2+</sup> supplementation improved glucose use in vivo in response to an intravenous glucose test when no changes in insulin secretion on sensitivity were seen. This suggests that Zn<sup>2+</sup> alone was responsible for the increased in glucose tolerance. Further studies need to be completed to investigate the mechanism of RBC glucose uptake and increase ATP release after incubation with Zn<sup>2+</sup>-activated C-peptide.

When starting this area of research, it was hypothesized that C-peptide required Zn<sup>2+</sup> for transport to the RBC or for its activity in some way. However, through the course of experimentation, it was discovered that while the C-peptide can interact with the RBC without Zn<sup>2+</sup>, the Zn<sup>2+</sup> cannot interact with the RBC without C-peptide, as seen in figure 3.7. While it has been shown that C-peptide interacts with the RBC without the

presence of  $Zn^{2+}$ , it is known that the increase ATP release will not occur unless the RBCs have been incubated with  $Zn^{2+}$  bound to C-peptide. This has led to the idea that C-peptide is a  $Zn^{2+}$  carrier to the RBC.

Previous work done by Wathsala Medawala shows that C-peptide binds to Zn<sup>2+</sup> in a 1:1 ratio. 41 Results shown in figure 3.8 support this finding. In normal PSS, only a 1:1 ratio of  $\mathrm{Zn}^{2+}$  to C-peptide exhibits  $\mathrm{Zn}^{2+}$  interaction with the RBC. C-peptide, having no histidine residues, is assumed to bind to Zn<sup>2+</sup> through the acidic amino acids, glutamic acid and aspartate. These amino acids bind monodentate through one carboxyl oxygen. Because of this, it is hypothesized that when Zn<sup>2+</sup> and C-peptide are combined in a 1:1 ratio, folding of the C-peptide occurs, binding to the Zn<sup>2+</sup> with multiple amino acids. A minimalistic diagram of this theory can be seen in figure 3.9. Results showing the lost of Zn<sup>2+</sup> interaction with the RBC with higher Zn<sup>2+</sup> to C-peptide ratios led to the hypothesis that multiple Zn<sup>2+</sup> ions may be binding to the C-peptide in those cases. Then, upon addition of serum albumin containing PSS, the Zn<sup>2+</sup> may be removed from the peptide by the albumin because of its high binding affinity. Further proof of this is seen in figure 3.8, when the E27A mutant of the peptide was used, along with the use of BSA-free PSS. When E27A is incubated with  $Zn^{2+}$  prior to the addition of normal PSS and RBCs, no  $Zn^{2+}$ 

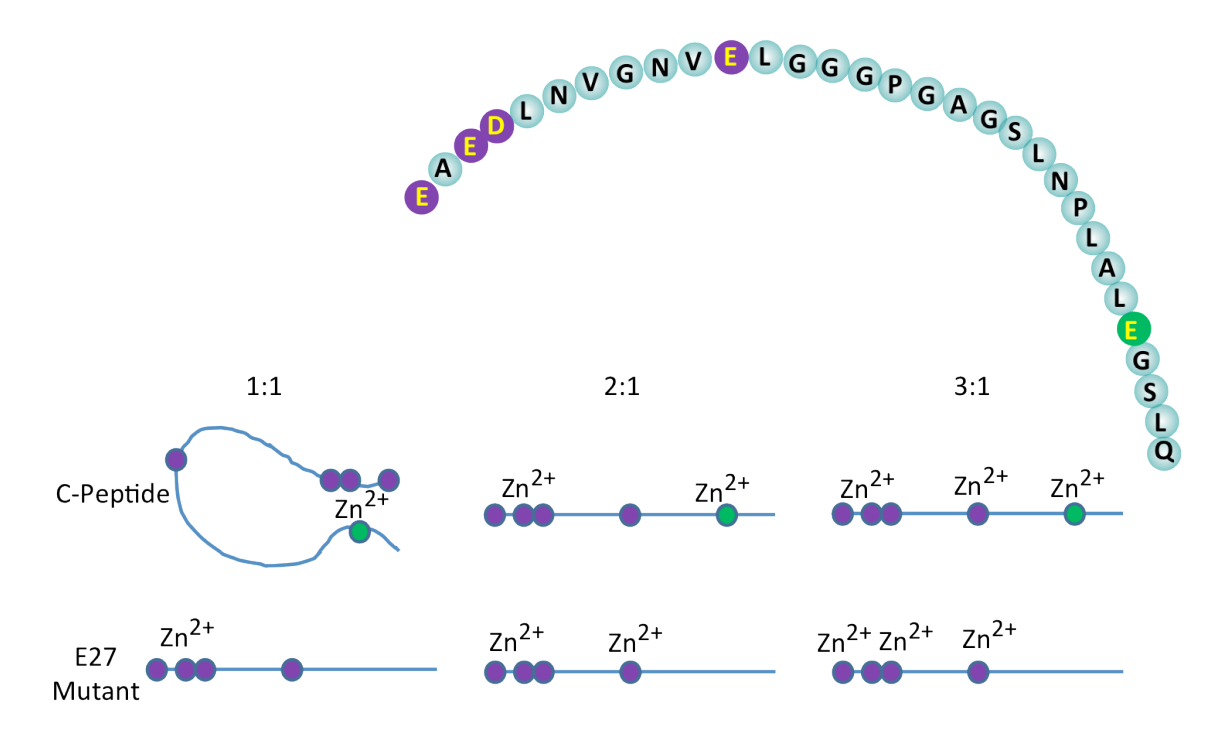


Figure 3.9 – Hypothesis of  $Zn^{2+}$  Binding to C-peptide and a Mutant – Results showing the loss of  $Zn^{2+}$  interaction with the RBC with higher  $Zn^{2+}$  to C-peptide ratios led to the hypothesis that multiple  $Zn^{2+}$  ions may be binding to the C-peptide in those cases. Then, upon addition of serum albumin containing PSS, the  $Zn^{2+}$  may be removed from the peptide by the albumin because of its high binding affinity. It is believed that the  $Zn^{2+}$  may bind to the E27A peptide, however there is no folding, and the  $Zn^{2+}$  ions are easily removed by the BSA. This hypothesis is related to the data in figure 3.8.

is seen on the RBCs. This was expected, as the glutamic acid in the  $27^{th}$  position has been shown to be necessary for biological effects on RBC-derived ATP release. It is believed that the Zn<sup>2+</sup> may bind to the E27A peptide, however there is no folding, and the Zn<sup>2+</sup> ions are easily removed by the BSA. Further proof of this is seen when the Zn<sup>2+</sup>-activated peptides are incubated with the RBCs in a BSA-free PSS. Here, the data shows that for C-peptide, approximately 2.4 picomoles of Zn<sup>2+</sup> are interacting with the RBC, regardless of the  $Zn^{2+}$  to C-peptide ratio. Additionally, the  $Zn^{2+}$  is also able to interact with the RBC after incubation with the mutant, though in a statistically lower quantity of approximately 1.3 picomoles. Interestingly, this data matches up with binding affinities found by Wathsala Medawala, who found that E27A has a decrease in  ${\rm Zn}^{2+}$  binding affinity of about 50% as compared to the  ${\rm Zn}^{2+}$  binding affinity for Cpeptide. 41 Because of these results, it is concluded that Zn 2+ cannot interact with the RBC without the presence of C-peptide, and that C-peptide and the mutant can carry  $Zn^{2+}$  to the RBC, regardless of the  $Zn^{2+}$  to peptide ratio without the presence of BSA. However, in in vivo conditions, with serum present, C-peptide will bind to Zn<sup>2+</sup> ions in a 1:1 ratio for the most effective delivery of  $Zn^{2+}$  to the RBC for biological effects.

Unpublished data from the Spence lab shows that purified C-peptide has biological effects only when co-administered with Zn<sup>2+</sup>-containing insulin and not when co-

administered with purified insulin alone. Specifically, Zn<sup>2+</sup> bound to C-peptide increases RBC-derived ATP and subsequently, NO release from endothelial cells lining the blood vessels causing vasodilation. Therefore, Zn<sup>2+</sup> bound to C-peptide has great potential in the relief of the vascular complications of diabetes. While this has obvious implications for diabetes research and potential treatment, Zn<sup>2+</sup> is also implicated in other diseases, such as multiple sclerosis (MS), as discussed in chapter 1.6. Because of the results presented here, Zn<sup>2+</sup> bound to C-peptide was used in future studies to investigate the differences in Zn<sup>2+</sup> interaction with the RBC between MS patients and healthy controls.

REFERENCES

#### REFERENCES

- Gavin, J. R., Alberti, K. G. M. M., Davidson M. B., DeFronzo, R. A., Drash, A., Gabbe, S. G., Genuth, S., Harris, M. I., Kahn, R., Keen, H., Knowler, W. C., Lebovitz, H., Maclaren, N. K., Palmer, J. P., Raskin, P., Rizza, R. A. & Stern, M. P. Report of the expert committee on the diagnosis and classification of diabetes mellitus. *Diabetes Care* 22, S5-S19 (1999).
- Alberti, K., Zimmet, P., Consultation, W. & Consultation, W. Definition, diagnosis and classification of diabetes mellitus and its complications part 1: Diagnosis and classification of diabetes mellitus Provisional report of a WHO consultation. *Diabetic Medicine* **15**, 539-553 (1998).
- Vaarala, O., Knip, M., Paronen, J., Hämäläinen, A. M., Muona, P., Väätäinen, M., Ilonen, J., Simell, O. & Akerblom, H. K. Cow's milk formula feeding induces primary immunization to insulin in infants at genetic risk for type 1 diabetes. *Diabetes* **48**, 1389-1394 (1999).
- Akerblom, H. K., Virtanen, S. M., Ilonen, J., Savilahti, E., Vaarala, O., Reunanen, A., Teramo, K., Hämäläinen, A. M., Paronen, J., Riikjärv, M. A., Ormisson, A., Ludvigsson, J., Dosch, H. M., Hakulinen, T. & Knip, M. Dietary manipulation of beta cell autoimmunity in infants at increased risk of type 1 diabetes: a pilot study *Diabetologia* **48**, 1676-1676 (2005).
- Fowler, M. J. Diabetes: Magnitude and Mechanism. *Clinical Diabetes* **25**, 25-28 (2007).
- 6 Lebovitz, H. Insulin resistance: definition and consequences. *Experimental and Clinical Endocrinology & Diabetes* **109**, S135-S148 (2001).
- Polansky, K. S. Dynamics of Insulin Secretion in Obesity and Diabetics. *International Journal of Obesity and Related Metabolic Disorders* **24**, S29-31 (2000).
- 8 Mokdad, A. H., Bowman, B. A., Ford, E. S., Vinicor, F., Marks, J. S. & Koplan, J. P. The continuing epidemics of obesity and diabetes in the United States. *Journal of the American Medical Association* **286**, 1195-1200 (2001).
- 9 Associat, A. D. & Associat, A. D. Diagnosis and classification of diabetes mellitus. *Diabetes Care* **31**, S55-S60 (2008).

- 10 Creager, M., Luscher, T., Cosentino, F. & Beckman, J. Diabetes and vascular disease Pathophysiology, clinical consequences, and medical therapy: Part I. *Circulation* **108**, 1527-1532 (2003).
- Libby, P. Coronary artery injury and the biology at atherosclerosis: Inflammation, thrombosis, and stabilization. *American Journal of Cardiology* **86**, 3J-8J (2000).
- Carroll, J., Raththagala, M., Subasinghe, W., Baguzis, S., D'amico Oblak, T., Root, P. & Spence, D. An altered oxidant defense system in red blood cells affects their ability to release nitric oxide-stimulating ATP. *Molecular Biosystems* **2**, 305-311 (2006).
- Sprague, R., Stephenson, A., Bowles. E., Stumpf, M., Ricketts, G. & Lonigro, A. Expression of the heterotrimeric G protein Gi and ATP release are impaired in erythrocytes of humans with diabetes mellitus. *Hypoxia and Exercise* **588**, 207-216 (2006).
- Johnstone, M. T., Creager, S. J., Scales, K. M., Cusco, J. A., Lee, B. K. & Creager, M.
   A. Impaired endothelium-dependent vasodilation in patients with insulindependent diabetes mellitus. *Circulation* 88, 2510-2516 (1993).
- 15 Icks, A., Trautner, C., Haastert, B., Berger, M. & Giani, G. Blindness due to diabetes: Population-based age- and sex-specific incidence rates. *Diabetic Medicine* **14**, 571-575 (1997).
- Sheetz, M. & King, G. Molecular understanding of hyperglycemia's adverse effects for diabetic complications. *Journal of the American Medical Association* **288**, 2579-2588 (2002).
- The Diabetes Control and Complications Trial Research Group. The effect of intensive treatment of diabetes on the development and progression of long-term complications in insulin-dependent diabetes mellitus. *New England Journal of Medicine* **329**, 977-986 (1993).
- Sima, A. The heterogeneity of diabetic neuropathy. *Frontiers in Bioscience* **13**, 4808-4816 (2008).
- Sugimoto, K., Murakawa, Y. & Sima, A. Diabetic neuropathy a continuing enigma. *Diabetes-Metabolism Research and Reviews* **16**, 408-433 (2000).
- Boulton, A. Neuropathy and diabetes Introduction. *Diabetes Reviews* **7**, 235-236 (1999).

- Aoun, S., Blacher, J., Safar, M. & Mourad, J. Diabetes mellitus and renal failure: effects on large artery stiffness. *Journal of Human Hypertension* **15**, 693-700 (2001).
- 22 Ritz, E., Rychlik, I., Locatelli, F. & Halimi, S. End-stage renal failure in type 2 diabetes: A medical catastrophe of worldwide dimensions. *American Journal of Kidney Diseases* **34**, 795-808 (1999).
- Helal, I., Fick-Brosnahan, G., Reed-Gitomer, B. & Schrier, R. Glomerular hyperfiltration: definitions, mechanisms and clinical implications. *Nature Reviews Nephrology* **8**, 293-300 (2012).
- Tervaert, T. W., Mooyaart, A. L., Amann. K., Cohen, A. H., Cook, H. T., Drachenberg, C. B., Ferrario, F., Fogo, A. B., Haas, M., de Heer, E., Joh, K., Noël, L. H., Radhakrishnan, J., Seshan, S. V., Bajema, I. M. & Bruijn, J. A. Pathologic Classification of Diabetic Nephropathy. *Journal of the American Society of Nephrology* 21, 556-563 (2010).
- Schleicher, E., Kolm, V., Ceol, M. & Nerlich, A. Structural and functional changes in diabetic glomerulopathy. *Kidney & Blood Pressure Research* **19**, 305-315 (1996).
- 26 Cryer, P. Hypoglycemia is the limiting factor in the management of diabetes. *Diabetes-Metabolism Research and Reviews* **15**, 42-46 (1999).
- Ahmed, A. History of diabetes mellitus. *Saudi Medical Journal* **23**, 373-378 (2002).
- Poretsky, L. *Principles of diabetes mellitus*. 2nd ed., (Springer, 2010).
- Orci, L. Patterns of cellular and subcellular organization in the endocrine pancreas The Henry Dale Lecture for 1983. *Journal of Endocrinology* **102**, 3-4, (1984).
- Hutton, J. Insulin secretory granule biogenesis and the proinsulin-processing endopeptidases. *Diabetologia* **37**, S48-S56 (1994).
- Chimienti, F., Favier, A. & Seve, M. ZnT-8, a pancreatic beta-cell-specific zinc transporter. *Biometals* **18**, 313-317 (2005).
- Hutton, J. The insulin secretory granule. *Diabetologia* **32**, 271-281 (1989).

- Emdin, S., Dodson, G., Cutfield, J. & Cutfield, S. Role of zinc in insulin-biosynthesis some possible zinc-insulin interactions in the pancreatic beta-cell. *Diabetologia* **19**, 174-182 (1980).
- Vanschaftingen, E., Detheux, M. & Dacunha, M. Short-term control of glucokinase activity role of a regulatory protein. *Faseb Journal* **8**, 414-419 (1994).
- Cook, D. & Hales, C. Intracellular ATP directly blocks K<sup>+</sup> channels in pancreatic beta-cells. *Nature* **311**, 271-273 (1984).
- Wollheim, C. & Sharp, G. Regulation of insulin release by calcium. *Physiological Reviews* **61**, 914-973 (1981).
- Jones, P., Persaud, S. & Howell, S. Time-course of Ca<sup>2+</sup>-induced insulin secretion from perifused, electrically permeablised Islets of Langerhans effects of cAMP and a phorbol ester. *Biochemical and Biophysical Research Communications* **162**, 998-1003 (1989).
- 38 Permutt, M. A. *The Islets of Langerhans*. (Academic Press, 1981).
- Henriksson, M., Nordling, E., Melles, E., Shafqat, J., Ståhlberg, M., Ekberg, K., Persson, B., Bergman, T., Wahren, J., Johansson, J. & Jörnvall, H. Separate functional features of proinsulin C-peptide. *Cellular and Molecular Life Sciences* **62**, 1772-1778 (2005).
- Henriksson, M., Shafqat, J., Liepinsh, E., Tally, M., Wahren, J., Jörnvall, H. & Johansson, J. Unordered structure of proinsulin C-peptide in aqueous solution and in the presence of lipid vesicles. *Cellular and Molecular Life Sciences* **57**, 337-342 (2000).
- 41 Medawala, W. Mechanistic and Functional Studies of Zinc Activation of C-Peptide and its Effect on Red Blood Cell Metabolism PhD thesis, Michigan State University, (2011).
- Rigler, R., Pramanik, A., Jonasson, P., Kratz, G., Jansson, O. T., Nygren, P. A., Stahl, S., Ekberg, K., Johansson, B. L., Uhlen, S., Uhlen, M., Jornvall, H. & Wahren, J. Specific binding of proinsulin C-peptide to human cell membranes. *Proceedings of the National Academy of Sciences of the United States of America* **96**, 13318-13323 (1999).

- Vague, P., Dufayet, D., Coste, T., Moriscot, C., Jannot, M. F. & Raccah, D. Association of diabetic neuropathy with Na/K ATPase gene polymorphism. *Diabetologia* **40**, 506-511 (1997).
- 44 Pieper, G., Siebeneich, W., MooreHilton, G. & Roza, A. Reversal by L-arginine of a dysfunctional arginine nitric oxide pathway in the endothelium of the genetic diabetic BB rat. *Diabetologia* **40**, 910-915 (1997).
- McNally, P. G., Watt, P. A., Rimmer, T., Burden, A. C., Hearnshaw, J. R. & Thurston, H. Impaired contraction and endothelium-dependent relaxation in isolated resistance vessels from patients with insulin-dependent diabetes mellitus. *Clinical Science* **87**, 31-36 (1994).
- Kitamura, T., Kimura, K., Makondo, K., Furuya, D. T., Suzuki, M., Yoshida, T. & Saito, M. Proinsulin C-peptide increases nitric oxide production by enhancing mitogen-activated protein-kinase-dependent transcription of endothelial nitric oxide synthase in aortic endothelial cells of Wistar rats. *Diabetologia* 46, 1698-1705 (2003).
- 47 Al-Rasheed, N. M., Meakin, F., Royal, E. L., Lewington, A. J., Brown, J., Willars, G. B. & Brunskill, N. J. Potent activation of multiple signalling pathways by C-peptide in opossum kidney proximal tubular cells. *Diabetologia* **47**, 987-997 (2004).
- Kitamura, T., Kimura, K., Jung, B. D., Makondo, K., Sakane, N., Yoshida, T. & Saito, M. Proinsulin C-peptide activates cAMP response element-binding proteins through the p38 mitogen-activated protein kinase pathway in mouse lung capillary endothelial cells. *Biochemical Journal* **366**, 737-744 (2002).
- 49 Steiner, D., Cunningham, D., Spigelman, L. & Aten, B. Insuling biosynthesis evidence for a precursor. *Science* **157**, 697-700 (1967).
- Ko, A., Smyth, D., Markussen, J. & Sundby, F. Amino acid sequence of C-peptide of human proinsulin. *European Journal of Biochemistry* **20**, 190-199 (1971).
- Horwitz, D., Starr, J., Mako, M., Blackard, W. & Rubenstein, A. Proinsulin, insulin, and C-peptide concentrations in human portal and peripheral blood. *Journal of Clinical Investigation* **55**, 1278-1283 (1975).
- Pramanik, A., Ekberg, K., Zhong, Z., Shafqat, J., Henriksson, M., Jansson, O., Tibell, A., Tally, M., Wahren, J., Jörnvall, H., Rigler, R. & Johansson, J. C-peptide binding to human cell membranes: Importance of Glu27. *Biochemical and Biophysical Research Communications* **284**, 94-98 (2001).

- Forst, T., De La Tour, D. D., Kunt, T., Pfützner, A., Goitom, K., Pohlmann, T., Schneider, S., Johansson, B. L., Wahren, J., Löbig, M., Engelbach, M., Beyer, J. & Vague, P. Effects of proinsulin C-peptide on nitric oxide, microvascular blood flow and erythrocyte Na<sup>+</sup>,K<sup>+</sup>-ATPase activity in diabetes mellitus type I. *Clinical Science* **98**, 283-290 (2000).
- Meyer, J. A., Subasinghe, W., Sima, A. A., Keltner, Z., Reid, G. E., Daleke, D. & Spence, D. M. Zinc-activated C-peptide resistance to the type 2 diabetic erythrocyte is associated with hyperglycemia-induced phosphatidylserine externalization and reversed by metformin. *Molecular Biosystems* **5**, 1157-1162 (2009).
- 55 Steiner, D. F. in *Diabetes & C-Peptide* (ed Anders A.F. Sima) (Humana Press, 2012).
- Wahren, J., Johansson, B. & Wallberg-Henriksson, H. Does C-peptide have a physiological role? *Diabetologia* **37**, S99-S107 (1994).
- Wahren, J. C-peptide: new findings and therapeutic implications in diabetes. Clinical Physiology and Functional Imaging **24**, 180-189 (2004).
- Forst, T. & Kunt, T. Effects of C-peptide on microvascular blood flow and blood hemorheology. *Experimental Diabesity Research* **5**, 51-64 (2004).
- Jensen, M. & Messina, E. C-peptide induces a concentration-dependent dilation of isolated skeletal muscle arterioles only in the presence of insulin. *Faseb Journal* **13**, A88-A88 (1999).
- Meyer, J. A., Froelich, J. M., Reid, G. E., Karunarathne, W. K. & Spence, D. M. Metal-activated C-peptide facilitates glucose clearance and the release of a nitric oxide stimulus via the GLUT1 transporter. *Diabetologia* **51**, 175-182 (2008).
- Johansson, B., Kernell, A., Sjoberg, S. & Wahren, J. Influence of combined C-peptide and insulin administration on renal function and metabolic control in diabetes type 1. *Journal of Clinical Endocrinology & Metabolism* **77**, 976-981 (1993).
- Shafqat, J., Melles, E., Sigmundsson, K., Johansson, B. L., Ekberg, K., Alvelius, G., Henriksson, M., Johansson, J., Wahren, J. & Jörnvall, H. Proinsulin C-peptide elicits disaggregation of insulin resulting in enhanced physiological insulin effects. *Cellular and Molecular Life Sciences* **63**, 1805-1811 (2006).

- Sprague, R. S., Ellsworth, M. L., Stephenson, A. H. & Lonigro, A. J. ATP: The red blood cell link to NO and local control of the pulmonary circulation. *American Journal of Physiology-Heart and Circulatory Physiology* **271**, H2717-H2722 (1996).
- Oblak, T. D. A., Root, P. & Spence, D. M. Fluorescence Monitoring of ATP-Stimulated, Endothelium-Derived Nitric Oxide Production in Channels of a Poly(dimethylsiloxane)-Based Microfluidic Device. *Analytical Chemistry* **78**, 3193-3197 (2006).
- Sprague, R. S., Olearczyk, J. J., Spence, D. M., Stephenson, A. H., Sprung. R. W. & Lonigro, A. J. Extracellular ATP signaling in the rabbit lung: erythrocytes as determinants of vascular resistance. *American Journal of Physiology-Heart and Circulatory Physiology* **285**, H693-H700 (2003).
- Keltner, Z., Meyer, J. A., Johnson, E. M., Palumbo, A. M., Spence, D. M. & Reid, G. E. Mass spectrometric characterization and activity of zinc-activated proinsulin C-peptide and C-peptide mutants. *Analyst* 135, 278-288 (2010).
- 67 Masuoka, J. & Saltman, P. Zinc (II) and copper (II) binding to serum albumin a comparative study of dog, bovine, and human albumin. *Journal of Biological Chemistry* **269**, 25557-25561 (1994).
- Shay, N. F. & Tang, X. H. Zinc has an insulin-like effect on glucose transport mediated by phosphoinositol-3-kinase and AKT in 3T3-L1 fibroblasts and adipocytes. *Journal of Nutrition* **131**, 1414-1420 (2001).
- Harmening, D. *Clinical Hematology and Fundamentals of Hemostasis*. (F. A. Davis Co, 2009).
- Brun, J. F., Guintrand-Hugret, R., Fons, C., Carvajal, J., Fedou, C., Fussellier, M., Bardet, L. & Orsetti, A. Effects of oral zinc gluconate on glucose effectiveness and insulin sensitivity in humans. *Biological Trace Element Research* **47**, 385-391 (1995).

## Chapter 4 – Potential Multiple Sclerosis Biomarkers

## 4.1 MS Diagnosis and the Need for Biomarkers

Because of the difficulty of diagnosis, the search for biomarkers for MS has been ongoing since 1922, when an abnormality was first discovered in the CSF of MS patients. Even after almost 100 years of investigation, there is still no biomarker used clinically. Biomarkers are defined as characteristics that can be objectively measured to be evaluated as an indicator of a biological process, normal or pathogenic, or as an indicator of response to pharmaceuticals. In other words, biomarkers should both correlate with how a patient feels, functions, and survives and with the effects of treatment on these areas. Because of the complexity of MS, it is unlikely that one biomarker will be able to encompass the full effect of the disease, but rather one of the many ongoing processes. As a result, there are four proposed biomarker categories for MS: diagnostic biomarkers, predictive biomarkers, process-specific biomarkers and treatment-related biomarkers.

A reliable diagnostic biomarker for MS would discern the difference between healthy persons, MS patients, and patients with other neurological, autoimmune or inflammatory diseases. Currently, IgG oligoclonal bands are used for diagnostics, as described in chapter 1, however they are not specific enough to be considered as a biomarker for the disease. Evidence of IgG oligoclonal bands in the CSF, but not in blood

serum, denotes a local immune response. While this is often seen in MS patients, it can also be seen in a variety of both inflammatory and non-inflammatory disorders as well. Additionally, it is unknown if oligoclonal bands are involved in the pathogenesis of the disease, or if they are a product of the disease, and therefore not a reflection of disease prognosis.<sup>2</sup>

Predictive biomarkers in MS would be used to determine if a patient with CIS would go on to develop the disease during the first clinical manifestation or early phase of the disease. In addition to being diagnostic, IgG has also been suggested to have the potential to be a predictive biomarker as well. The presence of IgG in the CSF has been considered as an indicator of the development of MS in CIS patients. While an increased risk of disease development has been noted in CIS patients with IgG presence, it is not a strong enough correlation to be considered a biomarker. 6 In 2012, Avsar et al. investigated five proteins that have been suggested as potential predictive biomarkers in the CSF: myelin oligodendrocyte glycoprotein (MOG), myelin basic protein (MBP), tau, glial fibrillary acidic protein (GFAP), and neurofilament light chain (NFL). MOG and MBP are both involved in the myelination of nerves and tau, GFAP and NFL are all known to be associated with neuronal damage. The investigators were seeking to predict if patients with CIS would develop MS and to be able to diagnose between the types of MS and determine prognosis. It was found that MOG, tau, GFAP and NFL were only successful predictors of disease classification and prognosis when considered together, and further investigation is needed in larger scale studies to attempt to confirm these findings.<sup>2</sup>

Process-specific biomarkers are not disease specific, but can be indicative of different processes occurring in the disease. In MS, the processes that have been measured with biomarkers include: inflammation, demyelination, oxidative stress, remyelination, and neuroaxonal damage. While these biomarkers do not help with diagnostics, they can be useful to measure disease course.

The final type of biomarker used to study MS is the treatment response biomarker. Genes, mRNA, and protein levels can be used to test the effectiveness of drug therapies. Most of the research in this area to date has focused on IFNs and the response to treatment as a function of genetic variants. These studies are aimed at determining the difference in effectiveness of the treatment in individual patients. If it can be determined that a certain gene allele makes patients more responsive to IFN treatment, that information can be used to aid in the decision of the course of treatment, helping the patient sooner, as well as saving time and money. 5,7

While recent biomarker findings are promising, most use CSF for testing and this is an invasive procedure. CSF is traditionally believed to be the most likely source of a MS biomarker because of the proximity to the inflammation and lesions in the CNS. This may not be the case, as CSF is collected through a lumbar puncture in the lower back and may not accurately reflect inflammatory markers in the brain regions where most

MS lesions occur. Because of the invasiveness of CSF collection, sampling can only be performed for a limited number of time points. Additionally, the production of CSF varies with the time of day and any results would therefore need to be standardized.<sup>8</sup>

As previously discussed, MS patients have been shown to have an increase in RBC-derived ATP release. The studies presented here will confirm those studies as well as show that the increase is, in fact, due to mechanical deformation as a result of shear stress. Based on previous research investigating the role of zinc in MS, the basal level of Zn<sup>2+</sup> was measured in order to show that it is higher in MS patients than in healthy controls, with controls to ensure the same number of cells was being studied in each sample. In addition, the amount of <sup>65</sup>Zn<sup>2+</sup> and the amount of C-peptide interaction with the RBC were also measure to demonstrate the effect of Zn<sup>2+</sup> delivery to the RBC. Finally, because of the increased ATP release from RBCs and the potential for altered glucose metabolism in MS patients, the amount of glucose uptake into the RBC was measured and was expected to be higher than that of normal controls to keep up with the demand for ATP release.

## 4.2 Experimental

### 4.2.1 Preparation of Reagents

Purified water with 18.2 M $\Omega$  resistance was used for all experiments. Zn $^{2+}$  stock solution was prepared by dissolving zinc (II) chloride (Jade Scientific, Canton, MI) in purified water and diluting to 400 nM. Crude C-peptide (Genscript, Piscataway, NJ) was purified using reverse phase high performance liquid chromatography (RP-HPLC) and dried. The purified C-peptide was dissolved in purified water and diluted to a 400 nM working solution. When  $Z_n^{2+}$  bound to C-peptide was added to samples, the  $Z_n^{2+}$  and C-peptide solutions were mixed in water before the addition of any other components or buffers. Physiological salt solution (PSS) was prepared, containing, in mM, 4.7 KCl (Fisher Scientific, Fair Lawn, NJ), 2.0 CaCl<sub>2</sub> (Fisher Scientific), 140.5 NaCl (Columbus Chemical Industries, Columbus, WI), 12  $MgSO_4$ (Fisher Scientific), 21.0 tris(hydroxymethylaminomethane) (Invitrogen, Carlsbad, CA), 5.6 glucose (Sigma, St. Louis, MO), and 5% bovine serum solution (Sigma) at a final pH of 7.4, adjusted with hydrochloric acid. ATP solutions were prepared by first dissolving ATP (Sigma) in purified water to a concentration of 100 μM. Standards were then prepared by dilution of the stock in buffer to concentrations of 0 to 1 µM. For the incubations involving glybenclamide, a 10 mM working solution was prepared dissolving 48 mg of glybenclamide (Sigma) in a 0.1 M sodium hydroxide (Fisher Scientific) solution also containing 50 mg/mL dextrose (Sigma). The glybenclamide was diluted to 100 µM in the

RBC samples. A solution of luciferin/luciferase was prepared by dissolving 2 mg of luciferin (Gold Biotechology, St. Louis, MO) in 5 mL DDW, and transferring this to a vial containing 100 mg of luciferase (Sigma, St. Louis, MO). Saline was prepared by dissolving 9 g of NaCl in 1 L of purified water. The Drabkin's solution used for the determination of hemoglobin was prepared by reconstituting a vial of Drabkin's reagent (Sigma) in 1 L of purified water, adding 0.5 mL of Brij 35 solution, product code B 4184 (Sigma) which contains sodium bicarbonate, potassium ferricyanide and potassium cyanide.

## 4.2.2 Collection and Preparation of Patient and Control Samples

Patient samples were collected at the Neurology and Ophthalmology Clinic at Michigan State University, following their informed consent. The patients also filled out questionnaires pertaining to their sex, age, disease type, duration, and medications. Following venipunture, the samples were refrigerated briefly before being transported to the Spence Lab. For control and patient samples, following venipuncture and collection into heparinized vacutainers (BD, Franklin Lakes, NJ), whole blood was centrifuged for 10 minutes at 500g to separate the RBCs from the other blood components. Following the removal of the plasma and buffy coat, by aspiration, the RBCs were washed three times with PSS and centrifuged as previously stated. After the final washing, the supernatant was removed and the hematocrit of the RBCs was measured using a CritSpin© analyzer.

## 4.2.3 Determination of Radiolabelled Zn<sup>2+</sup> Interaction with MS Patient RBCs

The amount of  $Zn^{2+}$  interacting with MS and healthy RBCs was determined using the radioligand <sup>65</sup>Zn<sup>2+</sup> and C-peptide. First, <sup>65</sup>Zn<sup>2+</sup> and C-peptide were incubated together in pure water for three minutes to ensure peptide activation. PSS was then added to the mixture, immediately followed by the addition of the appropriate volume of RBCs to prepare 1 mL samples with a 7% hematocrit. Following a two hour incubation at 37°C, samples were centrifuged at 500g for 4 minutes and the supernatant was collected. In a 96-well plate, 200 μL of supernatant were combined with 100 μL of scintillation cocktail (Optiphase Supermix, Perkin Elmer, Waltham, MA). An appropriate range of standards was also prepared and measured. The amount of radioactivity in each sample was then determined using a 1450 Microbeta Plus liquid scintillation counter (Wallac, Turku, Finland). The concentration of  $^{65}Zn^{2+}$  in each sample was quantified by comparing to a set of standards prepared in RBC supernatant. Knowing the amount of  $^{65}$ Zn  $^{2+}$  added to the original RBC sample, and how much was left in the supernatant, the amount of <sup>65</sup>Zn<sup>2+</sup> interacting with the RBCs can be determined by subtraction.

## 4.2.4 Determination of Radiolabelled Glucose Uptake of MS Patient RBCs

Radiolabeled <sup>14</sup>C-glucose was used to determine the amount of glucose taken into the RBC,. After the RBCs were purified, they were incubated with <sup>14</sup>C-glucose alone or <sup>14</sup>C-

glucose and  $Zn^{2+}$  bound to C-peptide. For the samples incubated with  $Zn^{2+}$  bound to Cpeptide, Zn<sup>2+</sup> and C-peptide were first combined in a 1:1 ratio and allowed to interact for three minutes before the addition of 36 μL of 5 millicurie per 50 mL sterile water <sup>14</sup>C-glucose (Moravek Biochemicals, Brea, CA) and the correct volumes of PSS and RBCs to make a 1 mL sample of 7% RBCs. For the samples without Zn<sup>2+</sup> bound to C-peptide, equivalent volumes of purified water were used in place of the Zn<sup>2+</sup> and C-peptide solutions. Following the addition of the RBCs, the samples were incubated for 4 hours at 37°C before being centrifuged at 500g for 4 minutes. The supernatant was then removed and discarded and the cells were resuspended in PSS and centrifuged again. This process was repeated three times to ensure the removal of excess <sup>14</sup>C-glucose from the RBCs. Once washed, the RBCs were then lysed with 1 mL of bleach. After waiting 30 minutes, the samples were centrifuged at 500g for 4 minutes for any debris to settle. A standard curve of <sup>14</sup>C-glucose was prepared by adding 5 µL of <sup>14</sup>C-glucose to 1 mL of bleach and making three 1:1 serial dilutions. A 96-well plate was then prepared with 200 μL of supernatant, combined with 100 μL of scintillation cocktail (optiphase supermix, Perkin Elmer, Waltham, MA), and the amount of radioactivity in each sample was then determined using a 1450 Microbeta Plus liquid scintillation counter (Wallac, Turku, Finland). While the radioactivity of the <sup>14</sup>C-glucose is known, the number of radiolabeled carbons on each glucose molecule can vary. Therefore, the amount of radioactivity cannot be directly calibrated to the amount of glucose uptake into the RBCs. For this reason, the amount of <sup>14</sup>C-glucose was normalized by counts per minute to the measurement for healthy RBCs.

## 4.2.5 Determination of ATP Release from MS Patient RBCs in Response to Flow

ATP release was determined in a manner than has been previously reported. 9 After purification, RBCs are diluted to a 7% hematocrit and pumped through tubing with dimensions similar to arterioles. In response to mechanical deformation, ATP is released from RBCs. To accomplish this, two syringes, one containing the sample solution and the other containing a luciferin/luciferase mixture, were used in a dual syringe pump. Solutions were pumped, at 6.7 μL/min, through 50 μm internal diameter microbore tubing. The solutions met at a mixing T-junction and the combined stream was pumped through an additional segment of 75 µm internal diameter tubing, with a portion of the polyimide coating removed, over a PMT in a light excluding box, as shown in figure 4.1. This allowed for the chemiluminescence resulting from the reaction of ATP with luciferin/luciferase to be detected. Comparing to a calibration curve of ATP standards with known concentrations, the amount of ATP released from the RBCs was calculated. To ensure the ATP was not the result of lysis, samples of the RBCs were incubated with glybenclamide for one hour before measurement.

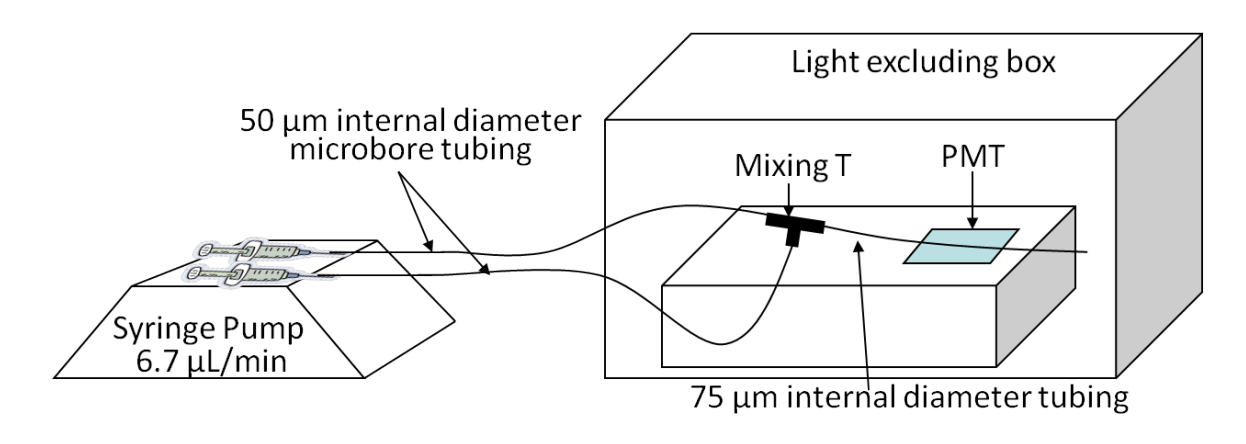


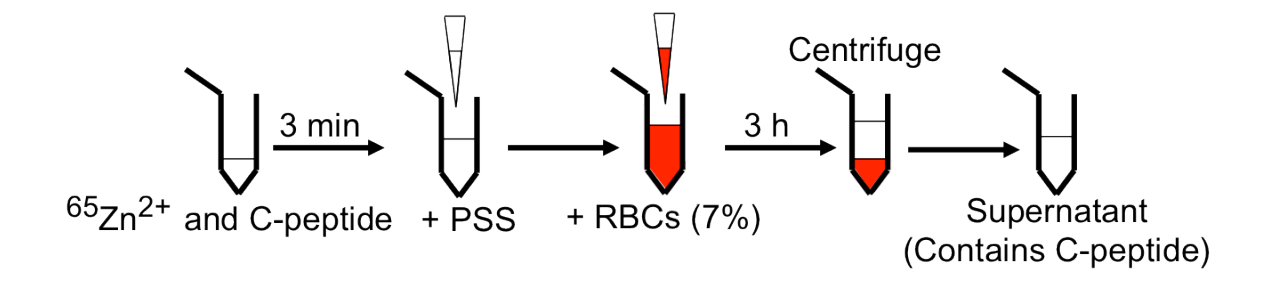
Figure 4.1 – Determination of ATP Release from MS Patient RBCs in Response to Flow – RBCs were diluted to a 7% hematocrit and pumped through tubing, one syringe containing the sample and the other containing luciferin/luciferase. Solutions were pumped, at 6.7  $\mu$ L/min, through 50  $\mu$ m internal diameter microbore tubing. The solutions met at a mixing T-junction and the combined stream was pumped through an additional segment of 75  $\mu$ m internal diameter tubing, with a portion of the polyimide coating removed, over a PMT in a light excluding box. This allowed for the chemiluminescence resulting from the reaction of ATP with luciferin/luciferase to be detected.

## 4.2.6 Determination of C-peptide Interaction with MS Patient RBCs and the Plasma Concentration of C-Peptide by Enzyme Linked Immunosorbent Assay

The interaction between Zn<sup>2+</sup> bound to C-peptide and RBCs was studied using solutions containing 7% RBCs and 20 nM each of Zn<sup>2+</sup> and C-peptide. Samples were prepared by mixing the appropriate volumes of Zn<sup>2+</sup> and C-peptide in water for several minutes before adding PSS, immediately followed by the RBCs from either MS patients or healthy controls. Following a three hour incubation at 37°C, the samples were centrifuged at 500g for 4 minutes and the C-peptide remaining in the supernatant was measured using an enzyme-link immunosorbent assay (ELISA) (Millipore, Billerica, MA). The process of an ELISA is depicted in figure 4.2. The amount of C-peptide in the supernatant was calculated using C-peptide standards that were prepared in the supernatant of a 7% RBC sample in order to account for any matrix effects. Knowing this, the amount of C-peptide interaction with the RBC was calculated.

# 4.2.7 Determination of Basal Zn<sup>2+</sup> Levels in MS Patient RBCs by Atomic Absorption Spectroscopy

To compare the basal levels of  ${\rm Zn}^{2+}$  on the RBCs from MS patients and healthy controls, the amount of  ${\rm Zn}^{2+}$ , relative to the amount of hemoglobin, was determined using atomic absorption spectroscopy. <sup>10</sup> After the initial centrifugation of the RBCs, 200  $\mu$ L of the cells were removed and set aside. These RBCs were washed three times with 1 mL



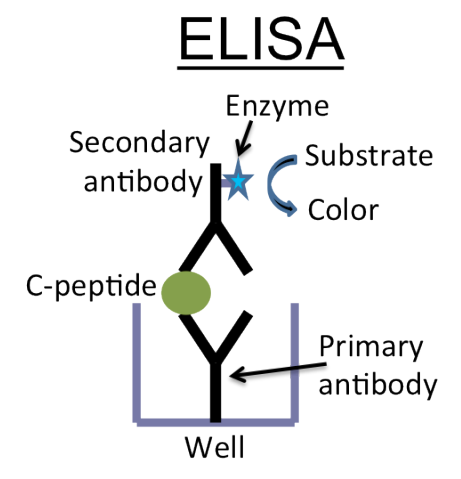


Figure 4.2 – Determining C-peptide Interaction with the RBCs of MS Patients using Enzyme-Linked Immunosorbent Assay – The interaction between  $Zn^{2+}$  bound to C-peptide and RBCs was studying using solutions containing 7% RBCs and 20 nM each of  $Zn^{2+}$  and C-peptide. Samples were prepared by mixing the appropriate volumes of  $Zn^{2+}$  and C-peptide in water for several minutes before adding PSS, immediately followed by the RBC of either MS patients or healthy controls. Following a three hour incubation at 37°C, the samples were centrifuged at 500g for four minutes and the C-peptide remaining in the supernatant was measured using an ELISA.

of saline, centrifuged at 500g for 4 minutes with removal of the supernatant after each washing. Following the washings,  $100~\mu L$  of the RBCs were lysed with  $200~\mu L$  of cold, purified water. Because of the complex matrix, samples were prepared using the standard addition method. In this method, an aliquot of lysed RBCs and a known amount of  $Zn^{2+}$  were added to each sample, allowing for the calculation of the original amount of  $Zn^{2+}$  in the solution using the equation:

$$c_X = \frac{bc_s}{mV_x}$$

where b and m are the intercept and slope, respectively, of the resulting calibration curve,  $c_x$  is the unknown concentration of  $Zn^{2+}$  in the initial solution,  $c_s$  is the known concentration of the standard solution added to each sample, and  $V_x$  is the volume of identical aliquots of the lysed RBC solution in each sample. A blank with only an aliquot of lysed RBCs was also measured. To account for differences in hematocrit and number of cells in the lysed RBC solutions, the amount of hemoglobin (Hb) in each lysate was also measured. A stock solution of hemoglobin was prepared by dissolving solid hemoglobin (Sigma) in purified water before being diluted to 0.72 mg/mL in Drabkin's Reagent. Several further dilutions were made in Drabkin's Reagent to create a calibration curve. The lysed RBC solutions were diluted 2:1000. 200  $\mu$ L of each solution were pipetted into a 96-well plate, and after 15 minutes, the absorbance was measured on a plate reader (SpectraMax M4, Molecular Devices, Sunnyvale, CA) at 540 nm. The

amount of  $Zn^{2+}$  in the RBC samples was then reported as micrograms of  $Zn^{2+}$  per gram of hemoglobin.

## 4.3 Results

The amount of ATP release from the RBCs of MS patients was found to be an average of  $344.7 \pm 46.8$  nM where the average release from healthy controls was  $132.1 \pm 14.1$  nM, as seen in figure 4.3. Reaffirming the preliminary studies, <sup>11</sup> the ATP release of the RBCs from the MS patients was nearly three times the amount of that from the healthy controls. When the RBCs of the MS patients were incubated with a CFTR inhibitor, glybenclamide, the ATP release is blocked back down below the amount of the healthy controls, to a level of  $65.3 \pm 11.6$  nM, showing that the increase in ATP release of the flowing RBCs of MS patients is not the result of RBC lysis.

Figure 4.4 shows the basal amount of  $Zn^{2+}$  in the RBCs of the MS patients was found to be 41.8  $\pm$  1.7  $\mu$ g of  $Zn^{2+}$ /g Hb, which is a 27% increase of the basal levels of  $Zn^{2+}$  of the RBCs of healthy controls, 32.9  $\pm$  2.2  $\mu$ g of  $Zn^{2+}$ /g Hb. Additionally, the amount of  $^{65}Zn^{2+}$  that is able to interact with the RBCs of MS patients is significantly higher, at a value of 3.61  $\pm$  0.22 picomoles, than that of healthy controls, at a value of 2.26  $\pm$  0.24 picomoles, as seen in figure 4.5. Similarly, it can be seen in figure 4.6 that the amount of C-peptide interacting with the RBCs of MS patients, 3.61  $\pm$  0.18 picomoles, is very similar to the

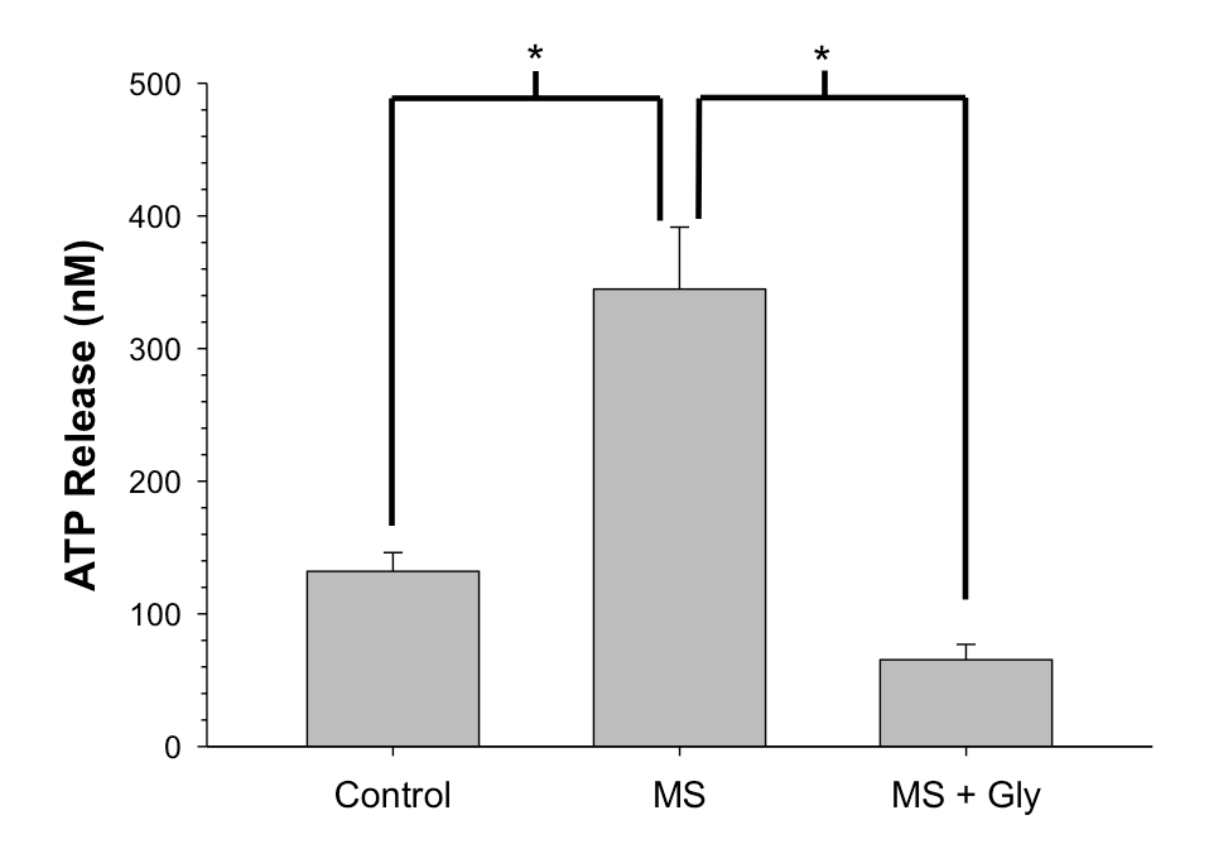


**Figure 4.3 – ATP Release from RBCs of MS Patients –** The results from the ATP release studies show that the ATP release from the RBCs of MS patients was found to be an average of  $344.7 \pm 46.8$  nM where the average release from healthy controls was  $132.1 \pm 14.1$  nM. When the RBCs of the MS patients were incubated with a CFTR inhibitor, glybenclamide, the ATP release is decreased back down below the amount of the healthy controls, to a level of  $65.3 \pm 11.6$  nM, showing that the increase in ATP release of the flowing RBCs of MS patients is not the result of RBC lysis. The error is reported as standard error of the mean, for N = 19 MS patients, 10 healthy controls and 12 glybenclamide inhibitions. The asterisk represents p < 0.001.

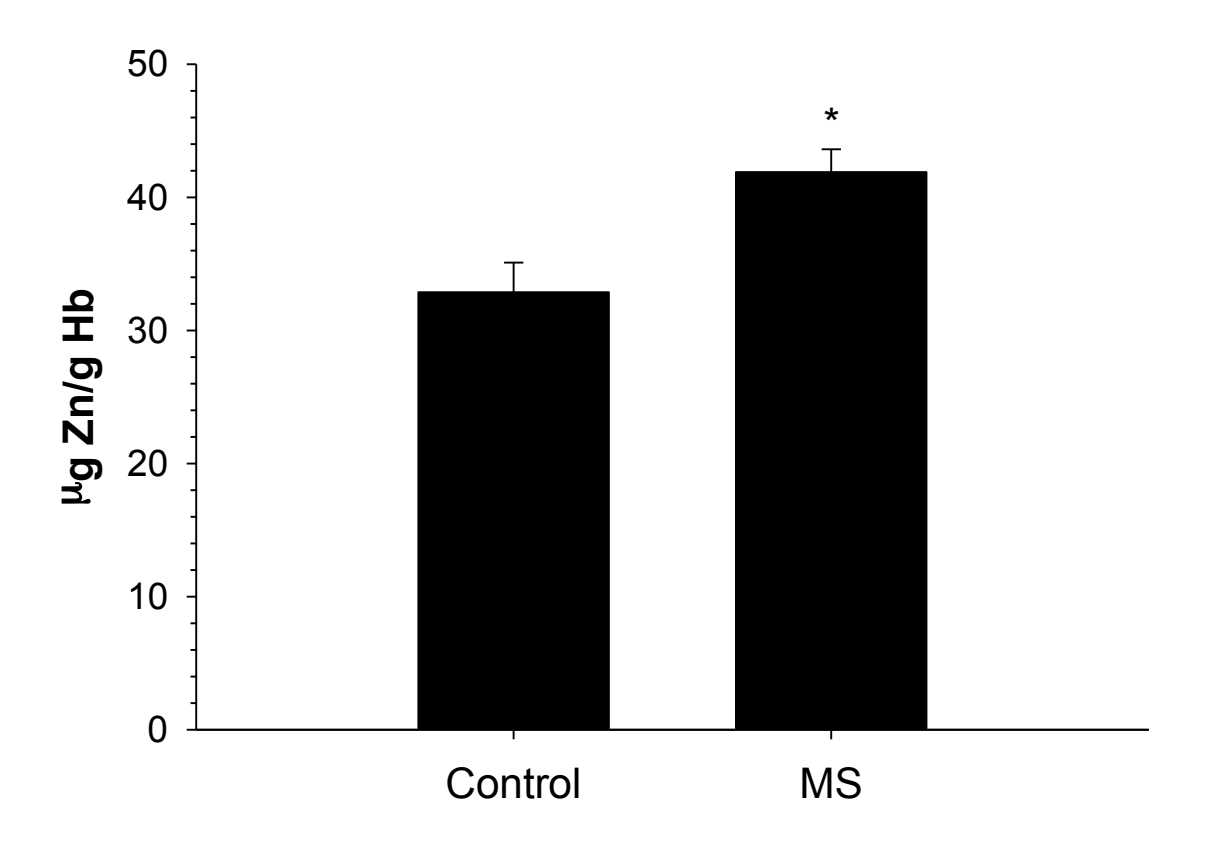


Figure 4.4 – Basal Levels of  $Zn^{2+}$  in the RBCs of MS Patients – The basal amount of  $Zn^{2+}$  in the RBCs of the MS patients was found to be 41.8  $\pm$  1.7  $\mu$ g of  $Zn^{2+}/g$  Hb, which is a 27% increase of the basal levels of  $Zn^{2+}$  of the RBCs of healthy controls, 32.9  $\pm$  2.2  $\mu$ g of  $Zn^{2+}/g$  Hb. The error is reported as standard error of the mean for N = 21 MS patients and 11 healthy controls. The asterisk represents p < 0.01 as compared to the control sample.

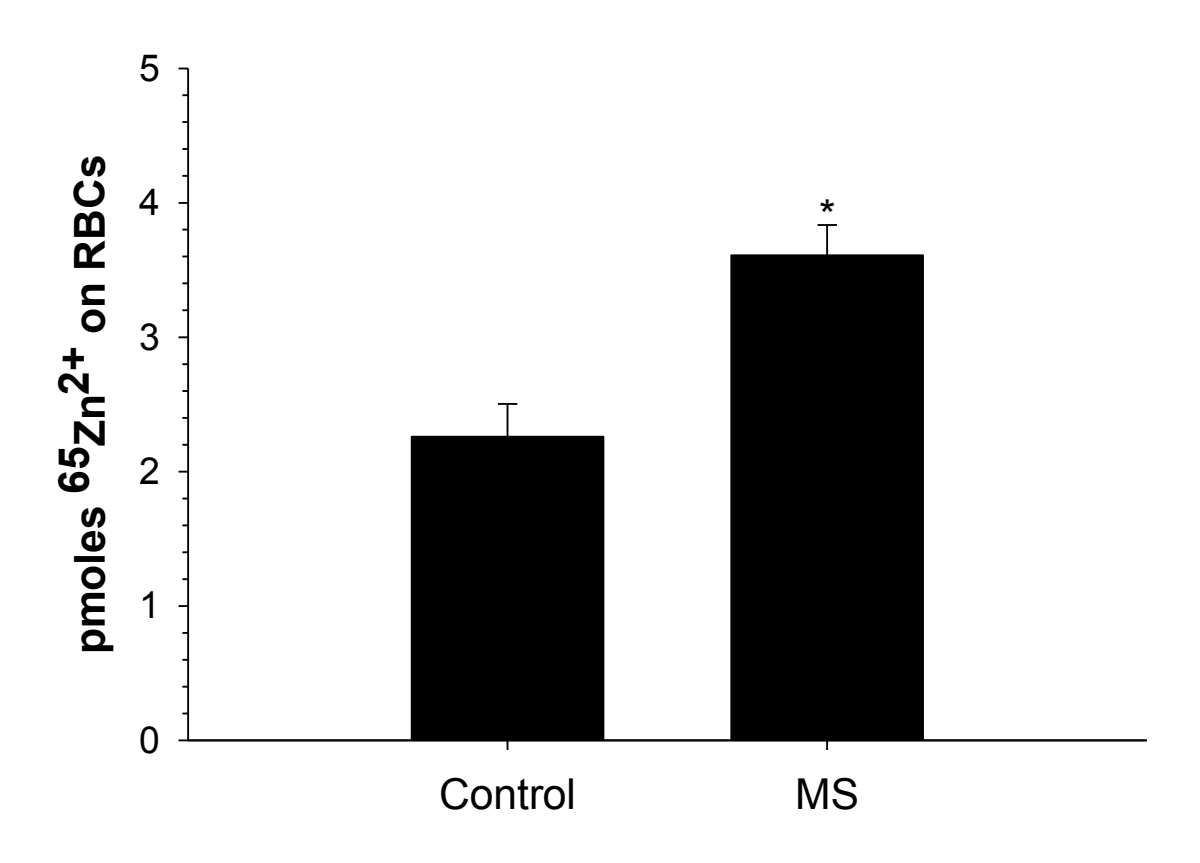
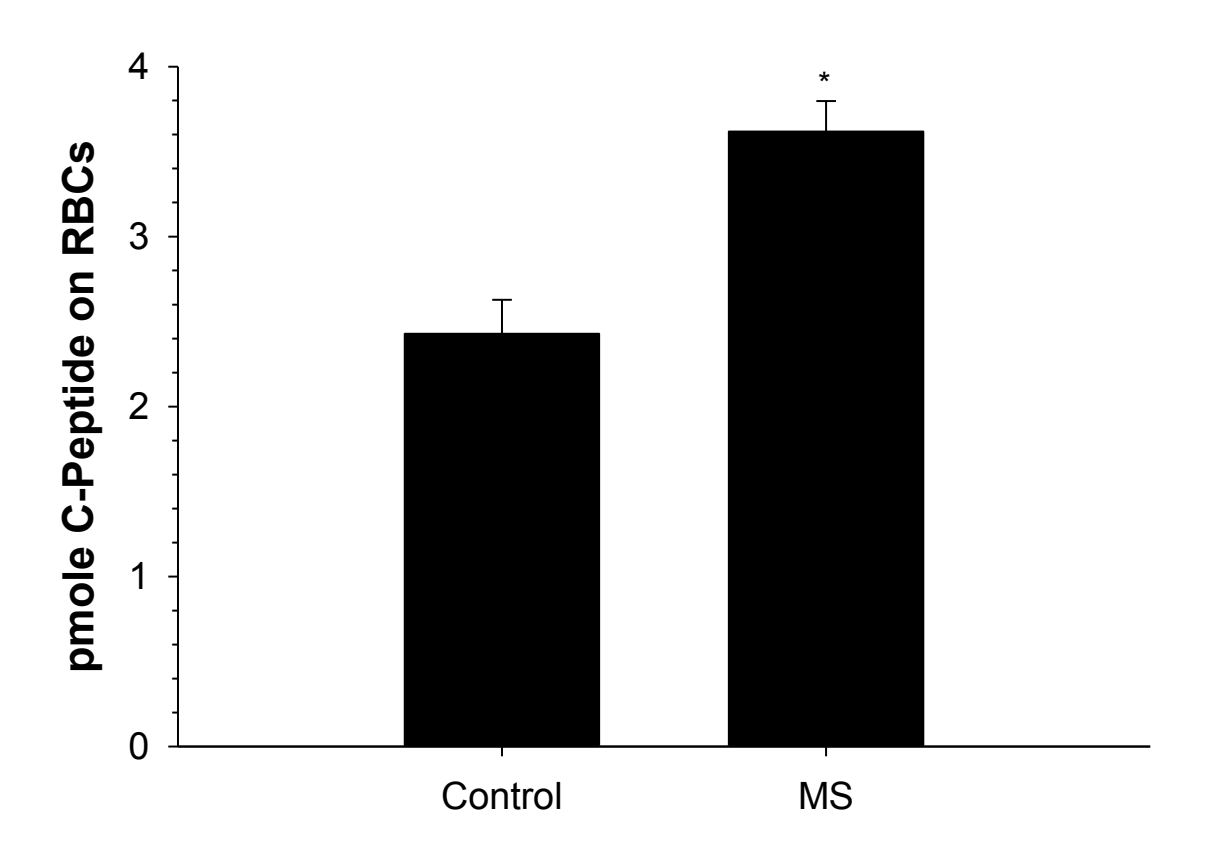


Figure 4.5 –  $^{65}$ Zn<sup>2+</sup> interaction with the RBCs of MS Patients – The amount of  $^{65}$ Zn<sup>2+</sup> that is able to interact with the RBCs of MS patients is significantly higher, at a value of 3.61  $\pm$  0.22 picomoles, than that of healthy controls, at a value of 2.26  $\pm$  0.24 picomoles. The amount of C-peptide interaction with the RBC correlates to this very well, as shown in figure 4.6. The error is reported as standard error of the mean for N = 22 MS patients and 11 healthy controls. The asterisk represents p < 0.001 as compared to the control samples.



**Figure 4.6 – C-peptide Interaction with the RBCs of MS Patients –** Correlating to the data in figure 4.5, it can be seen that the amount of C-peptide interacting with the RBCs is very similar to the amount of  $^{65}$ Zn $^{2+}$ .  $3.61 \pm 0.18$  picomoles of C-peptide interacted with the RBCs of MS patients, while only  $2.43 \pm 0.20$  picomoles interacted with the RBCs of healthy controls. The error is reported as standard error of the mean for N = 12 MS patients and 6 healthy controls. The asterisk represents p < 0.001 as compared to the control sample.

amount of  $^{65}$ Zn $^{2+}$  interacting with these cells. Also shown in these results, only 2.43 ± 0.20 picomoles of  $^{65}$ Zn $^{2+}$  interacted with the RBCs of healthy controls.

The final set of experiments completed with the MS patient samples was to investigate the glucose uptake into the RBCs of both the patient and healthy control groups. Figure 4.7 shows the results, and it should be noted that the x-axis does not start at zero, so while there are differences, they are not as extreme as they seem. Comparing the RBCs of the MS patients and those of the healthy control, no significant difference was seen in the amount of glucose uptake. However, when the RBCs were stimulated by  $\mathrm{Zn}^{2+}$  bound to C-peptide, those from the MS patients took in 6.0  $\pm$  0.1% more glucose than those of the healthy controls. While this seems like a small increase, it was a statistically significant one.

## 4.4 Discussion

As expected, the ATP release from the RBCs of MS patients was nearly three times that of the RBC from healthy controls. As shown in figure 4.3, while there is a statistical difference, the standard deviation for the average from the MS patients is quite large. This may be due to differences in the individual patients, such as age, sex disease type and duration, or even medications. While data was collected on these areas for each patient, the sample set is not yet large enough to separate by those factors. Additionally, for this data set, the MS samples were also incubated with glybenclamide. This pharmaceutical has been shown to be an inhibitor of the cystic fibrosis

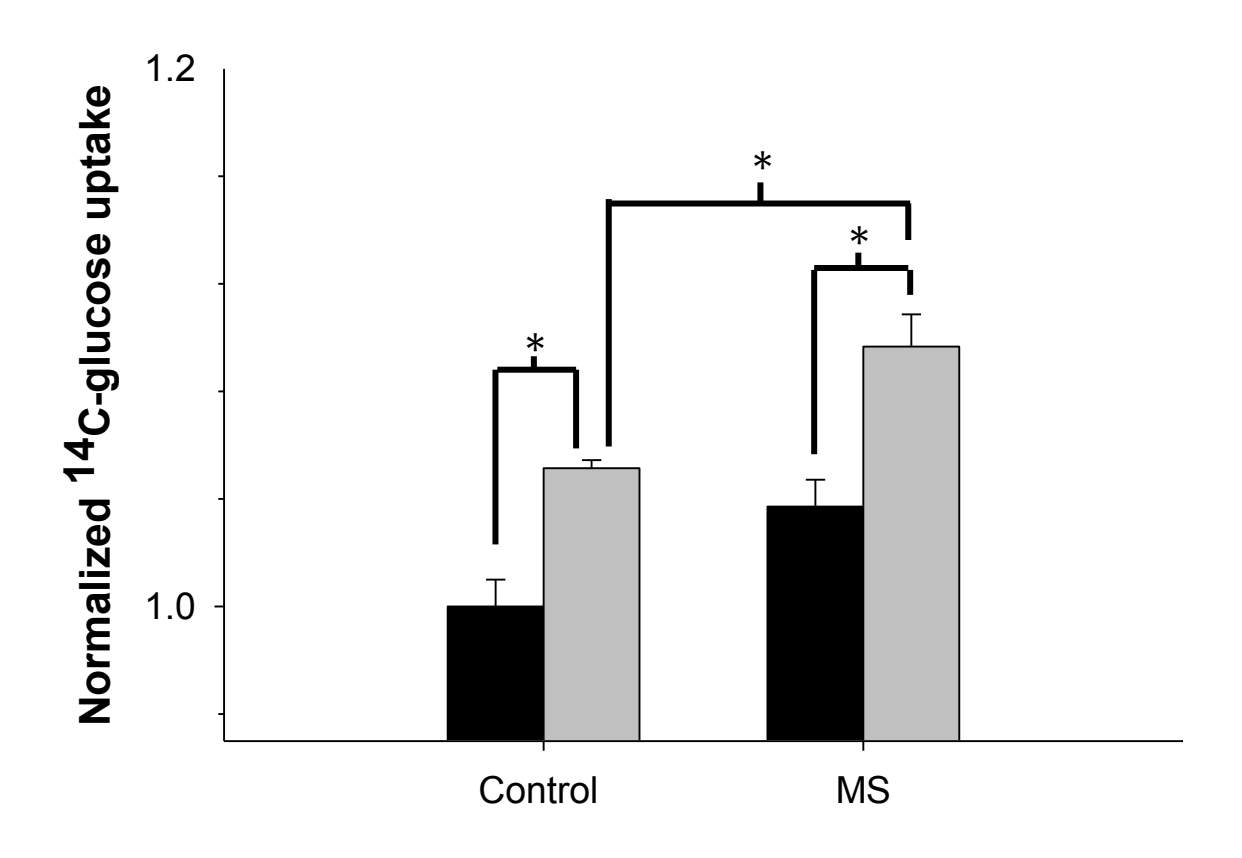


**Figure 4.7 – Glucose Uptake into the RBCs of MS Patients –** It should be noted that the x-axis does not start at zero, so while there are differences, they are not as extreme as they seem. Comparing the untreated RBCs (black) of the MS patients and those of the healthy control, no significant difference was seen in the amount of glucose uptake. However, when the RBCs were stimulated by  $Zn^{2+}$  bound to C-peptide (grey), those from the MS patients took in  $6.0 \pm 0.01\%$  more glucose than those of the healthy controls. While this seems like a small increase, it is a statistically significant one. The error is reported as standard error of the mean for N = 22 MS patient RBC samples and 11 healthy control RBC samples. The asterisk represents p < 0.001 and the pound sign represents p < 0.01.

transmembrane conductance regulator (CFTR).<sup>12</sup> CFTR has also been implicated as necessary in RBC-derived ATP in response to mechanical deformation.<sup>13</sup> Therefore, the subsequent decrease of ATP release from RBC following incubation with glybenclamide shows that the increase in ATP in the samples for the MS patients is not due to lysis of the cells, but is, in fact, due to an increase in ATP release from the RBCs. It is known that RBC-derived ATP increases the production of nitric oxide (NO) in the endothelial cells lining the blood vessels.<sup>14</sup>

This is significant due to previous reports showing the increased levels of NO and its metabolites in the lesions that occur as a result of demyelination and in the cerebral spinal fluid (CSF), serum and urine of MS patients. Knowing that there is an increase in RBC-derived ATP in MS patients, it logically follows that there would be an increase in NO production in these patients as well. NO has been suggested as one of the factors involved in the change in permeability of the blood brain barrier leading to its breakdown. The research presented here has potentially found another link further upstream in this process and may help the overall understanding of the etiology of MS.

While the increase in glucose uptake in the RBCs of MS patients as compared to healthy controls, as shown in figure 4.7, is not significant, the RBCs of both groups had a significant increase in glucose uptake when incubated with Zn<sup>2+</sup> bound to C-peptide and the increase glucose uptake of the RBCs of MS patents was significantly higher than that

of the RBCs of the healthy controls. These finding were expected, as glucose is used in glycolysis to produce ATP in the RBC. The increase in ATP release from the RBC would likely require an increase in ATP production, resulting in the need for an increase in glucose uptake. While glucose metabolism has only been investigated in MS in a very limited capacity, it had previously been shown that MS patients had a significant increase in the ATP content of their RBCs after an intake of 50 g of glucose that was not seen in healthy controls. 17 It has also been noted that there is an increase in glucose metabolism outside of the mitochondria in the CSF of MS patients. <sup>18</sup> This suggests that there may be some dysfunction of glucose metabolism in MS patients.  $Zn^{2+}$  has previously been implicated in increased glucose uptake in fibroblasts and adipocytes. 19 Until now, this had never been investigated in RBCs. When taken together, the results from chapter 3 showing the ability of Zn<sup>2+</sup> bound to C-peptide to deliver Zn<sup>2+</sup> to the RBC and data presented here showing an increase in glucose uptake in the RBCs of both MS patients and healthy controls when incubated with Zn<sup>2+</sup> bound to C-peptide lead to the conclusion that  ${\rm Zn}^{2+}$  also causes an increase in glucose uptake in human RBCs. It is interesting to note that while the idea of altered glucose metabolism in MS patients has only been limitedly explored, <sup>17,20</sup> there is genetic overlap between type 1 diabetes and MS, with a significant increase in prevalence of MS in the first-degree relatives of type 1 diabetics. <sup>21</sup> Genetic investigation is still ongoing, however, there has been some evidence of overlap between single neucleotide polymorphisms associated with type 1 diabetes and those associated with MS.  $^{22}$ 

As seen in figure 4.4, the basal level of Zn<sup>2+</sup> in the RBCs of MS patients is higher than that of healthy controls. Because of the nature of the samples, this level was measured in relation to the amount of hemoglobin to ensure that the same number of RBCs were being analyzed. There has been some previous discussion about the role of Zn<sup>2+</sup> in MS, though it has not been the focus of major MS research. It has been noted that in areas of Zn<sup>2+</sup> contamination, either in the soil and water, or from Zn<sup>2+</sup> smelters, clusters of MS have been found. 23-25 Other reports have shown that the RBCs of MS patients have increased levels of  $Zn^{2+}$ , even when they are not associated with an MS cluster. While the amount of  $Zn^{2+}$  in or on the RBC was increased, the serum  $Zn^{2+}$  levels did not differ between these groups, suggesting the increase in RBC  $\mathrm{Zn}^{2+}$  levels is not a result of defective Zn<sup>2+</sup> absorption or individual nutrition.<sup>26</sup> The previous research in this area has hypothesized that the amount of  $\mathrm{Zn}^{2+}$  in the RBC was correlated with a decrease in the amount of cholesterol in the cells as well. Here it is concluded that regardless of the amount of cholesterol, the amount of basal Zn<sup>2+</sup> in the RBCs of MS patients is higher than that of healthy controls.

While there has been previous research into the amount of Zn<sup>2+</sup> bound to the RBC, there has not been research performed investigating the ability of the RBCs of MS patients to bind  $Zn^{2+}$ . Looking at the amounts of  $^{65}Zn^{2+}$  and C-peptide interacting with the RBC in figures 4.5 and 4.6, respectively, it is clear that for both molecules the amount was higher with the RBCs of MS patients as compared to healthy controls. Comparing the data presented in figures 4.5 and 4.6, it can be observed that the average amounts of <sup>65</sup>Zn<sup>2+</sup> and C-peptide interacting with the RBC are nearly identical. This confirms the data described in chapter 2 showing the interaction of Zn<sup>2+</sup> and Cpeptide with the RBC occurs at a 1:1 ratio. While C-peptide has never been implicated in the etiology of MS, one of the following possibilities may serve to explain the increased interaction. The β-cells of MS patients may contain an increased amount of Zn<sup>2+</sup>, allowing for more of the C-peptide become Zn<sup>2+</sup> bound to C-peptide. Another possibility may be an increase in number of binding sites on each RBC in MS patients. While the identity of this binding site is not currently known, work is currently being done in the Spence group investigating GLUT1 as a potential target, hypothesizing that the larger increase in glucose uptake by the RBCs may be the result of Zn<sup>2+</sup> binding to the protein in the membrane. This will be discussed further in the future work section of chapter 5.

The collection of information from MS patients regarding age, sex, disease type and duration, and the usage of steroids and other medications was done in a hope to

discover a link between these areas and the biological effects of the disease on the RBC as studied. The vast majority of the pool of patients to date has been relapse-remitting MS patients, and the pool is not yet large enough to discern differences in many of the areas listed above. However, as seen in figure 4.8, there is a significant difference in the amount of  $^{65}Zn^{2+}$  interaction with the RBC between males and females patients with MS that is not seen in healthy controls. The highest amount of  $^{65}Zn^{2+}$  interacting with the RBC s is seen in male MS patients. While females are twice as likely as males to develop the disease, men with MS tend to progress to disability at a more rapid rate. With a larger sample size it will be interesting to see if the higher levels of  $^{65}Zn^{2+}$  will have down stream effects of increase glucose uptake and ATP release from the RBCs of male MS patients. This could potentially lead to discoveries into the etiology of MS and the sex differences seen in the disease.

While there needs to be more conclusive evidence before any one of these elements of MS etiology can be used as a clinical biomarker, the research presented here shows several potential targets. As further data is collected on the various types of MS, along with CIS patients, and immune disease and neurological controls, hopefully, one of these targets will prove to be a usable biomarker for the detection and monitoring of MS.

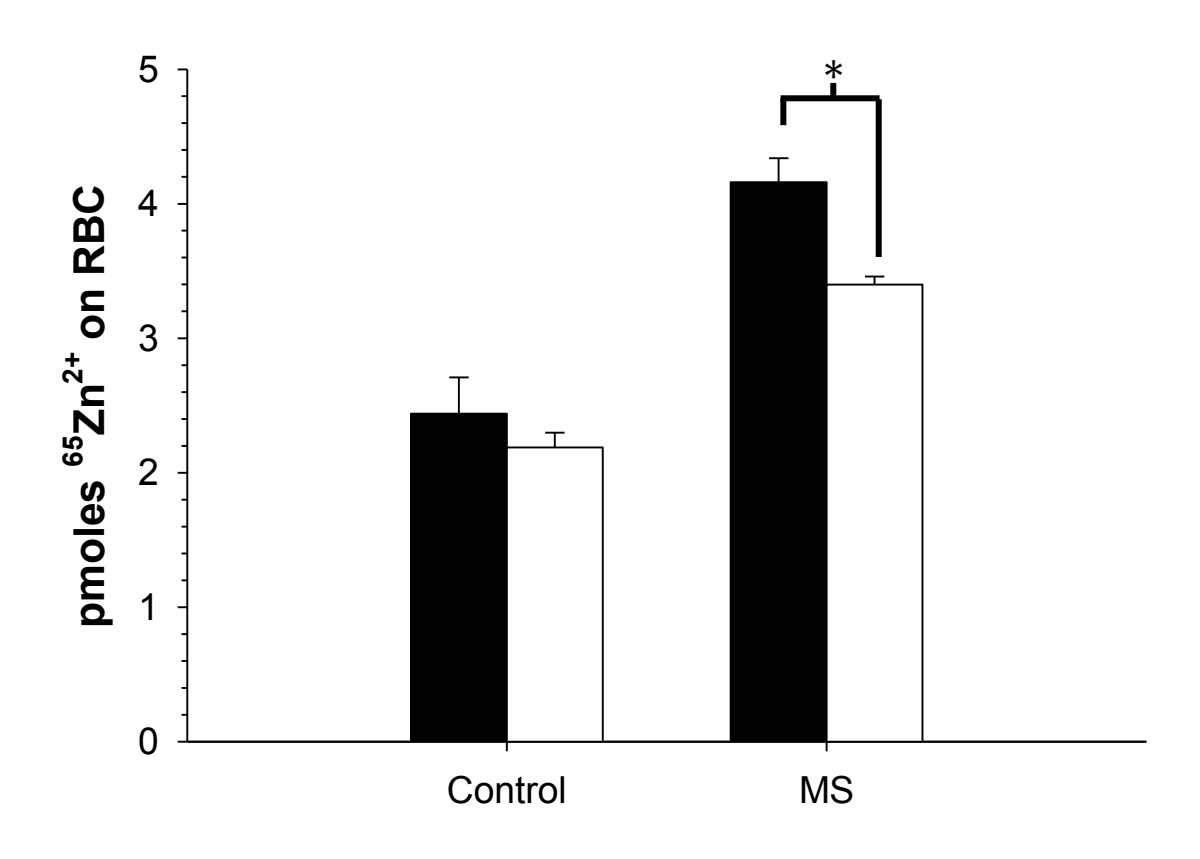


**Figure 4.8 – The Difference in**  $^{65}$ **Zn**  $^{2+}$  **interaction with the RBCs of Male and Female MS Patients –** There is a significant difference in the amount of  $^{65}$ Zn  $^{2+}$  interaction with the RBC between male (black bars) and female (white bars) patients with MS that is not seen in healthy controls. The highest amount of  $^{65}$ Zn  $^{2+}$  interacting with the RBC s is seen in male MS patients at a level of  $4.16 \pm 0.18$  picomoles. The error is shown as standard error of the mean for N = 6 male MS patients, 3 male healthy controls, 16 female MS patients, and 8 female healthy controls. The asterisk represents p < 0.001.

REFERENCES

#### REFERENCES

- Awad, A., Hemmer, B., Hartung, H. P., Kieseier, B., Bennett, J. L. & Stuve, O. Analyses of cerebrospinal fluid in the diagnosis and monitoring of multiple sclerosis. *Journal of Neuroimmunology* **219**, 1-7 (2010).
- Avsar, T., Korkmaz, D., Tütüncü, M., Demirci, N. O., Saip, S., Kamasak, M., Siva, A. & Turanli, E. T. Protein biomarkers for multiple sclerosis: semi-quantitative analysis of cerebrospinal fluid candidate protein biomarkers in different forms of multiple sclerosis. *Multiple Sclerosis Journal* **18**, 1081-1091 (2012).
- Biomarkers Definitions Working Group. Biomarkers and surrogate endpoints: Preferred definitions and conceptual framework. *Clinical Pharmacology & Therapeutics* **69**, 89-95 (2001).
- 4 Prentice, R. Surrogate endpoints in clinical trials definition and operational criteria. *Statistics in Medicine* **8**, 431-440 (1989).
- 5 Comabella, M. & Khoury, S. J. in *Multiple Sclerosis: Diagnosis and Therapy* (ed Howard L. Weiner) Ch. 2, 26-55 (2012).
- Villar, L. M., Masjuan, J., González-Porqué, P., Plaza, J., Sádaba, M. C., Roldán, E., Bootello, A. & Alvarez-Cermeño, J. C. Intrathecal IgM synthesis predicts the onset of new relapses and a worse disease course in MS. *Neurology* **59**, 555-559 (2002).
- 7 Cénit, M. D., Blanco-Kelly, F., de las Heras, V., Bartolomé, M., de la Concha, E. G., Urcelay, E., Arroyo, R. & Martínez, A. Glypican 5 is an interferon-beta response gene: a replication study. *Multiple Sclerosis* **15**, 913-917 (2009).
- Bielekova, B. & Martin, R. Development of biomarkers in multiple sclerosis. *Brain* **127**, 1463-1478 (2004).
- 9 Subasinghe, W. & Spence, D. M. Simultaneous determination of cell aging and ATP release from erythrocytes and its implications in type 2 diabetes. *Analytica Chimica Acta* **618**, 227-233 (2008).
- Whitehouse, R., Prasad, A., Rabbani, P. & Cossack, Z. Zn<sup>2+</sup> in plasma, neutrophils, lymphocytes, and erythrocytes as determined by flameless atomic absorption spectrophotometry. *Clinical Chemistry* **28**, 475-480 (1982).

- Spence, D. M., Letourneau, S., Hernandez, L. & Faris, A. N. Evaluating the effects of estradiol on endothelial nitric oxide stimulated by erythrocyte-derived ATP using a microfluidic approach. *Analytical and Bioanalytical Chemistry* **397**, 3369-3375 (2010).
- Schultz, B. D., DeRoos, A. D., Venglarik, C. J., Singh, A. K., Frizzell, R. A. & Bridges,
   R. J. Glibenclamide blockade of CFTR chloride channels. *American Journal of Physiology-Lung Cellular and Molecular Physiology* 271, L192-L200 (1996).
- Sprague, R. S., Ellsworth, M. L., Stephenson, A. H., Kleinhenz, M. E. & Lonigro, A. J. Deformation-induced ATP release from red blood cells requires CFTR activity. *American Journal of Physiology* **275**, H1726-1732 (1998).
- Sprague, R. S., Ellsworth, M. L., Stephenson, A. H. & Lonigro, A. J. ATP: The red blood cell link to NO and local control of the pulmonary circulation. *American Journal of Physiology-Heart and Circulatory Physiology* **271**, H2717-H2722 (1996).
- Smith, K. J. & Lassmann, H. The role of nitric oxide in multiple sclerosis. *Lancet Neurology* **1**, 232-241 (2002).
- Boje, K. M. K. & Lakhman, S. S. Nitric oxide redox species exert differential permeability effects on the blood-brain barrier. *Journal of Pharmacology and Experimental Therapeutics* **293**, 545-550 (2000).
- 17 Raczkiewicz, J. & Leyko, W. Adenine Nucleotide Content of Erythrocytes of Multiple Sclerosis Patients. *Clinica Chimica Acta* **14**, 408-409 (1966).
- Regenold, W. T., Phatak, P., Makley, M. J., Stone, R. D. & Kling, M. A. Cerebrospinal fluid evidence of increased extra-mitochondrial glucose metabolism implicates mitochondrial dysfunction in multiple sclerosis disease progression. *Journal of the Neurological Sciences* **275**, 106-112 (2008).
- Shay, N. F. & Tang, X. H. Zn<sup>2+</sup> has an insulin-like effect on glucose transport mediated by phosphoinositol-3-kinase and AKT in 3T3-L1 fibroblasts and adipocytes. *Journal of Nutrition* **131**, 1414-1420 (2001).
- 20 Regenold, W. T., Phatak, P., Makley, M. J., Stone, R. D. & Kling, M. A. Cerebrospinal fluid evidence of increased extra-mitochondrial glucose metabolism implicates mitochondrial dysfunction in multiple sclerosis disease progression. *Journal of the Neurological Sciences* **275**, (2008).

- Dorman, J. S., Steenkiste, A. R., Burke, J. P. & Songini, M. Type 1 diabetes and multiple sclerosis. *Diabetes Care* **26**, 3192-3193 (2003).
- Ban, M., Co, I. M. S. G. & Co, I. M. S. G. The expanding genetic overlap between multiple sclerosis and type 1 diabetes. *Multiple Sclerosis* **14**, S296-S296 (2008).
- Henry, J. P., Williamson, D. M., Schiffer, R., Wagner, L., Shire, J. & Garabedian, M. Investigation of a cluster of multiple sclerosis in two elementary school cohorts. *Journal of Environmental Health* **69**, 34-38 (2007).
- Schiffer, R. B., McDermott, M. P. & Copley, C. A multiple sclerosis cluster associated with a small, north-central Illinois community. *Archives Environmental Health* **56**, 389-395 (2001).
- Stein, E. C., Schiffer, R. B., Hall, W. J. & Young, N. Multiple-Sclerosis and the Workplace Report of an Industry-Based Cluster. *Neurology* **37**, 1672-1677 (1987).
- Dore-Duffy, P., Catalanotto, F., Donaldson, J. O., Ostrom, K. M. & Testa, M. A. Zn<sup>2+</sup> in Multiple-Sclerosis. *Annals of Neurology* **14**, 450-454 (1983).
- Vukusic, S. & Confavreux, C. Pregnancy and multiple sclerosis: the children of PRIMS. *Clin Neurol Neurosurg* **108**, 266-270 (2006).

# **Chapter 5 – Overall Conclusions and Future Directions**

# 5.1 Overall Conclusions

The results presented in this thesis further the understanding of the etiology of MS. In addition, the reason behind ameliorations of the disease seen with the use of estrogen begins to be explained. It was previously known that adenosine triphosphate (ATP) is released from RBCs in response to several stimuli and this ATP stimulates nitric oxide (NO) production in the endothelial cells lining the blood vessels. <sup>1,2</sup> The early studies presented in this thesis show that the estrogens, in the form of estriol and estradiol can decrease the amount of ATP released from the RBC, even in a non-flow system. <sup>3</sup> This is of note taking into consideration the knowledge that RBCs from patients with MS release three times the amount of ATP then RBCs from healthy controls, and that it has been shown that high levels of estrogens, due to pregnancy or drug therapy, can ameliorate MS. 4,5 It is believed that the increase in ATP release may be overstimulating the NO production in the endothelial cells, and NO is known to be toxic to the blood brain barrier (BBB). 6 If the overproduction of ATP from the RBCs can be returned to normal levels, the leakage in the BBB may be able to be stopped.

As discussed in chapter 1 and shown in figure 1.1, cystic fibrosis transmembrane conductance regulator (CFTR) activity is necessary for the release of ATP from the RBC in response to mechanical deformation.<sup>7</sup> There have been several reports showing the

effect of estrogen on the CFTR. Estrogens have been show to inhibit the chloride channel activity and have been called "glybenclamide-like inhibitors" in other cell types. Some very preliminary results that will be discussed shortly and shown in figure 5.1, show this to be the case with ATP release from RBCs. The data suggests that estrogens attenuate the excessive release of ATP from the RBCs of MS patients. If this is the case, the amount of NO production would also be decreased, potentially leading to less damage from the disease. The use of the microfluidic device to investigate the interactions occurring in the microvasculature showed that RBCs flowing through the channel of the microfluidic device release ATP as a result of sheer stress that stimulates the production of NO in bovine pulmonary artery endothelial cells (bPAECs) that are in proximity to the ATP.

Using this device, the role of estrogen in this process was determined, as shown in figure 2.16. Specifically, when acting on the RBCs, estrogen has a negative effect on the ATP release, subsequently decreasing the NO production in the bPAECs. However, the excess estrogen in the system interacted with the bPAECs, increasing the amount of NO production, though not above the levels seen in RBCs alone until a superphysiological amount of estrogen was incubated with the RBCs. The data presented here looks at the role of estrogen in this process in a distinctly different way from past studies in this area, where the hormone was applied directly to the cell to measure NO production. This reaffirms that it is essential to study drug interactions not only on a single cell type, but to also investigate the influence of cell-to-cell communication. Here, the

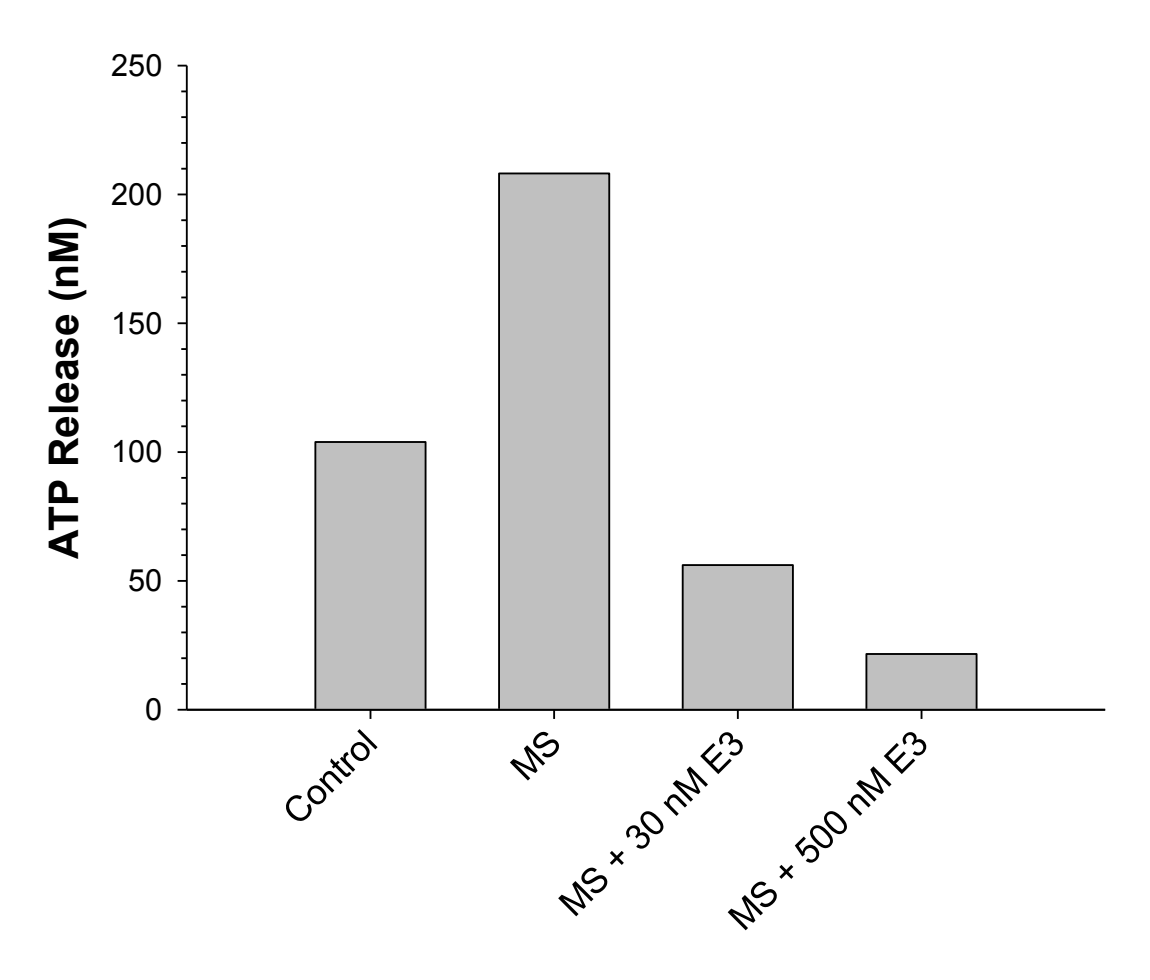


Figure 5.1 – The Effect of Estriol (E3) on ATP Release from the RBCs of MS Patients – Flow based studies were performed on one sample of RBCs from an MS patient with the addition of 30 and 500 nM estriol. Without estriol, the RBCs from the MS patient released 208.1 nM ATP, while the healthy control released 103.9 nM. When incubated for a half hour with 30 or 500 nM estriol, the ATP release dropped to 59.1 and 21.6 nM, respectively. N = 1.

microfluidic device was able to discern between endothelium-derived NO due directly to estradiol and the inhibition of NO production as a result of the decrease in RBC-derived ATP caused by the hormone.

Another major finding of this research is the evidence that C-peptide is the  $\operatorname{Zn}^{2+}$  carrier to the RBC. It was previously known that  $\operatorname{Zn}^{2+}$  bound to C-peptide will increase the ATP release from RBCs,  $^{11}$  and studies completed by Watshsala Medawala have shown that C-peptide binds to  $\operatorname{Zn}^{2+}$  in a 1:1 ratio.  $^{12}$  It was the expectation that C-peptide would need  $\operatorname{Zn}^{2+}$  to interact with the RBC, however, it was found that it is  $\operatorname{Zn}^{2+}$  that needs C-peptide for RBC interaction. Through the course of experimentation, it was discovered that while the C-peptide can interact with the RBC without  $\operatorname{Zn}^{2+}$ , the  $\operatorname{Zn}^{2+}$  cannot interact with the RBC without C-peptide, as seen in figure 3.7. Because C-peptide only causes an increase in ATP release from the RBC when it has been previously incubated with  $\operatorname{Zn}^{2+}$ , it was concluded that C-peptide is a  $\operatorname{Zn}^{2+}$  carrier to the RBC.

This knowledge was used in experimentations on the RBCs of MS patients, and may have significance in diabetes. Using  ${\rm Zn}^{2+}$  as the metal to bind C-peptide comes from the in vivo process in which C-peptide is cleaved and released into the blood stream. This occurs in the  $\beta$ -cells of the pancreas, where  ${\rm Zn}^{2+}$  is readily available to the C-peptide for binding before release into the body where there are many competitors for the metal.

As previously discussed, Zn<sup>2+</sup> bound to C-peptide has been shown to have a biological effect; it has also been shown to increase ATP release from RBCs obtained from a type 1 diabetic rat model back to the level of healthy controls. This effect is also seen in the RBCs from the type 2 diabetic rats, though only after incubation with metformin, a common pharmaceutical to treat the disease.<sup>13</sup>

It as been repeated shown that Zn<sup>2+</sup> bound to C-peptide increases RBC-derived ATP and subsequently NO release from endothelial cells lining the blood vessels causing vasodilation.<sup>2,14,15</sup> With further understanding of the structure, potential receptor and mechanism of the bioactivity of Zn<sup>2+</sup> bound to C-peptide, there is pharmaceutical potential for this molecule. Improving the blood flow of diabetic patients would help to ameliorate the complications seen with the disease, such as retinopathy, neuropathy, and nephropathy, and could vastly improve the health and quality of living of diabetic patients.

Working with the Neurology and Ophthalmology Clinic at Michigan Sate University and evaluating the RBCs of MS patients yielded a wealth of new information about the potential role of these cells in the disease. It was reaffirmed that the amount of ATP release from the RBCs of MS patients is significantly higher than that from the RBCs of healthy controls. The studies here went further than previous studies and, through the use of glybenclamide, it is now clear that the increase in ATP seen in the samples is the

result of an increased ATP release from the RBC, rather than from cell lysis. These findings are especially significant when discussed in the context of previous research showing the increased levels of NO and its metabolites in the lesions that occur as a result of demyelination and in the cerebral spinal fluid (CSF), serum and urine of MS patients. With the proven increase in ATP release from the RBCs of MS patients, an increase in NO production in these patients is expected. An increase in ATP-derived NO would be a significant discovery for the reasons mentioned above, as well as the knowledge that NO is one of the factors involved in the change in permeability of the blood brain barrier leading to its breakdown. Future work in this area will be discussed in section 5.2.2.

As discussed in chapter 1, high levels of ATP increases the pore size of the P2X<sub>7</sub> receptor to transport molecules with masses in the range of 100s of Daltons rather than just small cations. <sup>18</sup> This results in cytotoxic effects on oligodendrocytes forming lesions, in mice, that are similar to those seen in MS. <sup>19</sup> Interestingly, P2X<sub>7</sub> deficient mice were four times less likely to suffer from EAE than control mice, despite having the same increase in cytokine production. <sup>20</sup> Because of this, it seems that the increase in ATP release from the RBCs of MS patients may be having a direct cytotoxic effect on the oligodendrocytes, causing the lesions.

Early work evaluating the level of ATP release from healthy RBCs after incubation with estrogen showed a decrease in the concentration of ATP in these samples. Based on this, and reports in literature on the ability of this hormone to ameliorate the lesions of MS patients and in the animal model, 5,21,22 flow based studies were performed, as described in section 4.2.5, on one sample with the addition of 30 and 500 nM estriol. Although further work needs to be performed in this area, the early results are promising. As seen in figure 5.1, without estriol, the RBCs from the MS patient released 208.1 nM ATP, while the healthy control released 103.9 nM. When incubated for a half hour with 30 or 500 nM estriol, the ATP release dropped to 59.1 and 21.6 nM, respectively. This encouraging data shows that estriol does have the ability to inhibit RBC-derived ATP and may lend to the explanation of the effects of this hormone. It is believed by some that estrogens help to ameliorate MS by correcting an immune shift. 23 However, the data presented in chapter 2, combined with what was seen in this preliminary study and the previously mentioned ability of estrogen to interact directly with and inhibit CFTR, show that the effect of estrogen on MS may not be related to the immune system, but rather to its ability to decrease ATP release from the RBC.

Because ATP in the RBC is produced from glycolysis, the increase in ATP release from the RBC of MS patients suggests that there is an increase need for glucose in the cell and therefore it was expected that the glucose uptake into these cells would also be increased. While this was not the case when comparing the glucose uptake in the RBCs of MS patients to healthy controls, the RBCs of both groups had a significant increase in

glucose uptake when incubated with Zn<sup>2+</sup> bound to C-peptide, and the increased glucose uptake of the RBCs of MS patents was significantly higher than that of the RBCs of the healthy controls. Glucose metabolism has only been investigated in MS in a very limited capacity; however, as previously discussed, it has been noted that there may be some dysfunction of glucose metabolism in MS patients. While the data presented here is not the first to suggest that there is more than an autoimmune aspect to MS, nor the first to suggest altered glucose metabolism, it is the first to suggest a mechanism by which this abnormality can influence MS etiology. The increase in glucose uptake into the RBCs of MS patients likely results in an increase in ATP production and release. This ATP subsequently activated NO production in the endothelium, and this free radical has a damaging effect on both BBB, causing leaking and eventually leading to the formation of lesions.

While it is hypothesized that the increase in RBC-derived ATP results from an increase in glucose uptake, the reason for this increase remains unknown. One possibility for this may be related to some sort of mitochondrial dysfunction, though little research has been completed in this area. The belief of this thesis is that the increase in glucose uptake is related to the increased levels of  $Zn^{2+}$  on the RBC. As previously discussed, the role of  $Zn^{2+}$  in MS has not been the focus of major MS research, although it has been noted that clusters of MS have been found in areas of  $Zn^{2+}$  contamination, either in the soil and water, or from  $Zn^{2+}$  smelters. RBCs of MS patients have also been

shown to have an increased level of  $Zn^{2+}$ , even when not associated with an MS cluster. The previous research in this area was in support of the hypothesis that the amount of  $Zn^{2+}$  in the RBC was correlated with a decrease in the amount of cholesterol in the cells as well. The results presented here show that regardless of the amount of cholesterol, the amount of basal  $Zn^{2+}$  in the RBCs of MS patients is higher than that of healthy controls.

Glucose uptake stimulated by Zn<sup>2+</sup> has been seen previously in fibroblasts and adipocytes;<sup>30</sup> however, this is the first time it was investigated in RBCs. The ability of Zn<sup>2+</sup> bound to C-peptide to deliver Zn<sup>2+</sup> to the RBC and the increase in glucose uptake in the RBCs of both MS patients and healthy controls when incubated with Zn<sup>2+</sup> bound to C-peptide lead to the conclusion that Zn<sup>2+</sup> also causes an increase in glucose uptake in human RBCs. It is interesting to note that there has been research conducted looking into the genetic overlap between type 1 diabetes and MS, showing a significant increase in prevalence of MS in the first-degree relatives of type 1 diabetics.<sup>31</sup>

Using <sup>65</sup>Zn<sup>2+</sup> bound to C-peptide, it was shown that for both molecules that the amount of interaction was higher with the RBCs of MS patients as compared to healthy controls. Comparing the data presented in figures 4.5 and 4.6, it can be noted that the average

amounts of <sup>65</sup>Zn<sup>2+</sup> and C-peptide interacting with the RBC are nearly identical. In addition to showing the increased Zn<sup>2+</sup> interaction with the RBCs of MS patients, this data also reaffirms that the interaction of Zn<sup>2+</sup> and C-peptide with the RBC occurs at a 1:1 ratio. C-peptide has never been investigated in the etiology of MS, and there could be a number of different reasons for this increased binding. The β-cells of MS patients may contain an increased amount of  $\mathrm{Zn}^{2+}$ , either through an increased number of  $\mathrm{Zn}^{2+}$ transporters on the β-cell or because of an increased transporter efficiency, either of which would allow for more of the C-peptide to become Zn<sup>2+</sup> bound to C-peptide. Another possibility may be an increase in the number of binding sites on each RBC in MS patients for interaction with Zn<sup>2+</sup> bound to C-peptide. While the identity of this binding site is not currently known, work is currently being done in the Spence group investigating GLUT1 as a potential target, hypothesizing that the larger increase in glucose uptake by the RBCs may be the result of Zn<sup>2+</sup> binding to the protein in the membrane.

This research presented here is a leap forward in the understanding of MS etiology. More conclusive evidence, along with validation by several controls is still needed before any one of these elements can be used as a clinical biomarker. However, potential targets have been identified. As further data is collected on the various types of MS, along with CIS patients, and immune disease and neurological controls,

hopefully, one of these targets will prove to be a usable biomarker for the detection and monitoring of MS. Regardless, the data presented here shows that along with the autoimmune component in MS, there is clearly also some dysfunction with the glucose metabolism in these patients. Research into this area needs to continue until both the cause of the altered ATP release and the effect it has on the etiology of the disease are determined.

## 5.2 Future Directions

# 5.2.1 Zn<sup>2+</sup> and C-Peptide Binding

While work has previously been completed looking at the binding of Zn<sup>2+</sup> to C-peptide, there is still more to be learned in this area. Currently, isothermal calorimetry is being used to look at the interaction between these two molecules, as well as the interaction between each of them and albumin, a metal binding protein commonly found in blood plasma.

Work is on-going in the Spence Lab to further investigate the interactions of  $Zn^{2+}$  and C-peptide. Since it was first shown that C-peptide needed metal activation for biological activity, it has been assumed that C-peptide is somehow being activated by  $Zn^{2+}$  in the  $\beta$ -cell, as both molecules are present in high concentration. It is also the hypothesis that  $Zn^{2+}$  is binding to C-peptide in the  $\beta$ -cell, since once in the blood stream there would be

many strong competitors for  $Zn^{2+}$  binding. There is preliminary work in the creation of a circulation microfluidic device where the  $\beta$ -cell will be suspended in a well above a membrane over a long channel of circulating RBCs. After stimulation of the  $\beta$ -cell,  $Zn^{2+}$  and C-peptide will be release into the blood stream. There will be a measurement well in order to look at the ATP release from the RBCs. By blocking different parts of the secretion, the process of  $\beta$ -cell secretion and the interaction with RBCs and the subsequent ATP release will be investigated, to further prove that the effects seen in the lab also occur in vivo.

Despite decades of finding biological relevance, there has no been receptor found for C-peptide at the time of writing. Because of the effect of Zn<sup>2+</sup> bound to C-peptide on glucose uptake and ATP release, GLUT1, the major glucose transporter, is currently being investigated as the receptor on RBCs. It is known that Zn<sup>2+</sup> has an effect on glucose transport in certain cell types that is believed to be mediated through GLUT1. As previously mentioned, C-peptide will interact with the RBC whether or not Zn<sup>2+</sup> is present, however Zn<sup>2+</sup> is necessary for biological activity. GLUT1 can be purified from the membranes of RBCs and can be used for binding studies with C-peptide, Zn<sup>2+</sup>, and Zn<sup>2+</sup> bound to C-peptide. Work using gel electrophoresis has shown a potential increase in GLUT1 in the membrane of RBCs of MS patients as compared to those of healthy controls. To discern the actual amount of this protein present, future work will

use antibodies for GLUT1 to examine the concentration using either ELISA or flow cytometry.

## 5.2.2 Future MS Studies

While investigating blood samples from 22 MS patients has given a wealth of preliminary data, the large majority of these patients were diagnosed with relapsing-remitting MS and 16 of the 20 were female. Running the same tests of patients with the other types of MS, as well as clinically isolated syndrome (CIS) will result in further information about the disease, as well as show when these abnormalities begin to occur, and to what extent. With a large sample group, the effect of disease duration on these factors can be further investigated. It is the hope that the ATP release, glucose or  $Zn^{2+}$  uptake may correlate to disease state or severity, as well as being a specific biomarker for MS. To ensure this is the case, the RBCs of several control groups also need to be investigated. To prove that the effects seen are not simple the result of any neurological or inflammatory disease, control samples from these groups will be tested. For example RBCs from patients with Parkinson's disease and patients with arthritis will be collected and tested in the same manner as those from the MS patients.

Very preliminary results from MS patients, along with the results discussed in chapter 2, suggest that estriol, as well as estradiol, will be effective in reducing the ATP release from the RBCs of MS patients. Future MS patient RBC samples and controls will be incubated with various physiological concentrations of these estrogens and along with

the ATP release, glucose, Zn<sup>2+</sup> and C-peptide uptake will also be evaluated. Because of the increased cancer risk associated with estrogens, the effects of estrogen mimics, such as xenoestrogens, should be investigated for their effectiveness as well. Alternatively, if the reason for the ameliorating effects of estrogen can be determined and ameliorated with a different compound, that compound can also be tested.

## 5.2.3 Microfluidics and MS Studies

From the data presented in this thesis, it is hypothesized that the increase in ATP release from the RBCs of MS patients will result in an increase in NO production in the endothelial cells lining the blood vessels. In order to explore these interactions, the microfluidic device described and employed in chapter 2. Because it is known that RBC-derived ATP stimulates NO production in endothelial cells and that the RBCs of MS patients release extremely high amount of ATP in response to sheer stress, it is anticipated that an large increase in NO production will be seen using this method.

Because blood brain barrier (BBB) breakdown is a hallmark feature of MS, microfluidic studies should also be completed investigating the permeability of this barrier. Work has been completed in the Spence Lab on the measurement of cell confluency in a microfluidic device. Vogel, et al. described a system that employs transendothelial electrical resistance measurement (TEER) on a flow-based microfluidic device. As the confluency of cells cultured on the device increased, so did the electrical resistance, while the amount of charge that passed through the cells decreased. This allows for

objective measurement, rather than relying on visual inspection to determine confluency. The cells used in the preliminary experimentation were bovine pulmonary artery endothelial cells, though the work could easily be expanded to use brain microvascular endothelial cells, which form much tighter junctions in the BBB. The used of these cells would allow for the study of the effects for RBC-derived ATP and subsequent endothelial NO production on the integrity of BBB. These experiments would aid in the further understanding of the role of the RBC in the etiology of MS.

REFERENCES

#### REFERENCES

- Bergfeld, G. & Forrester, T. Release of ATP from Human Erythrocytes in Response to a Brief Period of Hypoxia and Hypercapnia. *Cardiovascular Research* **26**, 40-47 (1992).
- Sprague, R. S., Ellsworth, M. L., Stephenson, A. H. & Lonigro, A. J. ATP: The red blood cell link to NO and local control of the pulmonary circulation. *American Journal of Physiology-Heart and Circulatory Physiology* **271**, H2717-H2722 (1996).
- Letourneau, S., Hernandez, L., Faris, A. N. & Spence, D. M. Evaluating the effects of estradiol on endothelial nitric oxide stimulated by erythrocyte-derived ATP using a microfluidic approach. *Analytical and Bioanalytical Chemistry* **397**, 3369-3375 (2010).
- 4 Confavreux, C., Hutchinson, M., Hours, M. M., Cortinovis-Tourniaire, P. & Moreau, T. Rate of pregnancy-related relapse in multiple sclerosis. *New England Journal of Medicine* **339**, 285-291 (1998).
- Sicotte, N. L., Liva, S. M., Klutch, R., Pfeiffer, P., Bouvier, S., Odesa, S., Wu, T. C. & Voskuhl, R. R. Treatment of multiple sclerosis with the pregnancy hormone estriol. *Annals of Neurology* **52**, 421-428 (2002).
- Thiel, V. & Audus, K. Nitric oxide and blood-brain barrier integrity. *Antioxidants & Redox Signaling* **3**, 273-278 (2001).
- Sprague, R. S., Ellsworth, M. L., Stephenson, A. H., Kleinhenz, M. E. & Lonigro, A. J. Deformation-induced ATP release from red blood cells requires CFTR activity. *American Journal of Physiology* **275**, H1726-1732 (1998).
- Singh, A. K., Schultz, B. D., Katzenellenbogen, J. A., Price, E. M., Bridges, R. J. & Bradbury, N. A. Estrogen inhibition of cystic fibrosis transmembrane conductance regulator-mediated chloride secretion. *Journal of Pharmacology and Experimental Therapeutics* **295**, 195-204 (2000).
- 9 Sweezey, N., Ghibu, F. & Gagnon, S. Sex hormones regulate CFTR in developing fetal rat lung epithelial cells. *American Journal of Physiology-Lung Cellular and Molecular Physiology* **272**, L844-L851 (1997).
- 10 Chambliss, K. L. & Shaul, P. W. Estrogen modulation of endothelial nitric oxide synthase. *Endocrine Reviews* **23**, 665-686 (2002).

- Meyer, J. A., Froelich, J. M., Reid, G. E., Karunarathne, W. K. & Spence, D. M. Metal-activated C-peptide facilitates glucose clearance and the release of a nitric oxide stimulus via the GLUT1 transporter. *Diabetologia* **51**, 175-182 (2008).
- Medawala, W. *Mechanistic and Functional Studies of Zn*<sup>2+</sup> *Activation of C-Peptide and its Effect on Red Blood Cell Metabolism* PhD thesis, Michigan State University, (2011).
- Meyer, J. A., Subasinghe, W., Sima, A. A. F., Keltner Z., Reid, G. E., Daleke, D. & Spence, D. M. Zn<sup>2+</sup>-activated C-peptide resistance to the type 2 diabetic erythrocyte is associated with hyperglycemia-induced phosphatidylserine externalization and reversed by metformin. *Molecular Biosystems* **5**, 1157-1162 (2009).
- Oblak, T. D. A., Root, P. & Spence, D. M. Fluorescence Monitoring of ATP-Stimulated, Endothelium-Derived Nitric Oxide Production in Channels of a Poly(dimethylsiloxane)-Based Microfluidic Device. *Analytical Chemistry.* **78**, 3193-3197 (2006).
- Sprague, R. S., Olearczyk, J. J., Spence, D. M., Stephenson, A. H., Sprung, R. W. & Lonigro, A. J. Extracellular ATP signaling in the rabbit lung: erythrocytes as determinants of vascular resistance. *American Journal of Physiology-Heart and Circulatory Physiology* **285**, H693-H700 (2003).
- Smith, K. J. & Lassmann, H. The role of nitric oxide in multiple sclerosis. *Lancet Neurology* **1**, 232-241 (2002).
- Boje, K. M. K. & Lakhman, S. S. Nitric oxide redox species exert differential permeability effects on the blood-brain barrier. *Journal of Pharmacology and Experimental Therapeutics* **293**, 545-550 (2000).
- Adinolfi, E., Pizzirani, C., Idzko, M., Panther, E., Norgauer, J., Di Virgilio, F. & Ferrari, D. P2X(7) receptor: Death or life? *Purinergic Signal* 1, 219-227 (2005).
- Matute, C., Torre, I., Pérez-Cerdá, F., Pérez-Samartín, A., Alberdi, E., Etxebarria, E., Arranz, A. M., Ravid, R., Rodríguez-Antigüedad, A., Sánchez-Gómez, M. & Domercq, M. P2X(7) receptor blockade prevents ATP excitotoxicity in oligodendrocytes and ameliorates experimental autoimmune encephalomyelitis. *Journal of Neuroscience* 27, 9525-9533 (2007).
- Sharp, A. J., Polak, P. E., Simonini, V., Lin, S. X., Richardson, J. C., Bongarzone, E. R. & Feinstein, D. L. P2x7 deficiency suppresses development of experimental autoimmune encephalomyelitis. *Journal of Neuroinflammation* **5**, 33 (2008).

- Jansson, L., Olsson, T. & Holmdahl, R. Estrogen induces a potent suppression of experimental autoimmune encephalomyelitis and collagen-induced arthritis in mice. *Journal of Neuroimmunology* **53**, 203-207 (1994).
- Palaszynski, K. M., Liu, H., Loo, K. K. & Voskuhl, R. R. Estriol treatment ameliorates disease in males with experimental autoimmune encephalomyelitis: implications for multiple sclerosis. *Journal of Neuroimmunology* **149**, 84-89 (2004).
- Sicotte, N. L., Liva, S. M., Klutch, R., Pfeiffer, P., Bouvier, S., Odesa, S., Wu, T. C. & Voskuhl, R. R. Treatment of multiple sclerosis with the pregnancy hormone estriol. *Annals of Neurology* **52**, 421-428 (2002).
- 24 Raczkiewica, J. & Leyko, W. Adenine Nucleotide Content of Erythrocytes of Multiple Sclerosis Patients. *Clinica Chimica Acta* **14**, 408-409 (1966).
- Regenold, W. T., Phatak, P., Makley, M. J., Stone, R. D. & Kling, M. A. Cerebrospinal fluid evidence of increased extra-mitochondrial glucose metabolism implicates mitochondrial dysfunction in multiple sclerosis disease progression. *Journal of the Neurological Sciences* **275**, 106-112 (2008).
- Henry, J. P., Williamson, D. M., Schiffer, R., Wagner, L., Shire, J. & Garabedian, M. Investigation of a cluster of multiple sclerosis in two elementary school cohorts. *Journal of Environmental Health* **69**, 34-38 (2007).
- Schiffer, R. B., McDermott, M. P. & Copley, C. A multiple sclerosis cluster associated with a small, north-central Illinois community. *Archives of Environmental Health* **56**, 389-395 (2001).
- Stein, E. C., Schiffer, R. B., Hall, W. J. & Young, N. Multiple-Sclerosis and the Workplace Report of an Industry-Based Cluster. *Neurology* **37**, 1672-1677 (1987).
- Dore-Duffy, P., Catalanotto, F., Donaldson, J. O., Ostrom, K. M. & Testa, M. A. Zn<sup>2+</sup> in Multiple-Sclerosis. *Annals of Neurology* **14**, 450-454 (1983).
- 30 Shay, N. F. & Tang, X. H. Zn<sup>2+</sup> has an insulin-like effect on glucose transport mediated by phosphoinositol-3-kinase and AKT in 3T3-L1 fibroblasts and adipocytes. *Journal of Nutrition* **131**, 1414-1420 (2001).
- Dorman, J. S., Steenkiste, A. R., Burke, J. P. & Songini, M. Type 1 diabetes and multiple sclerosis. *Diabetes Care* **26**, 3192-3193 (2003).

Vogel, P., Halpin, S., Martin, R. & Spence, D. Microfluidic Transendothelial Electrical Resistance Measurement Device that Enables Blood Flow and Postgrowth Experiments. *Analytical Chemistry* **83**, 4296-4301 (2011).